CHALMERS
UNIVERSITY OF TECHNOLOGY

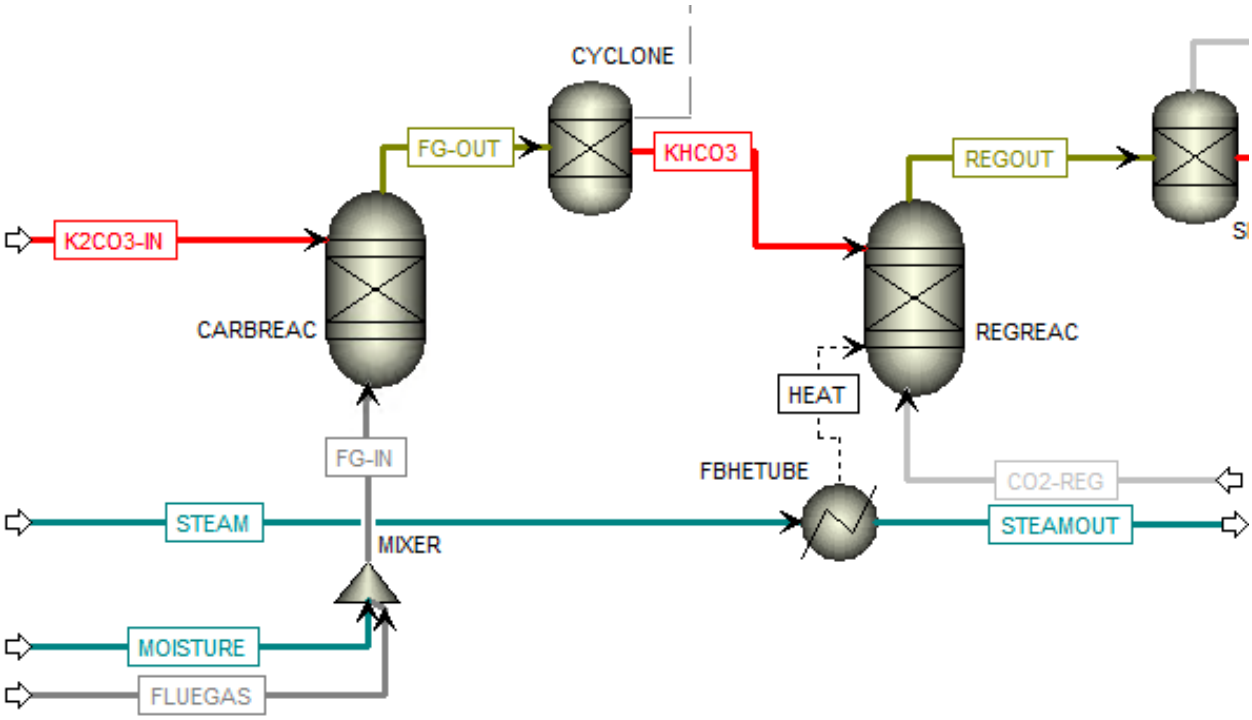

Implementation of Dry Hydrated Potassium Carbonate Carbon Capture

A case study of Renova's Waste-to-Energy plant in Sävenäs

Master's thesis in Sustainable Energy Systems

KAJSA JACOBSON, FRIDA TÖRNQVIST

DEPARTMENT OF SPACE, EARTH AND ENVIRONMENT
CHALMERS UNIVERSITY OF TECHNOLOGY
Gothenburg, Sweden 2024
www.chalmers.se

Master's thesis 2024

Implementation of Dry Hydrated Potassium Carbonate Carbon Capture

A case study of Renova's Waste-to-Energy plant in Sävenäs

KAJSA JACOBSON, FRIDA TÖRNQVIST

CHALMERS
UNIVERSITY OF TECHNOLOGY

DEPARTMENT OF SPACE, EARTH AND ENVIRONMENT
Division of Energy Technology
Chalmers University of Technology
Gothenburg, Sweden 2024

Implementation of Dry Hydrated Potassium Carbonate Carbon Capture
A case study of Renova's Waste-to-Energy plant in Sävenäs
KAJSA JACOBSON, FRIDA TÖRNQVIST

Supervisor: Ivana Staničić, Department of Space, Earth and Environment; Oscar Stenström, Department of Space, Earth and Environment; Andreas Hellström, Renova AB
Examiner: Magnus Rydén, Department of Space, Earth and Environment

Master's Thesis 2024
Department of Space, Earth and Environment
Division of Energy Technology
Chalmers University of Technology
SE-412 96 Gothenburg
Telephone +46 31 772 1000

Cover: Process diagram of the Dry Hydrated Potassium Carbon Capture system simulated in Aspen Plus.

Typeset in LaTeX
Printed by Chalmers Reproservice
Gothenburg, Sweden 2024

Implementation of Dry Hydrated Potassium Carbonate Carbon Capture
A case study of Renova's Waste-to-Energy plant in Sävenäs
KAJSA JACOBSON, FRIDA TÖRNQVIST
Department of Space, Earth and Environment
Chalmers University of Technology

Abstract

In near future, Waste-to-Energy (WtE) plants are required to reduce their CO_2 emissions drastically in order to achieve carbon neutrality. Since energy recovery from waste likely will persist, a necessary mitigation strategy is to implement a Carbon Capture and Storage (CCS) technology on site. In contrast to conventional methods, Dry Hydrated Potassium Carbonate (DHPC) carbon capture can provide low energy penalty, easy regeneration and opportunities to integrate the excess heat in the District Heating (DH) system. The DHPC process is based on solid absorption and performed by circulating a sorbent, potassium carbonate, K_2CO_3, between two fluidized bed reactors. This thesis performs a case study which implements the DHPC process at Renova's WtE plant in Sävenäs.

The application of the DHPC carbon capture is investigated by modeling the WtE and the DHPC process, using the simulation tools Ebsilon and Aspen Plus, respectively. When modeling the capture process according to the design proposed in research, an alternative design of the regeneration reactor is discovered able to reduce its steam demand, the fluidized bed heat exchanger (FBHE). The FBHE configuration as well as the original design of the DHPC process, lay the foundation for the construction of multiple system cases to analyse throughout the project. The potential for heat integration, in the different cases, is evaluated by performing a pinch analysis which creates the basis for retrofitting the WtE plant. In addition, the energy performance, reactor sizes and capture cost are investigated.

The thesis reveals that the DHPC process is a promising CCS method for Renova, especially the case using a FBHE. In particular, integrating this capture process increases the delivery of DH by 2.27-3.29% while reducing the electricity production by 2.09-8.51%, depending on the pressure level of the utilized steam. As a result, the total energy efficiency of the WtE plant is expected to increase by 1.47-1.57%, after applying the FBHE DHPC processes. In addition, the economic evaluation indicates on low capture costs including operational costs which are relatively insensitive in terms of future energy prices.

In conclusion, it is recommended for Renova to investigate the DHPC process further, since by choosing this method, the WtE plant can almost maintain its normal production of electricity and DH. However, in order to enable a future implementation of the process, it is of importance to verify the function of the FBHE reactor and evaluate the physical footprint of the system in the light of the found reactor sizes as well as the practical feasibility of the proposed retrofits.

Keywords: CCS, WtE, DHPC, Process Modeling, Heat Integration, Pinch analysis, FBHE.

Acknowledgements

First of all, we would like to thank our supervisors, Ivana Staničić and Oscar Stenström at the Department of Space, Earth and Environment, for their guidance in the completion of our project. You have provided us with useful feedback, forums for brainstorming and cheers when we have been in need for that. Also, we would like to thank our examiner, Magnus Rydén at the Department of Space, Earth and Environment, for guidance but also for spontaneous consulting sessions whenever technical problems have occurred.

Second of all, we want express our gratitude to Andreas Hellström at Renova for all the discussions, study visits as well as important information that he has provided. Thanks to you and your commitment, we have deepened our knowledge significantly in the field of waste incineration as well as heat and power processes.

Kajsa Jacobson and Frida Törnqvist, Gothenburg, May 2024

List of Abbreviations

Al_2O_3	Alumina
BFB	Bubbling Fluidized Bed
CAPEX	Capital Expenditures
CCS	Carbon Capture and Storage
CFB	Circulating Fluidized Bed
CHP	Combined Heat and Power
COP	Coefficient of Performance
CO_2	Carbon Dioxide
DC	Direct Condensation
DH	District Heating
DHPC	Dry Hydrated Potassium Carbonate
EP	Energy Penalty
ESP	Electrostatic Precipitator
FBHE	Fluidized Bed Heat Exchanger
FFB	Fast Fluidized Bed
HP	High Pressure
$KHCO_3$	Potassium bicarbonate
K_2CO_3	Potassium carbonate
LHV	Lower Heating Value
LP	Low Pressure
MEA	Mono-Ethanol-Amine
MKS	Internal cooling medium
OPEX	Operational Expenditures
RKS-BM	Reidlich-Kwong-Soave equation with Boston-Mathias modification
SCR	Selective Catalytic Reduction
SNCR	Selective Non-Catalytic Reduction
WtE	Waste-to-Energy

Nomenclature

Below is the nomenclature of indices, sets, parameters, and variables that have been used throughout this thesis.

Indices

tot	Index referring to total quantity
$loss$	Index referring to loss in energy efficiency
WtE	Index for WtE without carbon capture
$WtECC$	Index for WtE with carbon capture
El	Index referring to electricity
DH	Index referring to district heating

Sets

$CAPEX$	Set of capital expenditures
$OPEX$	Set of operational expenditures

Parameters

η_{tot}	Total energy efficiency
η_{loss}	Energy efficiency loss
η_{WtE}	Total energy efficiency of the WtE plant without carbon capture
η_{WtECC}	Total energy efficiency of the WtE plant with carbon capture
EP_{El}	Energy penalty in terms of electricity
EP_{DH}	Energy penalty in terms of district heating
X_{WtE}	Produced electricity or district heating of the WtE plant without carbon capture

X_{WtECC}	Produced electricity or district heating of the WtE plant with carbon capture

Variables

m_{fuel}	Mass flow of fuel
P	Electrical power
Q	Useful heat
LHV	Lower heating value
P_{WtE}	Electrical power produced in the WtE plant without carbon capture
P_{WtECC}	Electrical power produced in the WtE plant with carbon capture
Q_{WtE}	Useful heat produced in the WtE plant without carbon capture
Q_{WtECC}	Useful heat produced in the WtE plant with carbon capture

Contents

List of Figures

List of Tables

1
Introduction

The Paris Agreement establishes the overall climate goal of the world, limiting the global average temperature increase well below 2°C above pre-industrial levels. Although, in recent years, the UN's Intergovernmental Panel on Climate Change emphasizes that the increase in average temperature must not cross 1.5°C since it would cause severe climate change impacts [1]. The main reason for the global warming is the increase of greenhouse gas emissions, CO_2 being the most important, in the atmosphere [2].

In 2021, Waste-to-Energy, WtE, plants within the EU-27 generated 36.4 Mt of CO_2 emissions, which corresponds to 5.1% of the total greenhouse emissions from public electricity and heat production [3]. Despite alternative methods, energy recovery will likely always play some role in waste management. Consequently, to reach the climate goals, significant measures are needed in this field. A mitigation strategy available for the hard-to-abate emissions is to implement a Carbon Capture and Storage, CCS, technology at WtE sites.

Currently, there are numerous of different possible CCS technologies, some of which are in use in commercial facilities and some which still are in the conceptual design stage. Among these technologies are for instance solvent-based chemisorption, carbonate looping and oxy-fuel combustion [4]. Today, there are around 40 commercial CCS facilities in operation [5], but to reach the climate goals, more will be needed in the future.

One of the most studied capture methods is the Mono-Ethanol-Amine, MEA, absorption process which can reach a capture rate of 84-95% [6, 7, 8]. The main drawbacks of this method are the high energy penalty in the reboiler, corrosion problems as well as solvent degradation [9]. The energy penalty that follows the application of MEA CCS at a CHP plant, has been reported as 15-16% with a specific reboiler duty of 3.67 GJ/tCO_2 captured [10]. In contrast, solid absorption capture processes could provide low energy penalty, easy regeneration and high CO_2 capture capacity [11]. Particularly, the Dry Hydrated Potassium Carbonate, DHPC, process could be of interest for carbon capture.

The DHPC process is based on chemical absorption in which solid particles of potassium carbonate, K_2CO_3, supported by a material for mechanical strength, are circulated between two fluidized bed reactors with the aim to capture CO_2 from flue gas. In the carbonation reaction, where CO_2 reacts with K_2CO_3, heat is released as it

is an exothermic process [12]. The temperature of the excess heat is relatively high (50-100 °C) [12, 11] compared to the corresponding excess heat from MEA absorption (40-60 °C) [13, 14]. In particular, the excess heat could be used as a source for district heating purposes. Research on DHPC has been conducted in for instance Korea, where successful pilot plants have been built and operated [11]. Hence, it is interesting to investigate the impacts of DHPC implementation in Sweden where the heat and electricity generation is centralized, and the demand for heat is larger.

Renova is a waste management company that supplies a large geographical area with district heating, DH, and electricity. At their WtE plant in Sävenäs, Gothenburg, around 550 000 tons of waste is burned every year and in 2022, this plant produced 1 400 000 MWh of heat and 210 000 MWh of electricity in total [15, 16]. Considering that energy recovery from waste management will likely persist in the future, the CO_2 emissions from this WtE plant need to be adressed. Renova's plant in Sävenäs delivers DH water at 90-115°C [15], which evidently enables the potential use of waste heat from the DHPC process for DH purposes and could make DHPC a beneficial choice of CCS technology at this site. Therefore, this project presents a case study investigating the possibilities to implement the DHPC process at the WtE plant.

1.1 Aim and objectives

The main focus of the project is to design and simulate the DHPC carbon capture process by process modeling and to investigate the impacts of its implementation at the Renova's WtE plant. Hence, the WtE plant will be modeled, before incorporating both processes and performing a pinch analysis. Based on the outcome of the pinch analysis, the WtE plant will be retrofitted in order to integrate as much excess heat from the DHPC process as possible. The performance of the whole system will be evaluated in terms of energy performance parameters and capture cost.

The issue previously proposed is narrowed down to a several research questions in line with the aim of the project. These are:

Q1. How will the DHPC process design be constructed, if applied at the Renova WtE plant, and which operating conditions would be required?

Q2. How much excess heat from the DHPC process can be integrated at the Renova WtE plant and how will the implementation impact the supply of electricity and DH?

Q3. How does the DHPC system perform in terms of capture rate and capture cost?

1.2 Scope and limitations

The project scope will be partly limited due to restrictions in the system boundaries, as well as limited modelling complexity. Firstly, the system boundaries will be set to not include further treating of the CO_2 stream from the capture process. Consequently, liquefaction, which is crucial to enable transportation of CO_2 will not be included in this study, even though it might be of interest for Renova. Secondly, the complexity of the DHPC model will not be comparable with the complexity of the real process. For instance, the model will not take reaction kinetics into consideration even though this affects the performance of the process in reality. The real process involves a large number of free variables, and some of these will not be covered in this project. In other words, only a few design options are proposed in this thesis but certainly, there are more possible ways to design the process.

In addition to these limitations, the DHPC model will be constructed to only treat the flue gas generated by one of Renova's four combustion lines (Line 7). This boundary is set since the possibilities to implement carbon capture technologies at larger scales are limited at the time of this study. In addition, the remaining lifetime of the furnaces differs, implying that the newest, Line 7 is of interest. However, even though the flue gas from solely one combustion line will be treated, the heat sources and sinks of the entire WtE plant are available to satisfy the demands of the capture plant.

Consequently, the model of the WtE plant proposed in the project will be a simplified version of the real plant. Parts that are equal in two or more of the four combustion lines will be combined and represented by one component. This includes all four furnaces being modeled as one and the separate flue gas cleaning systems of all four lines being approximated as two. Another restriction in the WtE model is that it is instantaneous and will only be able to represent winter operation, full load capacity, at steady-state.

2
Theory

This chapter introduces the theory behind the different studied processes, Renova's Waste-to-Energy, WtE, plant and the DHPC carbon capture. Initially, the existing WtE plant design will be described, pointing out the most important components and their function in the system, or subsystem. As a way of justifying the relevance of this project, Renova's emission mitigation strategy will be presented as well. Thereafter, the fundamentals of the DHPC process will be explained, including the main principle and previous research. Later, detailed information about the involved reactors is presented as well as alternative ways of designing one of them. Lastly, different pathways for the global reactions and possible byproducts are explained.

2.1 Renova's WtE plant in Sävenäs, Gothenburg

In this section, the studied WtE plant at Renova will be described in detail. Later on, the company's current emission mitigation strategy will be presented.

2.1.1 Plant design

In Figure 2.1, a schematic representation of Renova's WtE plant focusing on the steam cycle, is shown. The plant consists of four different combustion lines that each proceed from separate incineration furnaces, furnace 1, 4, 5 and 7 [16]. The primary steam generated in each furnace is fed to a joint steam chest from which streams are led to different applications in the complex system. Firstly, steam is directed to the turbine for electricity generation [16]. The high-pressure steam (HP) is expanded to low-pressure (LP) steam where there is an extraction and then further down to the condensing pressure. The steam in the steam chest is also used to drive a feedwater pump and for furnace 4 and 5, it is used to preheat the air before combustion. Both line 1 and 7 instead use low-pressure steam from the extraction point for this purpose [17].

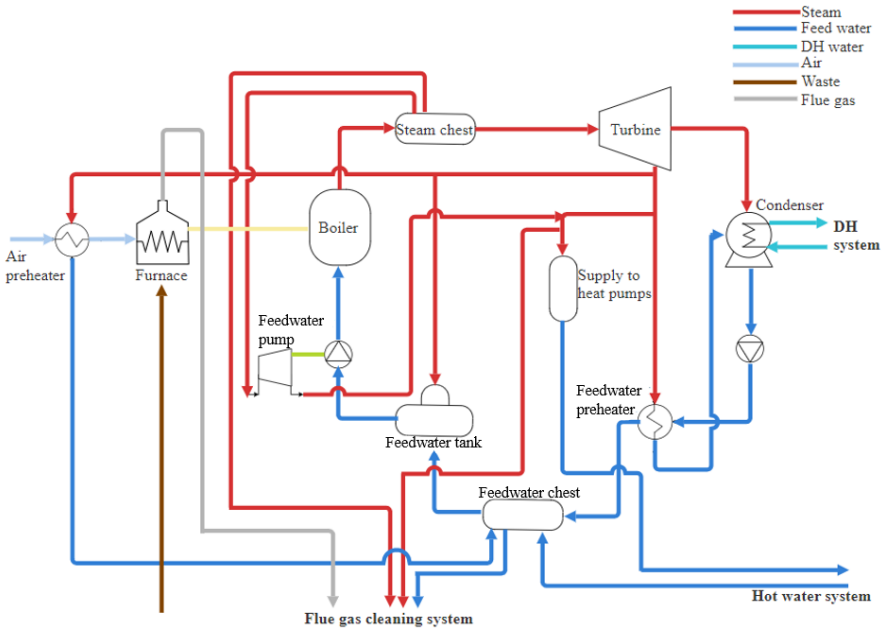

Figure 2.1: Schematic figure of the WtE process, focusing on the steam cycle.

Furthermore, the outlet stream from the turbine is condensed which generates heat of condensation utilized in the DH system. The condensate is then passed through a feedwater preheater, before entering the feedwater chest and later the feedwater tank. As mentioned, a steam driven feedwater pump provides the pressure increase before the stream of feedwater is led back to the boiler. An alternative feedwater pump, powered by electricity and functioning as a back-up, is also integrated at the plant.

As previously explained, low-pressure steam is extracted from the turbine. The utilization of it includes regulating the pressure in the feedwater tank, powering absorption heat pumps and heating the feedwater in a preheater [17]. After condensing in the heat pumps, the LP steam condensate is further utilized as a heat source to the hot water system. The hot water system is used to cool the flue gas as well as supplying heat to the district heating cycle via direct heat exchange and heat pumps. The temperature of the hot water is held above 110°C in all parts of the cycle [17].

The DH water leaves the plant at roughly 100°C and is returned at 40°C. The temperature is initially increased with heat from the direct condensation of the flue gas and then further increased with the use of heat pumps consuming heat at other parts of the plant, more specifically from the low-pressure steam and the hot water cycle. All heat pumps are of the type absorption heat pump and there are eight of them in total. Two of them are driven by hot water whereas the other six are consuming LP steam. After the heat provision by the heat pumps, a part of the DH water is directly heat exchanged with the hot water system, before it is heated in the turbine condenser and delivered to the DH costumers [17]. A process scheme of the hot water system and the DH system is presented in Figure 2.2.

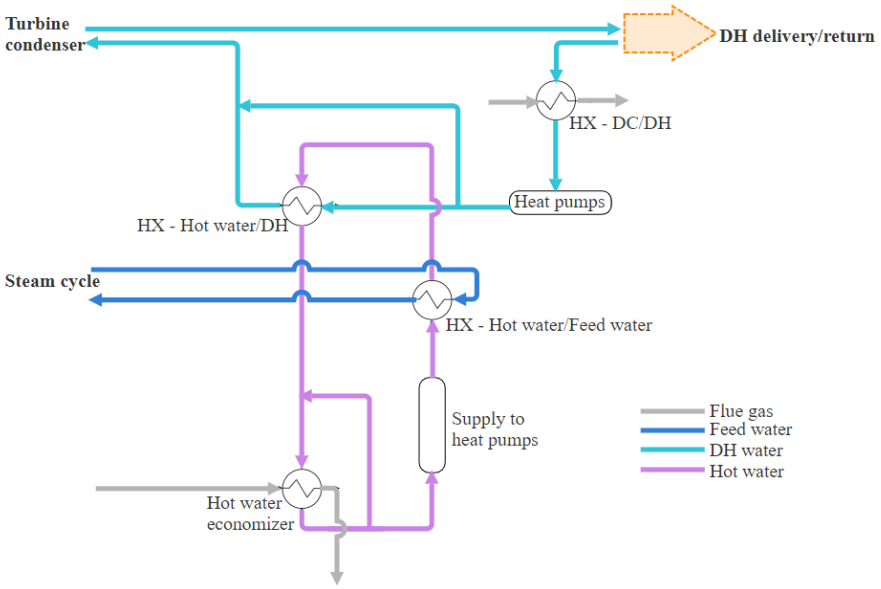

Figure 2.2: Schematic figure of the hot water and DH system of the WtE process. Note that DC refers to direct condensation.

The flue gas cleaning system is an important feature of the WtE in order to get rid of soot and impurities. In addition, it is connected to the rest of the plant in terms of steam demand and generation of heat. Therefore, it is of importance to include it when describing, and later modeling, the WtE plant. However, due to the different times of construction of the furnaces, the flue gas treatment systems differs between the four combustion lines. An overview of the flue gas cleaning system for line 1 and 7 is shown in Figure 2.3.

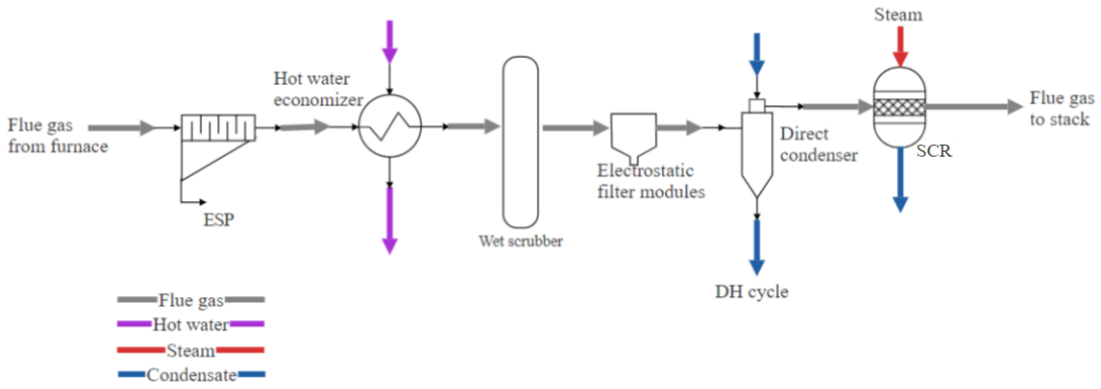

Figure 2.3: Schematic figure of the flue gas cleaning system of line 1 and 7 at Renova's WtE plant.

The first steps of the flue gas treatment are equal for all four lines. The flue gas is initially treated in Electrostatic Precipitators, ESP, which removes 99.5% of the solid

ash particles by inducing an electric charge [16]. Secondly, the flue gas temperature is reduced by heat exchanging with the hot water system in an economizer. Thirdly, the exhaust gas is treated step-wise in a wet scrubber to remove hydrochloric acid, heavy metals and sulphur dioxide. Further removal of particles is then performed in electrostatic filter modules, before the flue gas is condensed to decrease the water content and to recover heat [17]. The heat is utilized directly in the DH system and indirectly in the absorption heat pumps via an internal cooling medium, referred to as MKS. Lastly, the exhaust gas of line 1 and 7 is fed to a Selective Catalytic Reduction, SCR, reactor to reduce the concentration of nitrogen oxides by reacting with ammonia on a catalyst bed. The flue gas treatments in the other lines instead use a Selective Non-Catalytic Reduction, SNCR, for the same purpose but in this case, ammonia is usually added directly in the furnace [16]. Thereafter, the flue gas is led to the stack.

2.1.2 Emission mitigation strategy

As previously mentioned, the flue gas generated at the WtE plant in Sävenäs is cleaned in multiple steps, but currently there is no possibility to separate CO_2 from the emitted gases at the site. Around 540 000 tons of CO_2 are emitted yearly from the plant, whereas 40 % of these are from fossil sources. The company is aiming towards reducing their emissions drastically in order to mitigate their contribution to global warming and climate change impacts [15]. Consequently, Renova is investigating the possibilities of implementing a CCS technology to Line 7 at their plant in Sävenäs. Together with Göteborg Energi, Renova is working on a project that, if carried out, will lead to implementation of a CCS technology, such as the DHPC process, and separation of around 100 000 tonnes of CO_2 by the year 2030 [15].

2.2 DHPC process

This section will initially present the fundamentals of the DHPC process and previous research done in the field. Secondly, the overall set-up of a DHPC system and the required equipment, particularly focusing on the fluidized bed reactors, will be introduced.

2.2.1 The fundamentals of DHPC

The DHPC process is a post-combustion carbon capture technology which is based on chemical absorption [18]. The general principle of chemisorption for carbon capture is reaction between a sorbent, or absorbent, and the acidic CO_2 gas forming chemical bonds. Consequently, the regeneration of the sorbent and breaking the bonds of the new complex, involve an energy penalty [19].

In the DHPC process, CO_2 is separated from flue gas by the use of two fluidized bed reactors, one carbonation reactor and one regeneration reactor, with a solid sorbent as bed material. In particular, the sorbent is potassium carbonate, K_2CO_3. The

process also involves a cyclone that separates solid particles from gas and a sorbent cooler that cools the sorbent between the two reactors [20] by the use of air [12]. A simplified schematic figure of the process is shown in Figure 2.4.

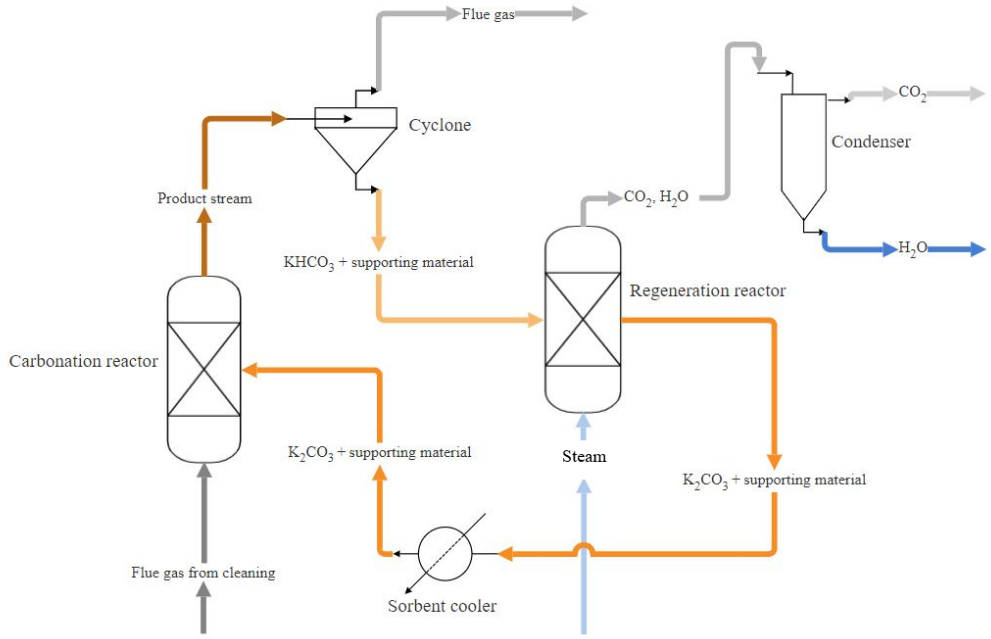

Figure 2.4: Flowchart of the DHPC capture process designed as proposed in literature.

Besides K_2CO_3, multiple sorbents have been used in experiments of the process. These include mostly alkali and alkaline metal-based ones such as Na_2CO_3 and Li_4SiO_4 [11]. Among them, the potassium based sorbents have shown the most promising results due to their cost and energy efficiency [11]. However, pure K_2CO_3 has slow kinetics due to the formed product inhibiting further diffusion of CO_2 and H_2O (more details on the reaction can be found in Section 2.2.3). Therefore, the solid particles in the DHPC process also contain a supporting material. Besides enhancing the reactivity, the support improves the mechanical strength [12]. As a result, the weight ratio of K_2CO_3 is important since a surplus can block pores which prevents the reaction [18]. Several supporting materials have been found in research. Among these are alumina (Al_2O_3), silica (SiO_2), magnesium oxide (MgO) and activated carbon [11]. However, considering costs and overall performance concerns of the capture process, Al_2O_3 is proposed as a preferable supporting material. In addition, it has beneficial pore structure and high surface area [11]. The average particle size for the described K_2CO_3 and Al_2O_3 mixtures has been reported to be between 103-120 µm [12].

Multiple small-scale setups of the process have been investigated but there is only one close to industrial-scale pilot plant, located in Hadong, Korea. The pilot plant is at 10 MWe-scale, was finalized in 2013 and managed to achieve a 80% CO_2 removal [21]. At this site, the bed material consisted of 35 weight% K_2CO_3 and 65 weight% of the supporting material Al_2O_3 [21]. When it comes to the relevant equipment, a

fast fluidized bed reactor, FFB, was used as a carbonator and a bubbling fluidized bed reactor, BFB, was used for regeneration of the sorbent [20]. These types of reactors will be described in more detail in the section below.

2.2.2 Fluidized bed reactors used for DHPC

The typical applications of fluidized bed reactors, FB, are in industries such as petroleum, fuel and mineral processing as well as wastewater treatment and combustion [22]. In general, FB reactors possess several advantageous characteristics. Among these are rapid mixing of phases, excellent mass and heat transfer, isothermal temperature distribution and good control of reaction parameters [22, 23, 24]. The general working principle of the FB reactor is fluid flow (either gas or liquid) through a bed of solid particles with high enough velocity to suspend the particles and cause them to act as a fluid [24]. There are two main types of fluidized bed reactors: fast fluidized bed reactor, FFB, and bubbling fluidized bed reactor, BFB [25].

The main difference between the FFB and the BFB reactors is the fluidization velocity, where the latter has the lowest. As a consequence, the bed material in the BFB remains in the lower region of the vessel whereas the bed material in the FFB is accelerated and dispersed throughout the whole reactor. The higher velocities in the FFB also results in lower residence time than for the BFB. [25]

2.2.3 Carbonation reactor

The working principle of the carbonation reactor is infusing the flue gas in the bottom of the reactor, fluidizing the bed of the solid particles of K_2CO_3 and supporting material [26]. Thereby, carbonation takes place according to the following reaction formula

$$K_2CO_3(s) + CO_2(g) + H_2O\,(g) \longrightarrow 2\,KHCO_3(s) \qquad \Delta H = -141\,kJ/mol \qquad \{1\}$$

which consumes CO_2 and produces heat as the carbonation reaction is exothermic. Consequently, the carbonation reactor requires cooling and the typical temperature range for this stage is 50-100°C [26, 11], at an ambient operating pressure [25]. In most research, the carbonation reactor is a fast fluidized bed reactor [27]. Additionally, in the pilot plant tests, the reactor vessel is mantled with tubes containing water which enables cooling [21]. For the carbonation reaction to take place at high degree, it is important that there is enough water vapor present in the reactor [12]. In previous studies, this has been ensured by letting the flue gas bubble through water in a gas bubbler before entering the carbonation reactor [27].

As previously mentioned, the main characteristic of the fast fluidized bed reactor is the high fluidization velocity which causes the bed material to expand and fill the whole reactor [25]. Consequently, the solid particles and the gas are well-mixed throughout the vessel, which requires subsequent separation achieved by the use of a cyclone. In reaction 1, solid potassium bicarbonate is formed, $KHCO_3$, which is continuously transported, due to the fast characteristics of the FFB reactor, to the

second reactor where the regeneration of the sorbent occurs [26].

The main disadvantage of utilizing the fast fluidized bed reactor for the carbonation reaction is the low residence time. To address this issue, a two-stage absorption reactor has been proposed instead. Instead of performing reaction 1 in solely a fast fluidized bed reactor, two bubbling fluidized bed reactors are connected in series [28]. The advantage of the bubbling fluidized bed reactor is the low gas velocity permitting a better contact between the gas and the sorbent, allowing for an increased capture efficiency. In addition, by combining the two stages of bubbling beds with features of the fast fluidized bed reactor, the sorbent circulation rate is more stable which enhances the operation of the process on industrial scale [28].

2.2.4 Regeneration reactor

In the second reactor the sorbent is regenerated. The regeneration reactor is of the type bubbling fluidized bed [12]. As the regeneration is an endothermic process, heat is required to drive the reaction. The reaction formula, being the reversed version of reaction 1, reads as follows

$$2\,KHCO_3(s) \longrightarrow K_2CO_3(s) + CO_2(g) + H_2O\,(g) \qquad \Delta H = 141\,kJ/mol \qquad \{2\}$$

In the regeneration reactor, the CO_2 is released from the $KHCO_3$ and thereby separated from the rest of the flue gas while the sorbent is converted back to K_2CO_3 [26]. As a consequence of the slow fluidization velocity in the BFB, the sorbent is extracted from the bottom of the reactor before it is cooled by a sorbent cooler and led back to the carbonation reactor [12].

Multiple different regeneration environments have been tested to identify the most effective conditions for regenerating the sorbent. The temperature in the regeneration reactor is most commonly within the range 150-200°C [20, 29] but lower temperatures have also been investigated [30]. The fluidization gas in the regeneration reactor is usually air or steam [26]. Previous research states that using one of the two products in the regeneration reaction, CO_2 or steam, as fluidization gas and to deliver heat to the reaction, gives a purer CO_2 stream than when air is used. This is due to easier gas separation after regeneration [31]. It was also concluded that a higher partial pressure of steam compared to CO_2, was more beneficial for the regeneration property of the sorbent than vice versa [31]. One could also argue against using products from the reaction as fluidization gas, if considering Le Chatelier's principle. However, as previously explained, using air would entail a difficult subsequent gas separation [31].

2.2.5 Alternative design of regeneration reactor - Fluidized Bed Heat Exchanger

An alternative way to construct and design the regeneration reactor could be as a Fluidized Bed Heat Exchanger, FBHE. A FBHE often consists of heat exchanger tubes, containing a fluid, within a BFB [32]. A fluidized bed can achieve very high

heat transfer rates which makes it possible for the reactor bed to attain almost a completely uniform temperature [32]. Because of these heat transfer properties, it could be suitable to use a FBHE in the DHPC process to supply heat to the endothermic reaction in the regeneration reactor. In a FBHE, the bed particles are often fine and in the size range 100-300 μm and the fluidization gas velocity is often around 0.5 m/s [33]. The bed material has in most previous research consisted of inert silica sand, but some reports have been done on beds that partly consist of a more active material, namely ilmenit which serves as an oxygen carrier. It has also been mentioned that a possible future application of FBHE would be as heat source for chemical reactions [32], which supports the idea of using this process for DHPC carbon capture.

In research, there are different applications for FBHE such as in Circulating Fluidized Bed, CFB, boilers where the FBHE is placed past the cyclone to cool bed particles before they are returned to the furnace. At the same time as the hot particles are cooled, steam is generated and superheated within the tubes [33]. Most research on FBHE has been conducted on a laborative scale, but there are examples where pilot plant scale investigations have been done [33].

2.2.6 Reaction pathways and byproducts

The overall reaction pathway of the carbonation process is in accordance with reaction 1. However, there are disagreements regarding how it occurs in detail, if parallel reactions are present and if it is a sequential reaction implying that intermediates are formed. In literature, it has been confirmed that an intermediate, $K_2CO_3{\cdot}(1.5H_2O)$, is formed from reaction of K_2CO_3 and water [11] according to reaction 3 [34, 35, 36, 37].

$$K_2CO_3(s) + 1.5\,H_2O\,(g) \rightleftharpoons K_2CO_3 \cdot (1.5\,H_2O)\,(s), \qquad \{3\}$$

This means that reaction 1 and 3 are competing parallel reactions in the carbonation reactor. Some research papers conclude that $K_2CO_3{\cdot}(1.5H_2O)$ is further converted into $2KHCO_3$ by reaction 4 [37, 38].

$$K_2CO_3 \cdot (1.5\,H_2O)\,(s) + CO_2(g) \rightleftharpoons 2\,KHCO_3(s) + 0.5\,H_2O\,(g), \qquad \{4\}$$

While some claim that reaction 4 does not occur [34, 35, 36]. In this case, the water content in the flue gas need to be carefully controlled to limit the formation of $K_2CO_3{\cdot}(1.5H_2O)$ [11]. In the regeneration reactor, if reaction 4 occurs in the reverse direction, it can absorb moisture from the fluidizing steam flow which allows for the steam to release latent heat in the reactor vessel [37].

Other than the different reaction pathways in the carbonation reactor, research has also touched upon the CO_2 uptake capacity of the different K_2CO_3 phases and intermediates. It has been shown that K_2CO_3 regenerated directly from $KHCO_3$ through reaction 1 has faster kinetics and higher CO_2 uptake than $KHCO_3$ regenerated from the intermediate through reactions 4 and 3 [34].

As discussed in Section 2.2.1, several different supporting materials have been used in research. Among these, there are materials that are inert and some that participate in reactions. For instance, alumina, Al_2O_3, is generally inactive but can form $KAl(CO_3)(OH)_2$ which can hinder the sorbent performance since it decreases the degree of carbonation. In addition, it requires a higher regeneration temperature than the pure potassium bicarbonate ($KHCO_3$). Furthermore, if utilizing MgO as supporting material, issues with byproducts can arise since it is active in the carbonation process, see Section 2.2.1. [11]

3
Methods

The methodology of the project is summarized in Figure 3.1. As seen in the figure, it consists of several main steps, represented in blue, which are linked to the research questions of the thesis, presented in green. First, the research aim and objectives were set, before conducting a generic literature review of the existing research examining the DHPC process. This included gathering information and gain knowledge about the process in terms of key parameters, such as related chemical reactions and process data from existing pilot plants.

Furthermore, relevant data for the simulation of the WtE plant was collected on-site at Renova in Sävenäs. Thereafter, the CHP plant as well as the DHPC process could be designed and modeled. Later, heat integration calculations were performed and the energy performance of the plant, capture cost as well as the sizes of capture process reactors were analyzed.

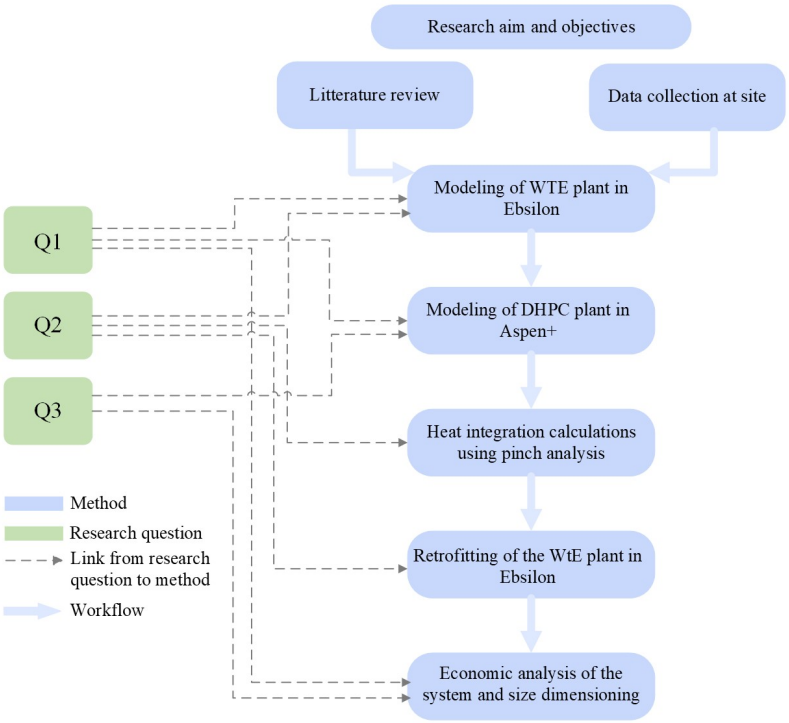

Figure 3.1: Flowchart of the methodology used in the thesis, representing the links between the main parts of the method and the research questions.

3.1 Collection of data

After formulating the research aim, relevant data for the simulation of the WtE plant were collected at Renova. In order to gain knowledge about the process, several study visits were carried out. The different learning elements of the visits included going on a detailed tour of the plant, discussing the layout of the process with operational staff and studying the process schemes in the control room. Data of important parameters and specifications in the WtE plant were collected through examining process schemes and measurements from the control room.

In order to make sure that the capture process is able to handle the maximum amount of CO_2 emissions from the plant and simultaneously account for the full potential of the available heating and cooling sources on-site, the simulation of the WtE plant was made in winter mode. In particular, this means that all input data was gathered from the 6th of November in 2022 at 1:42 pm.

3.2 Modeling of the WtE plant

In the following section, the modeling tool used for the simulation of the WtE plant is introduced as well as the overall strategy when creating the model.

3.2.1 Modeling tool

The chosen modeling tool for the WtE plant simulation was Ebsilon®Professional. The software is capable of simulating thermodynamic cycles in order to design and optimize plants. In addition, it allows to input specific parameters and study retrofit options [39] which made it suitable for this project.

3.2.2 WtE plant design

To set the basis for later integration of the DHPC capture process, a model representative of Renova's WtE plant in its current state was generated. The model was constructed by combining the main parts of the plant: the steam cycle, district heating cycle, the hot water cycle and the flue gas cleaning system. To facilitate the simulations, the stand-alone steam cycle was modeled firstly and then the remaining parts were added one by one. While Figure 2.1 displays a schematic representation of the process including the main parts of the WtE plant, Figure 3.2, 3.3 and 3.4 show more detailed views of each part and how they were modeled in Ebsilon. Figure 3.2 represents the steam cycle while the DH system, as well as the hot water cycle, are shown in Figure 3.3. Lastly, the flue gas cleaning systems are shown in Figure 3.4. Note that these figures are cleaned versions of the original Ebsilon model. Figures showing the original model as well as a complete list of the components used in the WtE model are found in Appendix A.

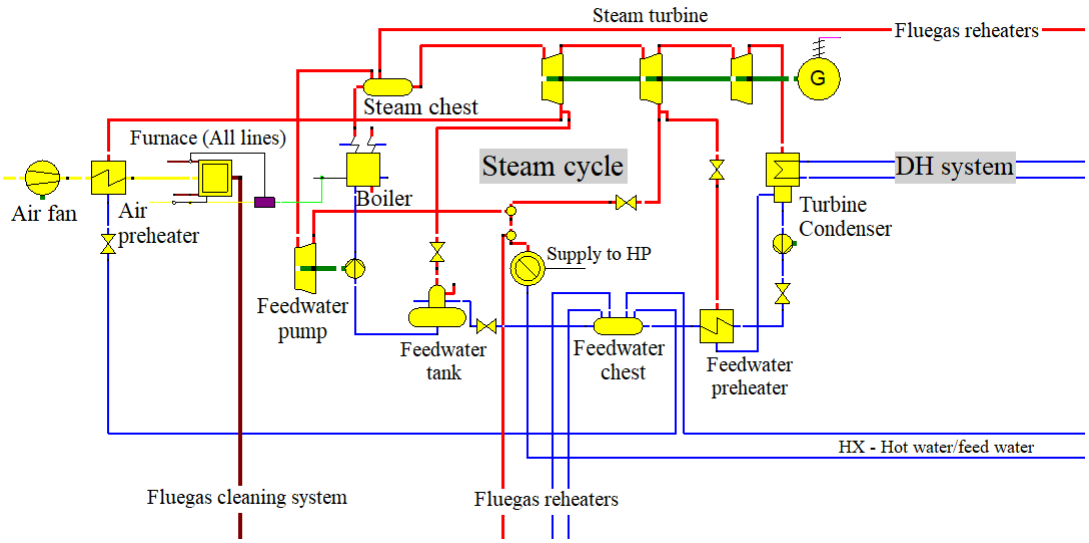

Figure 3.2: The steam cycle from the model in Ebsilon.

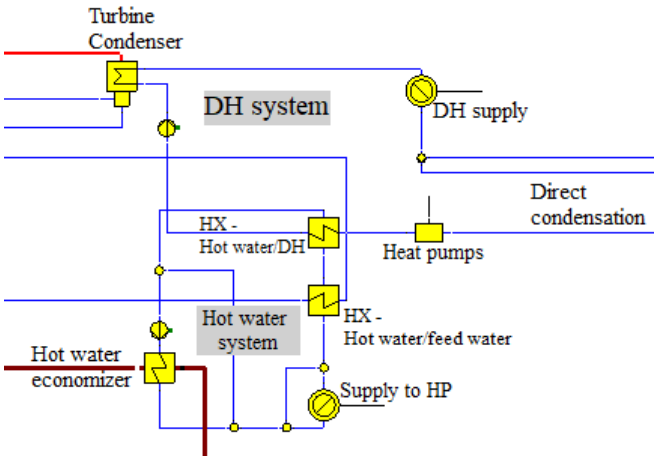

Figure 3.3: The DH system and hot water cycle from the model in Ebsilon.

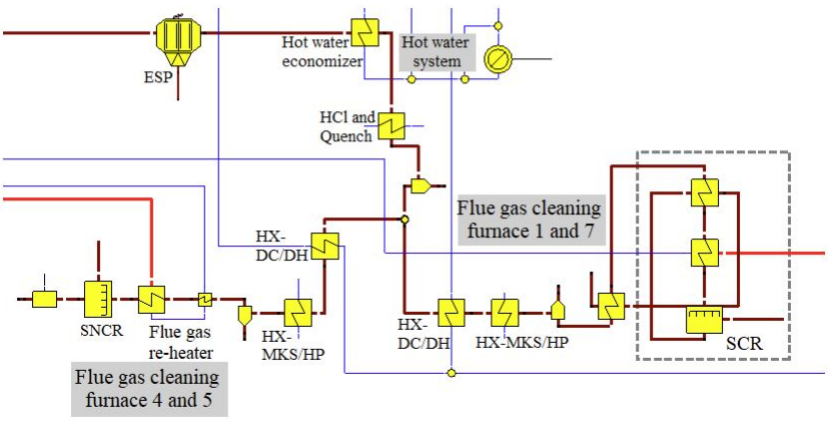

Figure 3.4: The flue gas cleaning systems from the model in Ebsilon.

Multiple design specifications from the collected data were implemented in different parts of the model such as temperatures, pressures and mass flows. As mentioned, all data were collected on the 6th of November at 1:42 pm. Therefore, it is important to note that the model is instantaneous, representing one specific point in time, while the real operation at the WtE plant is transient. Most of data collected at the site were implemented in the model by using "General input values", but some were also set with the use of "Controllers". Some important model specifications are presented in Table 3.1 while the remaining parameters can be seen in Table A.3 in Appendix A. The composition of waste was assumed to be the same as the waste treated at Lillesjöverket in Uddevalla, due to lack of data on this subject. This composition can be seen in Table A.2 found in Appendix A.

Table 3.1: Important input data for modeling the WtE plant in Ebsilon.

Steam conditions		
HP steam		
Temperature	400	°C
Pressure	40	bar
LP steam		
Temperature	150	°C
Pressure	3.5	bar
DH system		
Delivery temperature	90.2	°C
Return temperature	40.2	°C

Even though the objective of the project is to capture CO_2 solely from line 7, the heat sources and heat sinks of the entire WtE plant are available for satisfying the demands of the capture plant. Therefore, in the model, all four furnaces were simulated as one, implying that the total amount of flue gas in the WtE plant was fed in one stream to the cleaning system. Since there is a clear distinction between the cleaning systems of line 7 and 1 compared to line 4 and 5, two separate processes were created and the total flue gas flow was divided into two streams. This was done to account for the integration of the different flue gas cleaning systems in the WtE plant model in terms of steam demand, returned condensate etc.

Another important note to make about the model is that the absorption heat pumps were simulated using different components depending on which load they corresponded to. In other words, if the purpose was to represent the heat delivered to the DH system, also referred to as the sum of the absorber and desorber loads in the absorption heat pump, this was done by the use of a heat injection component. In contrast, the generator loads, meaning the heat sources in the absorption heat pumps, were modeled by the use of a heat consumer component. An additional note is that the heat pumps are dictated by a coefficient of performance (COP), implying that this has to be taken into consideration when evaluating the heat delivered and required for the heat pumps. For instance, the heat extracted from the

LP steam and the hot water system need to be multiplied by the COP to receive the heat delivered to the DH system. However, by the time of data extraction, one of the heat pumps in the hot water system was out of operation. This implied that the heat lift was not achieved and its function was rather similar to the function of a heat exchanger. In the model, this was accounted for by solely multiplying the heat extraction with the COP for one of the heat pumps in the hot water system.

The main parameters used to validate the model of the plant were the generation of electricity, delivered DH, total steam production and total heat pump load. The aim was that the model would manage to generate values of these parameters as close as possible to the corresponding values generated from the real plant at the specific time of input data generation.

3.3 Modeling of the DHPC capture process

The methodology of designing and modeling the DHPC capture process consisted of several steps which are described in the following section. Firstly, the modeling tool is introduced and the capture model design, as done in previous research, is described. Thereafter, alternative designs of the regeneration reactor are presented which later are used to establish several system cases. The parameter study, aiming to set the process variables in the capture designs, is also explained.

3.3.1 Modeling tool

The capture process was modeled using Aspen Plus® which is a software for chemical processes [40]. It can perform integrated process modeling taking into consideration for instance economics, energy and sustainability performance. In addition, the software includes a wide range of templates for chemical processes such as carbon capture which validates its usage for this project [40].

3.3.2 Capture process design

Based on the design of the DHPC process found in previous research and pilot plants, the model in Figure 3.5 was derived using Aspen Plus. In the initial stage of the simulation, several decisions were made. Among these, the property method was defined. In this simulation, Reidlich-Kwong-Soave equation of state with Boston-Mathias modification (RKS-BM) was used since it is suitable for gas processing applications [41]. In addition, the relevant chemical components of the process were added in to Aspen Plus, see Appendix B (Section B.1) for a complete list. These include the constituents of the flue gas, K_2CO_3, $KHCO_3$ and the supporting material. The complete flue gas composition is presented in Table 3.2. According to Section 2.2.6, there could be alternative reaction pathways and byproducts associated with the reactions. In particular, $K_2CO_3{\cdot}(1.5H_2O)$ and $KAl(CO_3)(OH)_2$. Consequently, to represent the real process and potential operational issues, these components were favorable to add into Aspen Plus as well. However, solely $K_2CO_3{\cdot}(1.5H_2O)$ could

be found in the data bank. Therefore, $KAl(CO_3)(OH)_2$ was excluded from the simulation. Besides these species, no other potential side reactions and corresponding products, such as reactions between impurities in the flue gas and the sorbent, were added into Aspen Plus. A summary of the general key simulation settings are listed in Appendix B (Section B.1).

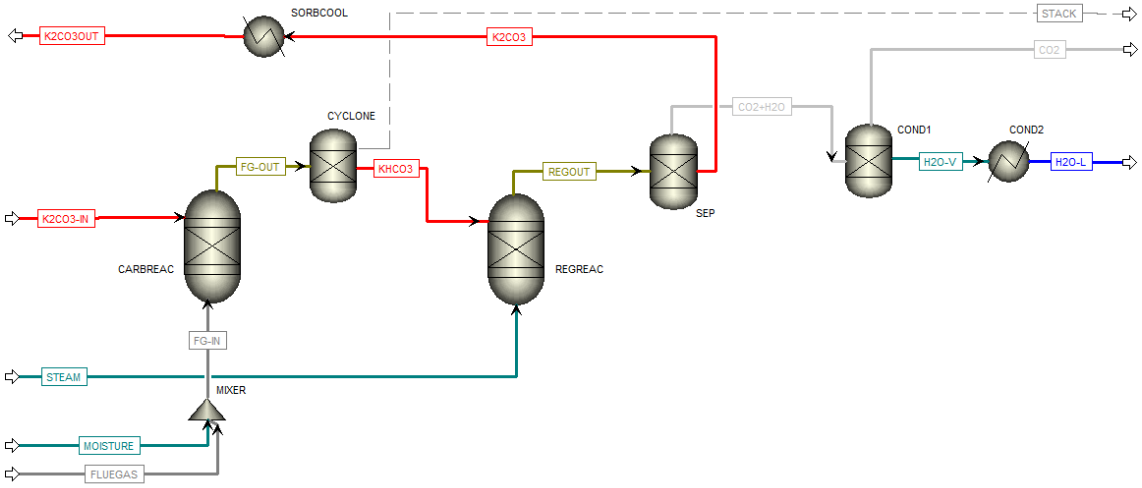

Figure 3.5: Aspen model of the DHPC capture process based on the design found in previous research and pilot plants.

As described in the theory section, see Section 2.2, the main components of the DHPC process are the two fluidized bed reactors, the cyclone and the sorbent cooler. The fundamental reactions of the DHPC process, reaction 1 and 2, and the corresponding reactors were simulated using Gibbs reactors (named CARBREAC and REGREAC in Figure 3.5). The principle of the Gibbs reactor is to calculate the equilibrium by minimizing Gibbs free energy [42]. In literature, both one-stage and two-stage carbonation reactors have been proposed. However, in the model, the carbonation reactor will solely consist of one reactor. To simulate the carbonation reaction, two streams, one containing the flue gas with known composition and flow rate and one with the sorbent K_2CO_3 supported by alumina, were fed to the reactor. A moisture stream was added and mixed with the flue gas to make sure that water was not a limiting reactant in the carbonation reaction. The size of this stream was set to obtain a maximum capture rate which will be discussed further in the results section. As the reaction is exothermic, cooling of the reactor is required in a real plant. However, in the model, the cooling was not included. Therefore, the heat produced, representing the required cooling duty of the reactor, was registered solely as the reactor duty.

Since the flue gas cleaning system of the WtE plant reduces the temperature of the flue gas, its inlet temperature into the mixer was approximately 43°C. The flow rate and composition of the flue gas entering the capture process were also known parameters. As proposed previously (see Section 2.2.3), the suggested temperature range for the carbonation reaction is 50-100°C. All these parameters, along with

other key inputs are summarized in Table 3.2.

Table 3.2: Key parameters for the simulation of the carbonation reactor.

Flue gas conditions		
Flue gas inlet temperature	43	°C
Flue gas flow	22.3	kg/s
Composition		
H_2O	4.5	mole%
HCl	1.0e-5	mole%
CO_2	12.3	mole%
CO	1.7e-3	mole%
O_2	5.7	mole%
SO_2	3.0e-5	mole%
N_2	77.5	mole%
NH_3	5.3e-5	mole%
NOx	1.4e-3	mole%
Reactor conditions		
Reactor temperature range	50-100	°C
Reactor pressure	1	bar
Sorbent conditions		
Composition		
K_2CO_3	35	mass%
Al_2O_3	65	mass%

According to reaction 1, water and CO_2 in the flue gas react and form $KHCO_3$. Since the carbonation reactor is a fast fluidized bed in reality and the product stream is mixed, the solid particles need to be separated from the gas stream. This is normally done using a cyclone, but for this model, the separation was carried out using a standard separator (CYCLONE in Figure 3.5). The gas stream was then sent to the stack while the solid stream was fed to the regeneration reactor.

As the regeneration reaction is endothermic, heat is necessary to enable reaction. This is normally provided by the fluidizing agent such as steam or hot air. Since air would require more complicated separation, as mentioned in Section 2.2.4, a stream of steam was fed to the reactor. The steam was extracted either directly from the steam chest or from the LP steam extraction point, depending on the desired conditions. The steam conditions were the ones already available at the plant, seen in Table 3.1. The given reactor temperature interval for the regeneration reaction is 150-200°C according to theory, see Section 2.2.4. However, to capture the behaviour of the reactions at lower temperatures as well, the evaluated temperature interval was extended to 100-200 °C.

In the regeneration reactor, CO_2 is released from the sorbent which in turn is regenerated back to K_2CO_3. In addition, water vapor is also formed. Consequently, a separator (SEP in Figure 3.5) was required to separate the product stream. Ev-

idently, from the separator there were two outlet streams, one in gas phase which contained CO_2 and water vapor as well as one in solid phase. To obtain a pure stream of CO_2, two components were added, one separator to separate the species as well as one cooler to condense the water vapor (COND1 and COND2 in Figure 3.5). In order to reduce the temperature of the solid stream before being led back to the carbonation reactor, a sorbent cooler was implemented which was simulated by a simple cooler extracting heat.

3.3.3 Alternative designs of regeneration reactor

The DHPC capture process design described in the previous section was constructed to mimic the setup used in previous pilot plant studies. However, in this project, alternative ways to design the process in order to decrease the demand of steam, were found. More precisely, the regeneration reactor could be redesigned while the carbonation rector was kept at its initial conditions. Two novel designs of the regeneration reactor are described below.

3.3.3.1 Preheated CO_2 as fluidization gas

As mentioned in Section 2.2.4, previous studies have evaluated CO_2 as fluidization gas in the regeneration reactor. An alternative design could therefore be to change the gas for fluidization from steam to CO_2. However, as the steam also provides heat to the reaction, the CO_2 would have to be preheated in order to serve the same purpose. Consequently a new design of the regeneration reactor system was created in Aspen Plus, which can be seen in Figure 3.6. As is evident, the reactor is still a Gibbs reactor. The main change lies in the fluidization gas feed.

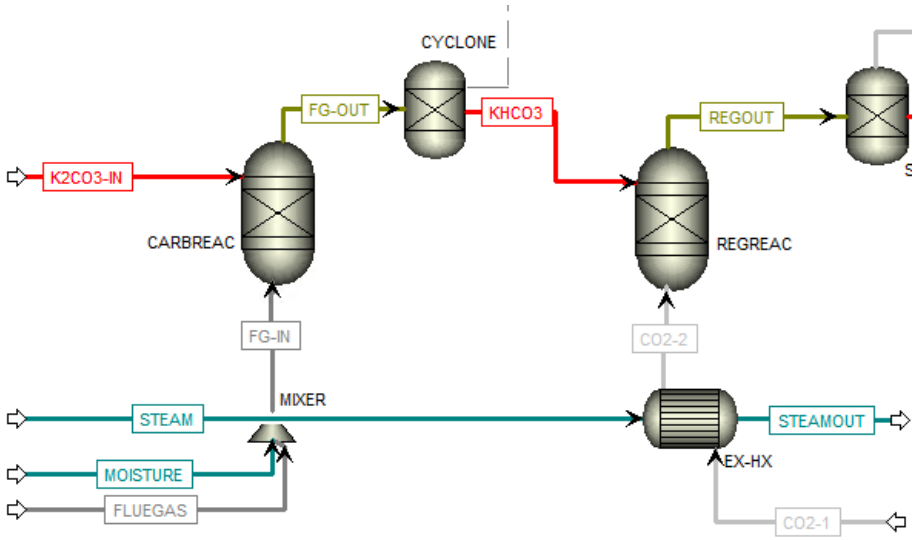

Figure 3.6: Aspen model of the DHPC capture process using the same regeneration reactor as in the initial design but with preheated CO_2 as fluidization gas.

In this design, a stream of CO_2 was preheated and fed to the regeneration reactor, before it was recirculated back in a closed loop. In other words, the product

stream will only partly consist of the CO_2 actually captured in the process. The outlet stream of the reactor was split to two separate streams of different size, one considered as the captured CO_2 and the other recirculated to the preheater. In the preheater, the CO_2 stream was heated by the use of primary HP steam or LP steam from the WtE plant. This component was modeled with the use of a shell and tube heat exchanger, see Table 3.3 for details, and allowed the steam to condense, making use of a large fraction of the heat content. As the steam undergoes a phase change, it was allocated to the shell side.

Table 3.3: Specifications of the shell and tube heat exchanger for the Preheated CO_2 case.

Shell and tube heat exchanger	
Flow direction	Countercurrent
Steam	Shell side
CO_2	Tube side
Minimum temperature approach	10°C

3.3.3.2 Fluidized Bed Heat Exchanger, FBHE

In contrast to the direct heating of CO_2 before being led to the reactor, as proposed above, the steam could instead be used as a indirect heating medium in the regeneration reactor by the use of a fluidized bed heat exchanger, FBHE. As described in Section 2.2.5, the principle of the FBHE is to recover heat from solid particles by heat exchanging with a medium flowing in tubes. For the application in the DHPC process, the principle would be reversed. Instead, it would imply installing tubes inside the fluidized bed. In the tubes, the primary steam could condense which would provide heat to the reaction while fluidization occurs in the bed by the use of recirculated CO_2. A graphical representation of the FBHE reactor is shown in Figure 3.7.

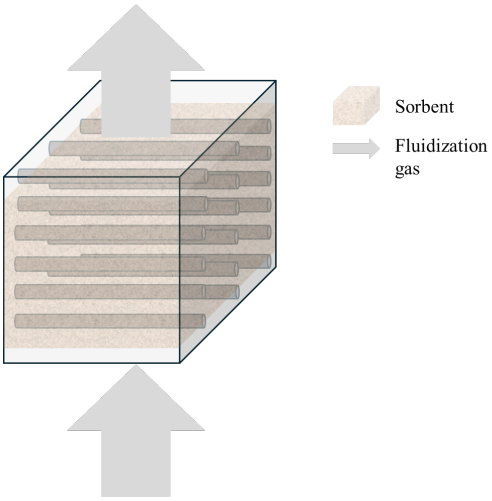

Figure 3.7: A graphical representation of the FBHE reactor showing the distribution of tubes in the reactor body as well as the inlet of the fluidization gas and the bed material.

In Aspen Plus, the FBHE reactor was modeled using the same Gibbs reactor as previously, but with an additional external cooler which condensed the steam and transferred the heat to the reactor. The outlet temperature of the steam was set according to a minimum temperature difference approach of 10°C in relation to the reactor temperature. As mentioned, the fluidization gas entering the reactor was split off from the pure CO_2 product stream and circulated in a closed loop within the system. This implies that the stream of CO_2 entering the preheater will be at reactor temperature. An image of this system design from Aspen Plus can be found in Figure 3.8.

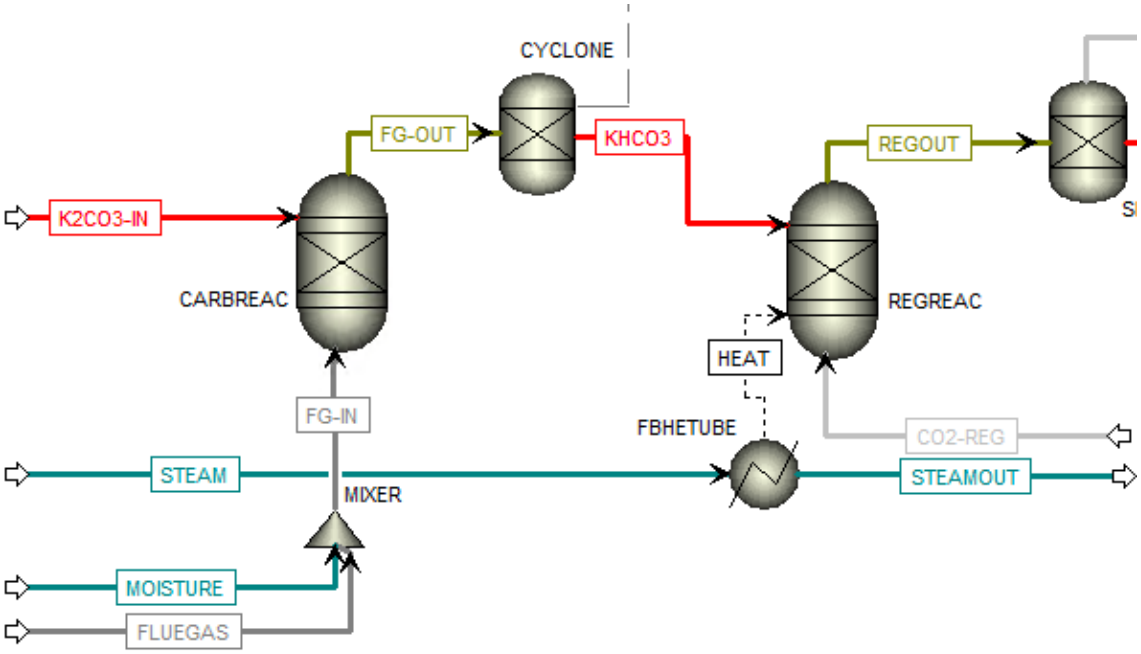

Figure 3.8: Aspen model of the DHPC capture process using the FBHE as the regeneration reactor. The cooler represents the internal tubes supplying the reactor with heat. The fluidization gas is CO_2.

As this design will not require fluidization gas to heat the reactor, it will only be required to drive the reaction and to fluidize the bed. Therefore, the mass flow of CO_2 fluidizing the reactor bed will be calculated through the estimated superficial velocity and cross sectional area of the reactor. These calculations will be explained in Section 3.6, where the dimensioning of the reactors are described in detail.

3.3.4 Parameter study

In order to finalize the model of the DHPC process, the critical parameters in each reactor had to be determined. This was done through strategic sensitivity analysis of each parameter having significant effect on the performance of the two reactors. The temperature in both reactors were analysed as well as the flow of solid sorbent in the carbonation reactor and the flow of gas for fluidization in the regeneration reactor.

3.3.4.1 Carbonation reactor

The reactor temperature was varied from 50 to 100°C, with a 10°C interval, and for each temperature, the sorbent (only K_2CO_3) and moisture flows were varied from 8 to 15 kg/s and 100 to 500 kmol/hr respectively. For each combination, the mole percentage of reacted CO_2 was registered which was defined as the mole flow of reacted CO_2 divided by the inlet amount of the species. In addition, for the combination of reactor temperature, moisture and sorbent flow where the reacted amount of CO_2 was the most, the percentage excess of K_2CO_3 and the respective product split of $K_2CO_3 \cdot (1.5H_2O)$ and $KHCO_3$ were noted. In this context, the product split was defined as the amount of the relevant species divided by the total reacted amount of K_2CO_3 in the carbonation reactor.

3.3.4.2 Regeneration reactor

The reactor temperature was varied between 100 and 200°C, with a 10°C interval, and for all temperatures, the flow of fluidization gas was varied in a suitable range. For each temperature and fluidization gas flow combination, the conversion of $KHCO_3$ and the heat duty of the reactor were noted. In this context, the conversion was defined as the reacted amount of $KHCO_2$ divided by the inlet amount. The analysis procedure was done with small alterations depending on the design of the studied situation.

For the cases where LP steam, HP steam and preheated CO_2 were used as fluidization gas, the mass flow of each gas was analyzed to find the flow that could satisfy the heat duty of the reactor. However, for the case with preheated CO_2 as fluidization gas, the mass flow was also strictly dependent on the achieved temperature of the gas. As previously described, this case was modeled by adding an external heat exchanger to the process, transferring heat from the condensing steam to the fluidizing stream of CO_2. The amount of steam condensed in this heat exchanger was set so that the exchanged heat was equal to the heat required by the reactor. Assuming a minimum temperature difference of 10°C and an outlet temperature of the condensate at 140°C in this heat exchanger, the temperature and mass flow of the CO_2 fed to the reactor were determined by successively increasing the flow until the reactor heat demand was fulfilled without violating the minimum temperature difference.

For the cases using a FBHE regeneration reactor, the important parameters could be determined through a more straight forward approach. In this case, the only purpose of the fluidization gas was to fluidize the bed and not to act as a heating medium. As explained before, the heat required in the reactor is transferred from condensing steam within heat exchanger tubes simulated through an external cooler. The mass flow of steam required to satisfy the heat demand was determined by setting the condensate outlet temperature to 140°C and evaluating which mass flow of steam would be required to supply enough latent heat to fulfill the reactor heat demand. The mass flow of CO_2 fluidizing the bed was calculated according to Section 3.6.

3.3.5 Case construction

To facilitate the analysis of the different modifications of the DHPC process further on in the report, three design cases were established based on the options for the regeneration reactor. The design of the carbonation reactor remained the same in all cases. In Table 3.4, they are presented together with their respective characteristics.

Table 3.4: Summary of the key parameters for the different DHPC cases. Note that the fluidization gas and heat source are relating to the regeneration reactor.

	Steam case	**Preheated CO_2 case**	**FBHE case**
Fluidization gas	Steam	Recirculated and preheated CO_2	Recirculated CO_2
Heat source	Provided by the fluidizing steam	External shell and tube heat exchanger (CO_2 or steam)	Internal tubes containing steam in reactor

As previously discussed and as evident in the table, the cases differ mainly in terms of the fluidization gas. The cases "Preheated CO_2" and "FBHE" also contain some kind of heat exchange, which was done with the objective to decrease the steam demand. In all three cases, steam will be required for heating. Steam of both conditions, LP and HP, will be used in each case, resulting in six cases in total.

For all six DHPC cases, the total degree of regeneration of sorbent was calculated. In this context, the definition was the percentage of the inlet mass flow of K_2CO_3 in the carbonator obtained after the regeneration reactor and consequently recirculated.

3.4 Application and heat integration of the DHPC process at the WtE plant

In general, CCS technologies imply a large energy penalty, either in the form of heat, which is evident in Table 3.4, or electricity [11]. Previous studies have shown that utilizing excess heat from industrial plants reduces the specific cost of carbon capture and enables an increased energy efficiency [43, 44]. Therefore, evaluating the possible extent of heat integration between the site and the capture plant is an important feature of a feasibility assessment of CCS.

In previous sections of this chapter, the methodology for constructing models of the two separate systems, Renova's WtE plant and the DHPC capture process, have been demonstrated. A big part of the project scope was to investigate the interconnection of these two systems and what impacts the application of the DHPC

process would have on the outputs from the WtE plant. The first step of applying the DHPC process was to extract steam from the plant, which will be described in the upcoming section. To make the inclusion of the DHPC process more feasible for Renova, this methodology will also contain the computation of a pinch analysis and retrofit of the WtE plant with the aim to integrate as much heat as possible.

3.4.1 Steam extraction

To simulate the implementation of the DHPC process to the WtE plant, the steam demand of the process was extracted from a suitable location in the Ebsilon model. This formed a reference case for further integration of heat, representing a situation where the capture process was applied to the plant but no further heat recovery was considered. Since this means that a part of the energy in the system would go to the DHPC process instead of being used for electricity and DH production, the plant would become less efficient after the extraction had been made. To make the integration of the capture process more realistic, and possibly more profitable for Renova, measures had to be made to recover and take advantage of as much heat as possible. These actions will be further explained in the Section 3.4.2 below.

The location of the steam extraction depended on whether HP or LP steam was required which can be seen in Figure 3.9. For the HP steam, also known as primary steam, the extraction was placed before the turbine. More specifically, steam was taken out directly from the steam chest. In contrast, the LP steam, is allowed to expand in the turbine before being extracted in the LP pressure discharge.

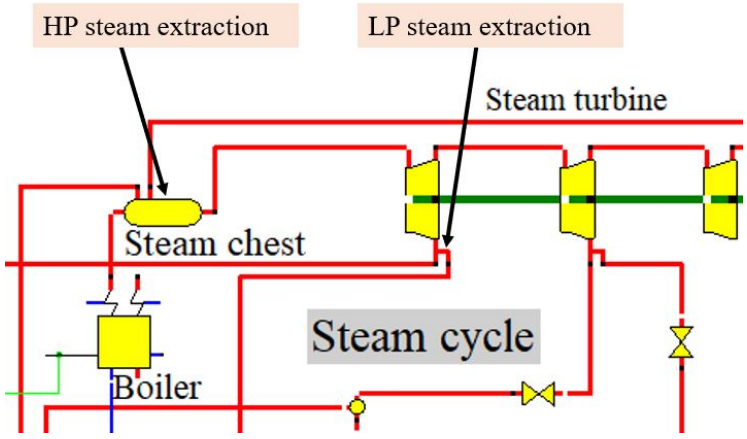

Figure 3.9: The locations for the steam extraction in the Ebsilon model for HP and LP steam, respectively.

The steam extracted to fluidize reactors and supply heat to the DHPC process had to be returned to the WtE plant to assure the consistency of the water balance. The condensate was returned to the feedwater chest directly in the cases where this was possible, without disturbing the energy balance in the proceeding feedwater tank. The motivation behind this was to avoid a potential cooling duty for the hot streams as well as decrease the steam demand for pressure and temperature regulation in

the succeeding feedwater tank.

In other cases where the energy balance was violated when returning the condensate directly, the condensate stream was cooled further before being brought back to the system in the feedwater tank. The cooling duty of this stream could therefore be seen as a heat source in these cases and as a result, it was included in the pinch analysis.

3.4.2 Pinch analysis

To get an idea of how large the heat recovery could be at most, a pinch analysis was made as the first step towards retrofitting the design. The method of pinch analysis seeks to optimize the energy usage of plants. It can be applied in system design planning, but also as a tool for identifying potential retrofits to existing plants [45].

An important part of a pinch analysis is the identification of hot and cold streams available for heat integration. A hot stream is defined as a stream that requires cooling in order to reach its target temperature. In contrast to a cold stream that is defined as a stream that requires heating to reach its corresponding target temperature [46].

The overall methodology for a pinch analysis follows the pattern: identification of hot and cold streams, creation of hot and cold composite curves and finally the combined composite curve, in which the minimum heat and cooling demand as well as the maximum heat recovery are established.

3.4.2.1 Identification of streams

The initial step of the pinch analysis was to identify the streams suitable to be included in the analysis. In the capture process, there are several cooling demands associated with the main equipment. These include the carbonation reactor, sorbent cooler and the water condenser separating CO_2 and H_2O. All these cooling demands were included in the pinch analysis and they are presented in Table 3.5 under the title "Hot streams".

At the WtE plant, there are also several components in need of heating. In a lot of cases, the primary source of heat in the equipment is steam. Components using steam as heating medium in the WtE plant are the air preheater, feedwater preheater, flue gas reheater and the SCR reheater. Replacing the steam demand with integrated heat from the hot streams presented above could result in decreasing the impact of the steam extraction discussed in Section 3.4.1. The equipment were therefore seen as heat sinks and included in the analysis as cold streams. Moreover, as the DH system is an important provider of residential heating and could be considered a heat sink, it was also included as a cold stream in the pinch analysis. All the cold streams are presented in Table 3.5 under the title "Cold streams".

Table 3.5: List of the streams included in the pinch analysis.

Hot streams	
Name	*Location*
H1	Carbonation reactor load
H2	Sorbent cooler load
H3	Water condenser (H_2O/CO_2)
Cold streams	
Name	*Location*
C1	Air preheater
C2	feedwater preheater
C3	Flue gas reheater
C4	SCR reheater
C5	DH system

For each identified stream in Table 3.5, the start and end temperatures were noted as well as the cooling/heating demand of the stream. Using the extracted information from each stream, the CP-value could be calculated. The CP-value is defined as the change in enthalpy per unit of temperature change. All thermodynamic data were generated from the final models in Aspen Plus and Ebsilon.

3.4.2.2 Composite Curves

When the stream data was collected, hot and cold composite curves were constructed for each case and analysed, in order to identify the possible amount of recovered heat as well as the minimum heating and cooling demands of the system. Both the hot and cold composite curves were created using the same methodology, the only difference being which streams that were considered.

At first, the streams were sorted according to the temperature intervals they covered. For each temperature interval, the heat duty was calculated by summarizing the CP-values of the streams included and multiply it with the respective interval temperature difference. These heat duties were summed up, starting from the lowest temperature range to achieve the cumulative heat duty. Thereafter, the cumulative heat duties were plotted against the temperature intervals, resulting in the composite curve.

The hot and cold composite curves were then combined in the same graph. Considering a minimum temperature difference of 10 K, the cold composite curve was adjusted to avoid pinch point violations. Finally, the minimum heating and cooling demands could be established as well as the maximum heat recovery potential of the system.

3.4.3 Retrofit of the WtE plant

From the pinch analysis described above, the heat recovery potential for the different DHPC cases was found. This gave an idea of what could be achieved by retrofitting the utility system. However, since there are multiple integration possibilities and ways of performing the retrofit, a systemic strategy for decision making and prioritization was needed. First of all, several overriding retrofit rules were established. These included a minimum recovery size at 1 MW for the retrofit measures and a generic minimum temperature difference at 10 K.

When performing the retrofit, two different operational modes, in terms of the heat pump loads, were investigated for each DHPC case. Please note that the WtE plant is still operating at full capacity. The first approach was to inject as much heat as possible, while keeping the heat pumps working at full load. The second approach was to decrease the heat pump load partly or to a minimum, and inject as much as possible of the available heat without violating any energy balances. The definition of part load in this context, was decreasing the heat pump load with the same amount as the retrofit integrated before the heat pump, thus replacing a part of its load. The definition of the minimum load of the heat pump is the total load generated from condensing the steam from the feedwater pump turbine and the hot water system. In other words, no LP steam is extracted from the steam turbine directly to supply it.

3.4.3.1 Rules of prioritization for cold streams

The main objective of the heat integration was to make use of the excess heat in the hot streams, possessing a load exceeding 1 MW, of Table 3.5. Therefore, in order to decide upon which cold streams (see Table 3.5) should be targeted, and in which order, a set of prioritization rules were implemented. As described in previous sections, the regeneration reactor requires steam as a heat source. Even though the application and demand of the steam differs among the regeneration reactor cases, the capture process will require an extraction of steam from the WtE plant in all of them. Consequently, the electricity and district heating generation of the WtE plant will be affected as the steam is the main energy carrier in the system. To make up for the potential reduction on the plant outputs when implementing the capture process, the main priority of the heat integration was to decrease the steam demand in existing equipment. In other words, replacing the heat load provided by steam partially or fully with excess heat from the capture plant.

The secondary priority in the retrofit strategy was to integrate excess heat into the district heating system. This was done to reduce the losses of delivered heat and potentially even increase the delivery compared to the WtE plant before the implementation of the DHPC process. There were a couple of available locations for integration with this purpose in the DH system. The position considered the most suitable for integration of heat, depended on the temperature level. The order of prioritization as well as the corresponding available locations are summarized in Table 3.6.

Table 3.6: Order of prioritization for cold streams.

Prioritization order for cold streams		
Order	**Action**	**Location**
1.	Decrease steam demand in existing equipment	Air preheater, Feedwater preheater, Flue gas reheater, SCR reheater
2.	Integrate heat into the DH system	Before heat pumps, after turbine condenser.

3.4.3.2 Stream matching

Following the strategy described in the previous section resulted in an order of prioritization of the cold streams. It was then of interest to find a matching hot stream. Firstly, the duty of the cold stream was compared to the loads of the hot streams. In order to utilize the maximum potential excess heat, it was desirable to match the hot streams with cold streams capable of extracting the entire heat load as this would minimize the number of new installations of heat exchangers. Secondly, the temperature level of the hot stream needed to exceed the cold stream, preferably allowing heat exchange along the whole temperature range. If all requirements were fulfilled, the heat integration was feasible. If not, the next cold stream in the prioritization order (Table 3.6) was evaluated, matched with a suitable hot stream and so on. This was done until all adequate hot streams were integrated. The remaining heat in hot streams that could not be matched to any of the cold streams, due to temperature levels or the load being too small, was considered requiring cooling and thereby seen as a cooling demand in process.

3.5 Energy performance evaluation

To evaluate the performance of a combined heat and power plant, CHP, plant, the total energy efficiency, η_{tot}, is a useful parameter. The η_{tot} of a CHP plant describes the share of the fuel energy input that is converted into useful heat and electricity [47]. The parameter is defined in Equation 3.1, where P is the net electrical power output, Q is the useful heat delivery, m_{fuel} is the mass flow of fuel and LHV is the lower heating value [47].

$$\eta_{tot} = \frac{P + Q}{m_{fuel} * LHV} \tag{3.1}$$

Equation 3.1 was applied to the WtE plant with and without including the DHPC carbon capture process. However, it is important to note that total energy efficiency utilizes the net electricity production. Consequently, it accounts for internal usage of electricity at the WtE plant, by for instance the operation of pumps and other electricity consuming equipment. However, this was not included in the WtE model created in Ebsilon and thereby, the electricity output needed to be adjusted

to obtain the net generation. Based on the data collected at Renova, this internal usage was 8.2 MW at the time of data extraction. Another note to make about equation 3.1 is that, in this context, the useful heat corresponds to the delivered district heating. When evaluating the retrofit of the WtE plant with the carbon capture applied, this meant that the effect of the measures, in terms of heat, were accounted for by reporting the amount of delivered DH.

When the η_{tot} was calculated for the WtE plant both with and without carbon capture, the results were used to compute a loss in energy efficiency [48]. The efficiency loss is defined in equation 3.2, where η_{WtE} is the total energy efficiency for the plant without carbon capture and η_{WtECC} is the corresponding value including a carbon capture process [48].

$$\eta_{loss} = \eta_{WtE} - \eta_{WtECC} \tag{3.2}$$

To investigate the potential losses in electricity production and DH delivery specifically, the energy penalty for both of these were also calculated [48]. The energy penalty relates the produced electricity or district heating from a plant without carbon capture to the corresponding value when a carbon capture process has been applied [48]. The definition of the energy penalty in electricity, EP_{El}, is shown in equation 3.3 and in equation 3.4 for DH delivery, EP_{DH}. Using the same indices as in the previous equation, P_{WtE} and P_{WtECC} relate to the net electricity production without and with carbon capture respectively. Similarly, Q_{WtE} is the useful heat delivery without carbon capture and Q_{WtECC} represents the case with the DHPC process integrated.

$$EP_{El} = 100 * \frac{P_{WtE} - P_{WtECC}}{P_{WtE}} \tag{3.3}$$

$$EP_{DH} = 100 * \frac{Q_{WtE} - Q_{WtECC}}{Q_{WtE}} \tag{3.4}$$

For a CCS process, another important performance indicator is the capture rate of CO_2. In this context, the capture rate is defined as the mass flow of the CO_2 captured in the process divided by the inlet mass flow of CO_2 in the flue gas.

3.6 Size dimensioning

To evaluate the feasibility of the DHPC process in terms of physical footprint and to enable cost evaluation of the equipment required, the dimensions of the reactors were estimated. The sizes of other process equipment were approximated in conjunction with the economic calculations and can be seen in Appendix D. Alongside the calculations of the reactor dimensions, the pressure drop in each reactor was calculated using equation C.4 found in Appendix C.

3.6.1 Carbonation reactor dimensions

To dimension the carbonation reactor used in all cases, the first action was to calculate the cross section area. This was done using the flue gas flow entering the reactor and an assumed fluidization velocity of 3 m/s. Using the results from previous research and pilot plants of the DHPC process [20], a residence time within the carbonation reactor at pilot scale could be calculated. A central point in the size calculations was to assume the same residence time in the full scale reactor. This assumption entailed that the height of the reactor could be established by multiplying the residence time with the superficial velocity within the reactor.

3.6.2 Dimensions of Steam HP regeneration reactor

In the Steam HP regeneration reactor, the flow of steam to fluidize the bed was already determined in the parameter study. Similarly as for the carbonation reactor, the cross section area was calculated through the use of volume flow of steam fluidizing the bed and an assumed superficial velocity of 0.5 m/s. The height of the Steam HP reactor was calculated in the same way as described for the carbonation reactor, using the superficial velocity while assuming the same residence time as in the pilot scaled plant. However, there were two equally sized regeneration reactors used at the pilot plant. Consequently, the residence time considered when designing the Steam HP case reactor was a sum of the two. Another assumption made was that the mass of the reactor bed was the same as the bed mass of the FBHE HP reactor, explained in the next Section, resulting in a reactor bed height and a pressure drop over the reactor bed.

3.6.3 Dimensions of FBHE HP/LP regeneration reactor

In contrast to the calculations described for the Steam HP regeneration reactor, in the FBHE cases, the flow of CO_2 fluidizing the reactor bed was not known in advance. Therefore, these size calculations were done in a different way. The method included estimating the total heat transfer area by the use of correlations for the Nusselt number, estimating specifications for the internal tubes of the FBHE reactor to obtain the cross section area of the reactor and finally, using the cross section area and a calculated pressure drop to evaluate the mass of bed material in the reactor. The procedure is based on a method used to dimension a fluidized bed reactor used for chemical looping combustion applications [49] and is described in detail in Appendix C.

3.7 Economic analysis

A common way of evaluating the economics of a carbon capture application at an industrial plant, is by evaluating the capture cost in the unit of EUR/tCO_2. The metric includes the annualized capital, CAPEX, and operational expenditures,

OPEX, as well as the annual captured amount of CO_2. This amount was obtained by multiplying the captured mass flow of CO_2 in the DHPC process with the assumed operational hours of 8000 hr/yr. In order to predict the capture cost as accurately as possible, the investment costs should preferably be estimated by the intended vendor. However, as this investigation can be time consuming, cost functions are often used in research to predict investment costs despite the uncertainty they are associated with [50].

In this project, the capture cost was selected as a relevant economical parameter and the definition used, equation 3.5, was inspired by the definition in literature [50]. However, the main objective with the capture cost calculations was not to study its absolute value, but to compare the capture cost between the studied cases. In other words, a lot of assumptions has been made in the calculations using equation 3.5 and the numerical value obtained from the equation may not be representative to the actual capture cost.

$$Capture\ cost \quad (\frac{EUR}{tCO_2}) = \frac{Annualized\ CAPEX + Yearly\ OPEX \quad (\frac{EUR}{yr})}{Annual\ captured\ CO_2 \quad (\frac{tCO_2}{yr})} \tag{3.5}$$

In the annualized CAPEX term, the equipment investment costs from the capture plant as well as the heat integration were included. Mainly, these were approximated using direct cost functions from literature [51]. However, the CAPEX related to the fluidized bed reactors, for which there are limited financial information, were estimated by scaling down an investment presented in research [52]. The paper is studying, among other carbon capture technologies, a calcium carbonate looping process which have similarities with the DHPC process in terms of the solid transport from a CFB reactor. The scaling was performed based on the reactor volume. In other words, the volumes of the carbonation and regeneration reactors were compared to the reactor volume in the literature by calculating a scaling factor which was used to compute the investment costs. The annualization factor was calculated assuming 25 years of plant lifetime (23 years operational years) and an interest rate of 7.5% [50].

The yearly OPEX term consisted of fixed and variable expenditures. The fixed OPEX included an annual maintenance cost of 4% of the total equipment cost and a yearly labour cost corresponding to the salaries of six operators and one engineer [50]. Assuming that the steam demand of the DHPC carbon capture process is satisfied by the steam production of the WtE plant, there were few variable OPEX associated with the system. However, the potential reduction or increase in electricity and DH generation when applying the DHPC process were accounted for in the variable OPEX, as they represent loss or gain of revenue. The definition can be seen in equation 3.6.

$$VariableOPEX = \frac{X_{WtECC}}{X_{WtE}} * Price(El./DH) * Annualproduction(El./DH) \tag{3.6}$$

Where X represents the momentary production of either electricity or DH. The annual production was found for the year 2022. In equation 3.6, it can be seen

that loss or gain of revenue was calculated by finding a percentage factor of the increase or decrease of the electricity and DH supply after applying the DHPC cases. Thereafter, the factor was multiplied by the annual produced of electricity and DH at Renova in 2022 to estimate the changes in production when DHPC had been applied. From this, the changes in the revenues from the generation of electricity and DH were found by assuming a price of electricity of 700 SEK/MWh and 200 SEK/MWh for DH [17]. This combination of prices will represent the base scenario. To investigate how the capture cost can change in the future, the prices were varied, creating two additional scenarios to evaluate, see Table 3.7 for a summary of all scenarios.

Table 3.7: Summary of price scenarios applied in the three studied DHPC system cases.

Scenario	Base	Low	High
Electricity price [SEK/MWh]	700	200	1000
DH price [SEK/MWh]	200	200	500

The first scenario, with low electricity price (200 SEK/MWh) and same DH price (200 SEK/MWh), was selected to represent the future when more renewable electricity generation has been deployed and reduced the electricity price (called low price scenario). In the second scenario, both the electricity price and DH price were increased to 1000 SEK/MWh and 500 SEK/MWh respectively (high price scenario), representing a future with more expensive energy production, for instance due to a crisis.

Among the parameters not included in the capture cost, were the first fill cost of the sorbent material in the reactors, the circulating cooling water in the carbonation reactor as well as carbon taxes. In addition, the cost for the cooling utility was not considered. The procedure for estimating the equipment investment costs, a summary of them and assumptions made in the economic calculations can be found in Appendix D.

4
Results

This section provides the results from the procedure described in the methods section above. First of all, the evaluation and performance of the WtE model will be presented. Thereafter, the results from the simulation of the DHPC cases are introduced. The carbonation reactor is included in every case presented in Section 3.3.5 but as a start this reactor will be analyzed separately. All cases are considered as full DHPC process systems including one carbonation reactor and one regeneration reactor. What differs the cases from each other is the different configurations of the regeneration reactor, thus the same carbonation reactor is considered for all cases.

When all key parameters in the carbonation reactor have been established and presented, the analysis of the regeneration reactor conditions will be shown. The results from the parameter study, integration of the DHPC case at the WtE plant and the system evaluation will be presented for each case separately, except for the two FBHE cases which are presented in the same section. The presented cases are then summarized and compared in the last paragraph of the results section.

Some of the cases shown in Section 3.3.5 will not be presented in as much detail as others. The two preheated CO_2 cases and the Steam LP case were shown to be unfeasible due to results collected in the parameter study. Therefore, these are briefly shown in Section 4.5 whilst more details can be found in Appendix E.

One of the main specifications in the regeneration rector was the temperature, which in literature is shown to be between 150 to 200 °C [20, 29]. However, as mentioned in the theory section, 2.2.4, lower temperatures have also been researched and since a lower reactor temperature would lead to a lower heat duty, the analysis of reactor temperature, shown in the sections below, were only carried out for temperatures between 100 and 150 °C. Excluding temperatures above 150 °C was considered fair in all cases since the conversion of $KHCO_3$ was able to reach 100% already at 130 °C.

4.1 Evaluation of WtE plant model

The model of the WtE plant was evaluated in terms of how well key parameters matched the corresponding values at the real plant from the time of data generation. These parameters were the produced electricity, the delivered DH, the total steam production and the achieved total heat pump load. A comparison between the values

generated by the model and the ones generated by the plant can be seen in Table 4.1.

Table 4.1: Comparison between model values and real values of electricity production, DH delivery, total steam production and heat pump load. Additionally, the percentage deviation is also presented in the rightmost column to give insights into how much these values differ numerically.

	Real values	**Model values**	Deviation
Produced electricity [MW]	41.96	42.64	+1.6%
Delivered district heating [MW]	197.69	193.53	-2.1%
Total steam production [kg/s]	71.00	72.13	+1.6%
Total heat pump load [MW]	66.79	65.12	-2.5%

In Table 4.1 it can clearly be seen that all resulting model values are closely comparable to the real values from the plant. More precisely, the modeled values lie in a range with 2.5% margin to the real value at most. The calculated delivered DH and total heat pump load were a little bit underestimated by the model while the two other parameters were overestimated.

4.1.1 Energy performance

The performance of the original WtE plant was evaluated through the total energy efficiency in equation 3.1. Note that, in the equation for the total energy efficiency (equation 3.1), the net electrical output of 34.44 MW is used, resulting in a total energy efficiency, η_{WtE}, of 97.67%.

4.2 Carbonation reactor study

The results from the parameter study of the carbonation reactor and the reactor dimensions are presented in the following section.

4.2.1 Parameter study

The results from analyzing the sorbent mass flow in the carbonation reactor with a reactor temperature of 70°C is shown in Figure 4.1 and the graphs for all other reactor temperatures can be seen in Appendix B (Section B.2). The appearance of these graphs were similar to the one shown in Figure 4.1, viewing a successively increased amount of captured CO_2 as the sorbent flow increased, until reaching a plateau. Note that a reactor temperature of 100°C was excluded, as the capture rate was unacceptably low.

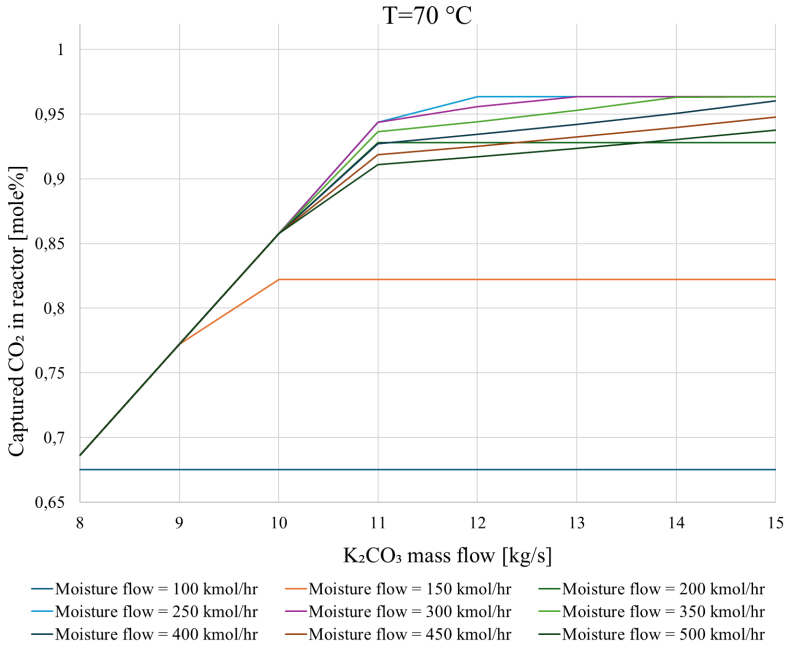

Figure 4.1: Amount of captured CO_2 obtained with a constant reactor temperature of 70°C as a function of sorbent mass flow at different moisture flows.

Two trends were noted when alternating the moisture and sorbent flow for different temperatures. The first one being that for higher reactor temperatures, a larger moisture flow is required in order to obtain amounts of captured CO_2 comparable to the level at lower temperatures, evident from the graphs in Section B.2. The other trend was that as soon as the sorbent flow reached an amount where there was a stoichiometric excess of K_2CO_3 in the reactor, the hydrated version of K_2CO_3 was generated through reaction 3. This pattern can be seen in Figure 4.2. Since the formation of $K_2CO_3{\cdot}(1.5H_2O)$ hinders the absorption of CO_2, it was desirable to minimize it, which was done by limiting the excess of K_2CO_3.

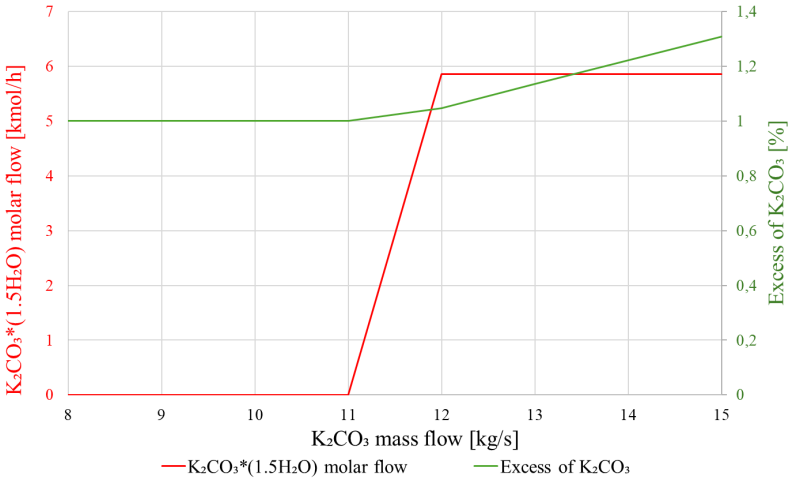

Figure 4.2: Excess of K_2CO_3 and molar flow of $K_2CO_3{\cdot}(1.5H_2O)$ obtained with a constant reactor temperature of 70°C as a function of sorbent mass flow.

The highest absorbed amount of CO_2 was found at different combinations of moisture flow and sorbent flow for each reactor temperature. These combinations for each temperature are shown in Table 4.2.

Table 4.2: Combination of moisture flow and sorbent flow to obtain the maximum amount of captured CO_2 for each reactor temperature.

Reactor temperature [°C]	Captured CO2 in reactor [mole%]	Sorbent flow [kg/s]	Moisture flow [kmol/hr]
50	0.993	13	250
60	0.984	13	250
70	0.963	12	250
80	0.919	11	300
90	0.819	10	400

As seen in Table 4.2, the highest amount of captured CO_2 in the reactor could be obtained when the reactor temperature was 50°C. However, since it was desirable to have a carbonation reactor working at higher temperatures to enable more effective heat integration with the DH system, 50°C was not chosen as reactor temperature for the process. Instead 70°C was chosen and further used in all following Aspen models of the capture process. The molar percentage of captured CO_2 in the reactor was lower in this case than for temperatures below 70°C, but still considered high enough, >95%. Especially considering that the capture rates for MEA lay in the range of 84-95% (see Section 1).

As previously mentioned and shown in Figure 4.2, $K_2CO_3{\cdot}(1.5H_2O)$ was formed to a small extent when running the carbonation reactor simulation. This was also the case when running the simulation with the chosen settings which indicates that the hydrate reaction, reaction 3, occurs at the same time as $KHCO_3$ is formed through the carbonation reaction. The share of K_2CO_3 that reacts to form $K_2CO_3{\cdot}(1.5H_2O)$ instead of $KHCO_3$ can be seen in Table 4.3 together with a summary of key parameters for the reactor. Note that the reactor duty of the carbonation reactor is negative, indicating that heat is delivered from the reactor due to the exothermic reaction.

Table 4.3: Key parameters and performance of the carbonation reactor.

Carbonation reactor		
Reactor temperature	70	°C
Moisture flow	250	kmol/h
K_2CO_3 feed	12	kg/s
Reacted CO_2	0.963	mole%
Excess of K_2CO_3	1.048	mole%
$KHCO_3$ product ratio	0.980	mole%
$K_2CO_3{\cdot}(1.5H_2O)$ product ratio	0.020	mole%
Reactor duty	-11.50	MW
Inlet flow of CO_2 (from flue gas)	3.711	kg/s

4.2.2 Reactor dimensions

Estimating the carbonation reactor dimensions as described in Section 3.6.1 resulted in a reactor cross section area of 7.2 m^2 and a height of 25.6 m.

4.3 Case: Steam HP

As described in Section 3.3.5, the Steam HP case uses primary steam both as fluidizing agent in the reactor bed, and as heating medium in the regeneration reactor. This section gathers the results for this case.

4.3.1 Parameter study

A graph showing the conversion of $KHCO_3$ as a function of steam flow, for different reactor temperatures in the Steam HP case, can be seen in Figure 4.3.

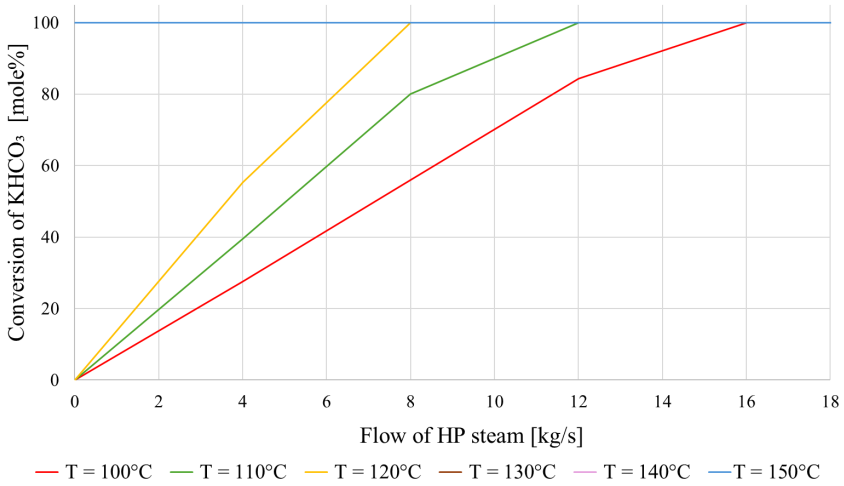

Figure 4.3: Conversion of $KHCO_3$ as a function of the flow of HP steam at different reactor temperatures. Note that the graphs for 130 and 140°C lay behind the 150°C graph.

In Figure 4.3, it is evident that for reactor temperatures at and above 130°C, conversion of $KHCO_3$ reaches 100% whereas for reactor temperatures at or below 120°C, complete conversion was not achievable at lower steam flows. Because of this, reactor temperatures at or below 120°C were not considered reasonable since they would require large flows of steam to convert all $KHCO_3$ in the reactor bed. Although Figure 4.3 gives an idea of which reactor temperatures that may be the most suitable for the conversion of $KHCO_3$, it gives no indications on which reactions occur. In other words, if $KHCO_3$ is converted to K_2CO_3 or the hydrated form, $K_2CO_3 \cdot (1.5H_2O)$, is not clear. This can be further investigated in Figure 4.4, where the regeneration reactor heat duty is plotted as a function of HP steam flow for the same reactor temperatures.

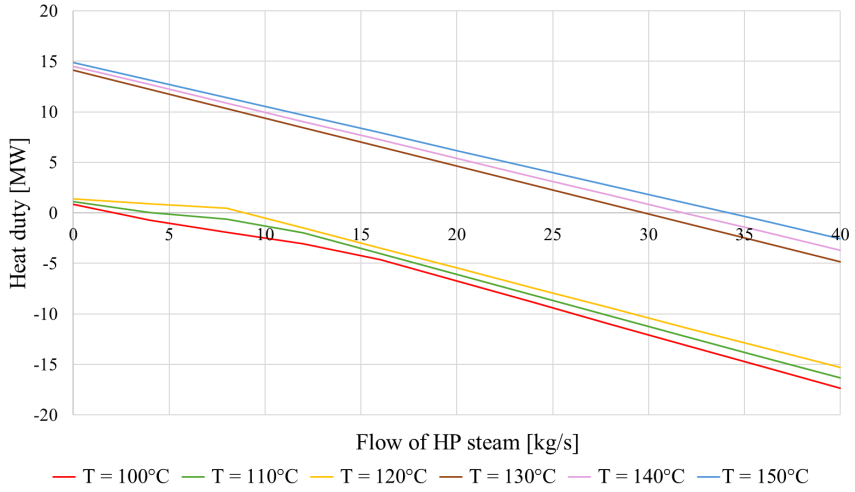

Figure 4.4: Regeneration reactor heat duty as a function of the flow of HP steam flow at different reactor temperatures.

In Figure 4.4, the graphs for the different reactor temperatures are aligned in two groupings, one with the higher reactor temperatures and another with lower reactor temperatures with a significant difference in reactor heat duty for the two groups. When investigating this further in the Aspen model, it was discovered that the reason for this was the different reactions occurring in different temperature ranges. For temperatures at and below 120°C, $KHCO_3$ was converted only to the hydrated version of K_2CO_3 through reaction 3. At temperatures above 120°C, $KHCO_3$ was exclusively converted to K_2CO_3 through the regeneration reaction, reaction 2. This pattern can be seen in Table 4.4 where a reactor temperature of 120°C is compared to 130°C. Evidently, the enthalpy of reaction for these two reactions differ which leads to dissimilar reactor heat duties.

Table 4.4: Molar flows of the different compounds forming products and reactants in the regeneration reactor for a reactor temperature of 120 and 130°C at 8 kg/s and 0 kg/s of HP steam, respectively, required for full conversion of $KHCO_3$.

Compound	Inlet molar flow [kmol/h]	Outlet molar flow [kmol/h] (120°C)	Outlet molar flow [kmol/h] (130°C)
K_2CO_3	14.18	0	312.58
$KHCO_3$	585.08	0	0
$K_2CO_3 \cdot (1.5H_2O)$	5.86	312.58	0

Formation of phases other than K_2CO_3 is also a motive for not choosing a temperature at or below 120°C. As mentioned in the theory section, literature discusses the reactivity of $K_2CO_3 \cdot (1.5H_2O)$ for absorbing CO_2 as a controversial subject, meaning that it is uncertain if reaction 4 can take place in the carbonation reactor. Because of this, and the amount of HP steam required to reach 100% conversion, the temperature of the regeneration reactor was set to 130°C. The HP steam flow through the reactor was chosen as the minimum amount that was able to satisfy the reactor

heat duty of 14.12 MW at the chosen reactor temperature. This steam flow is found in Figure 4.4 at the point where the 130°C graph crosses the x-axis, more precisely at 29.76 kg/s. The key parameters and settings for the regeneration reactor are summarized in Table 3.4.

Table 4.5: Key parameters of the regeneration reactor in the Steam HP case, using HP steam as both fluidizing agent and heating medium.

Steam HP case - Key parameters	
Steam condition	HP
Reactor temperature	130 °C
Reactor heat duty	14.12 MW
Steam demand	29.76 kg/s

4.3.1.1 Reactor dimensions

By estimating the dimensions of the regeneration reactor of the Steam HP case according to the methods section, Section 3.6.2, a cross section area of 2.6 m^2 and a reactor height of 6 m was obtained.

4.3.2 Integration of the DHPC process at the WtE plant

As previously mentioned in Section 3.4.1, the integration of the DHPC process at the WtE plant was done by extracting steam at a suitable location, depending on the pressure level, in the Ebsilon model to fulfill the steam demand. By doing so, the outputs from the model was affected to different extents depending on the regeneration reactor configuration. The produced electricity as well as the generation of DH after applying the Steam HP DHPC process to the plant, without heat integration, were 22.76 MW and 131.48 MW respectively.

4.3.2.1 Pinch analysis

As the cold streams originate from the WtE plant, they were the same for all cases. The thermodynamic data for the cold streams are summarized in Table 4.6. Note that the names of the streams corresponds to the ones used in Table 3.5.

Table 4.6: Stream data for the cold streams used in the pinch analysis for all DHPC cases.

Cold streams					
Name	*Location*	T_{start} *[°C]*	T_{end} *[°C]*	Q *[MW]*	CP *[MW/K]*
C1	Air preheater	36.48	120.75	8.78	0.10
C2	feedwater preheater	94.44	110.15	3.31	0.21
C3	Flue gas reheater	33.23	67.29	2.28	0.07
C4	SCR reheater	223.88	236.00	0.56	0.05
C5a	DH system (before heat pumps)	45.52	77.25	123.25	3.88
C5b	DH system (after turbine condenser)	90.15	120	115.96	3.88

Utilizing the data in Table 4.6, the cold composite curve was constructed and it can be seen in Figure 4.5. As evident, the cumulative cooling load is 253.58 MW.

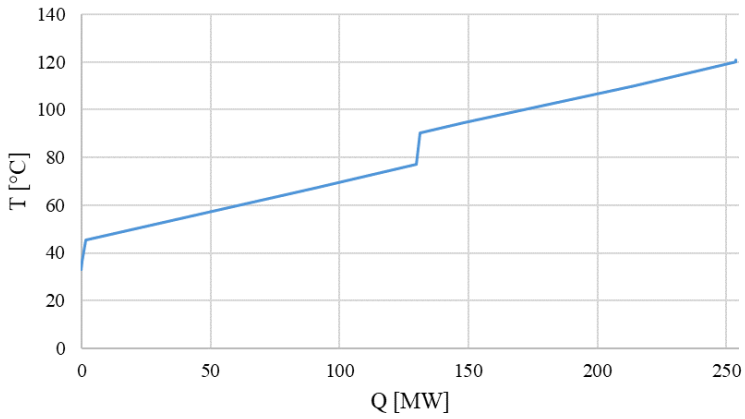

Figure 4.5: Cold composite curve for the streams included in the pinch analysis, valid for all DHPC cases.

Significant vapor flows are treated in the condenser separating CO_2 and H_2O. Thereby, the condenser load is large, which can be seen in Table 4.7, where the hot streams are presented. In the table, it is also evident that the stream H3 was divided into three separate streams. This was done to account for the phase change occurring in the condenser. H3a represents the cooling of the gas, whereas H3b corresponds to condensation. To maintain the water balance at the WtE plant, the cooling of the condensate in liquid phase (H3c) was treated by returning the stream to the feedwater chest as discussed in Section 3.4.1 and therefore excluded from the pinch analysis.

Table 4.7: List of the streams included in the pinch analysis for the Steam HP case.

Hot streams					
Name	*Location*	T_{start} *[°C]*	T_{end} *[°C]*	Q *[MW]*	CP *[MW/K]*
H1	Carbonation reactor load	70	55.52	11.50	0.79
H2	Sorbent cooler load	130	70	1.86	0.03
H3a	Water condenser (H_2O/CO_2)	130	100	1.78	0.06
H3b	Water condenser (H_2O/CO_2)	100.1	100	74.62	746.20

The hot streams in Table 4.7 were combined into a composite curve which is viewed in Figure 4.6. As is evident, the condenser load constitutes a significant share of the cumulative heat load of 89.76 MW.

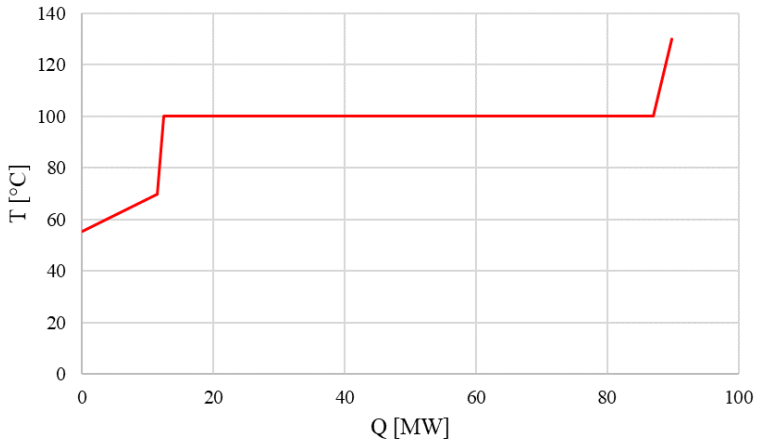

Figure 4.6: Hot composite curve for the streams included in the pinch analysis, which are related to the Steam HP case.

Combining the cold composite curve in Figure 4.5 with the hot composite in Figure 4.6 and shifting the cold composite curve, yielded Figure 4.7. Note that the minimum heating demand, $Q_{H,min}$, is not marked. This was due to that its relevancy in this context was limited since, despite the availability of the cold streams for heat integration, they have no heating demand that needs to be fulfilled by the pinch analysis. Another note to make is that the graph is zoomed in, resulting in that the entire hot composite curve is visible but the not the complete cold composite. In the figure, it is clear that there is no minimum cooling demand ($Q_{C,min}$) and the maximum heat recovery (Q_{rec}) is 89.76 MW.

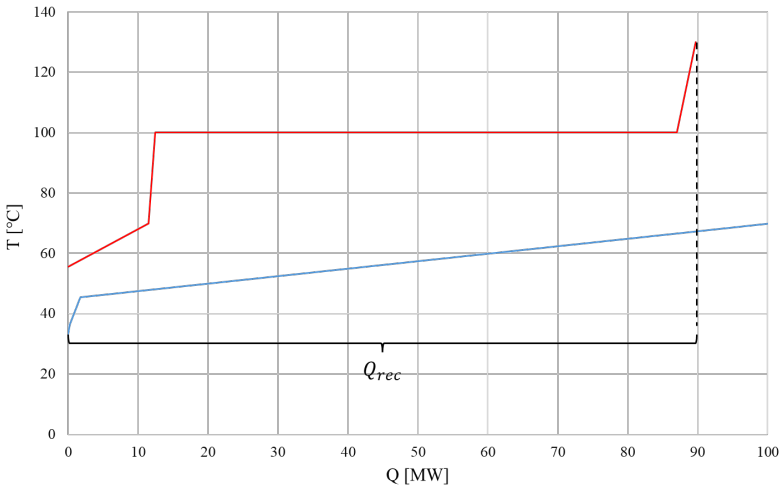

Figure 4.7: Combination of cold and hot composite curves for the Steam HP case shifted to satisfy the minimum temperature difference of 10 K.

4.3.2.2 Retrofit of the WtE plant

A summary of all retrofits done in the Steam HP case is shown in Table 4.8. A similarity between all three DHPC cases investigated was the stream matching for the sorbent cooler, H2. Since the sorbent cooler is the only equipment in the DHPC process using air as a cooling medium, the air preheater, C1, was the only integration possibility for its cooling demand. By exchanging heat between these two streams the air was preheated slightly before entering the air preheater. This resulted in a reduced demand for LP steam in the air preheater.

The next retrofit considered was also related to the air preheater, according to the prioritization order in Table 3.6. By exchanging heat between stream C1 and H3a in combination with a part of H3b, the air was heated additionally leading to a further decrease of steam demand in the air preheater. Secondly, the flue gas reheater was retrofitted. The steam used as a heating medium was completely exchanged by a part of stream H3b. The possibility to reduce the steam demand in the feedwater preheater was also investigated but none of the residual hot streams available were in the right temperature range to decrease this steam demand.

Considering the order of prioritization for the cold streams in Table 3.6, the next approach for integrating heat from the DHPC process was to add heat to the DH cycle. A retrofit was therefore done to match the carbonation reactor load, stream H1, with the DH water before the heat pumps, stream C5a. The temperature ranges of these two streams, as well as the loads of them, made it possible to fully inject the carbonation reactor load to the DH water. A second retrofit was done to the DH cycle with the aim of integrating the residual heat of hot stream H3b to the system. The suitable location for this retrofit was the same as for the previous, before the heat pumps.

Table 4.8: Description of all retrofits, their effects on the system as well as the streams matched in the Steam HP case.

Retrofit description	System effects	Streams matched		Load of retrofit [MW]
		Hot	Cold	
Sorbent cooler duty to preheat air	Reduced steam demand in the air preheater	H2	C1	1.86
Condensing steam to preheat air	Reduced steam demand in the air preheater	H3b	C1	5.27
Condensing steam to reheat flue gas	Elimination of steam demand in the flue gas reheater	Hb3	C3	2.28
Carbonation reactor duty for DH	Increased DH delivery	H1	C5a	11.50
Condensing steam for DH (Heat pumps at full load)	Increased DH delivery	H3b	C5a	58.10
Condensing steam for DH (Heat pumps at part load)	Increased DH delivery	H3b	C5a	68.86
Total recovered heat (Heat pumps at full load)				79.00
Total recovered heat (Heat pumps at part load)				89.76

With all retrofits in Table 4.8 carried out, all hot streams with a duty larger than 1 MW in Table 4.7 had been matched with a suitable cold stream from Table 4.6. To summarize the effects of all retrofits, the produced electricity, delivered DH, total amount of recovered heat are shown in Table 4.9 for both modes of heat pump operation.

Table 4.9: Outputs from retrofitted WtE plant with Steam HP DHPC process integrated.

Steam HP		
Heat pump load [MW]	Full load 65.12	Minimum load 13.75
Produced electricity [MW]	23.39	25.88
Produced DH [MW]	209.63	195.96
Recovered heat [%]	88	100

Table 4.9 shows that by decreasing the heat pump load to a minimum, more heat could be recovered in the system. In particular, 100% the maximum heat recovery potential, obtained in the pinch analysis could be achieved. When maintaining the heat pump load at full capacity the amount of recovered heat could not reach the maximum potential due to restrictions in the model. In particular, the temperature

of DH water received by the turbine condenser while keeping the heat pumps at full load ended up being too high, thereby violating the energy balance in the component. Consequently, for this operating condition, 88% of the maximum heat recovery was obtained resulting in a cooling demand of 10.76 MW for the process.

4.3.3 System evaluation

As described in the methods section, the plant, with and the without DHPC process integrated, was evaluated in terms of energy performance indicators, capture rate and capture cost, which are all included in the system evaluation. In this section the results from the system evaluation for the Steam HP case are presented.

4.3.3.1 Energy performance and capture rate

The energy performance of the plant with the Steam HP process integrated is summarized in Table 4.10. As described in the theory section, the efficiency penalty and energy penalty are relative to the WtE plant without carbon capture, meaning the case presented in Section 4.1.1. To recall, the total energy efficiency for the WtE plant is 97.67%.

Table 4.10: Energy performance indicator values for the Steam HP case.

Steam HP			
Mode of operation	No heat integration	Heat pump full load	Heat pump minimum load
Total energy efficiency, η_{WtECC} [%]	62.56	96.30	91.51
Efficiency penalty, η_{loss} [%-units]	35.10	1.35	6.14
Electricity energy penalty, EP_{El} [%]	57.72	55.91	48.67
DH energy penalty, EP_{DH} [%]	32.06	-8.32	-1.26

As expected, when applying the DHPC process in the Steam HP configuration to the WtE plant, the total energy efficiency dropped significantly. However, in the table, it is also evident that when integrating excess heat, the efficiency penalty decreased notably. Examining the energy penalties, when no heat integration is present, there are large penalties in terms of both electricity and DH. However, while the integration of excess heat does not change the electricity energy penalty to large extents, it results in significant improvements in the DH energy penalty. As a matter of fact, the negative DH penalty that is visible in Table 4.10 indicates on increased delivery of DH.

For the Steam HP case, the amount of captured CO_2 was 3.58 kg/s which corresponds to a capture rate of 96%. Consequently, the specific regeneration duty resulted in 3.95 GJ/tCO_2 captured.

4.3.3.2 Capture cost

Following the methodology proposed in Section 3.7, a capture cost was computed for the Steam HP case. In Figure 4.8, the different cost contributions, both CAPEX and OPEX, to the capture cost are shown together with the actual capture cost presented by the yellow dotted line and the text below it. See Appendix D for a complete list of the equipment included in the CAPEX for each DHPC case, their respective investment costs and a summary of the assumptions associated with the calculations.

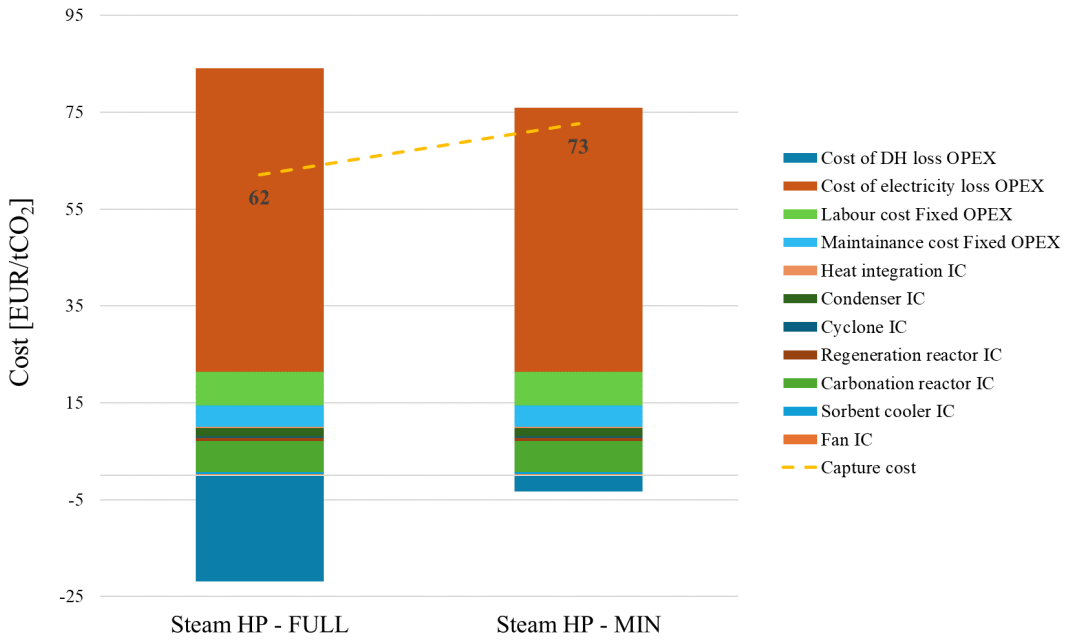

Figure 4.8: Cost contributions to the capture cost for the Steam HP case. Note that IC abbreviation refers to investment cost.

Focusing on the cost contributions seen in Figure 4.8, it is evident that the OPEX constitutes the largest share in the capture cost, particularly the electricity cost. Even though that statement holds for both operational modes, the absolute values and distribution of the OPEX differs. It may also be noted that the CAPEX is identical for the different modes of operation.

The difference in utility cost results in a lower capture cost when operating the heat pumps at full load. The reason behind this is the difference in the costs for electricity and DH loss, presented as red and blue bars. For the full load heat pump operation, the electricity cost is high, but the DH cost is negative which is interpreted as a revenue. In contrast, for the minimum load operation, the electricity cost is less but so is the revenue from the DH. Consequently, the net utility cost, adding electricity and DH, is lower for the full load operation. Therefore, this situation is further investigated by examining the changes in capture cost when applying the different price scenarios proposed in Section 3.7. The outcome of the price scenario analysis is shown in Figure 4.9.

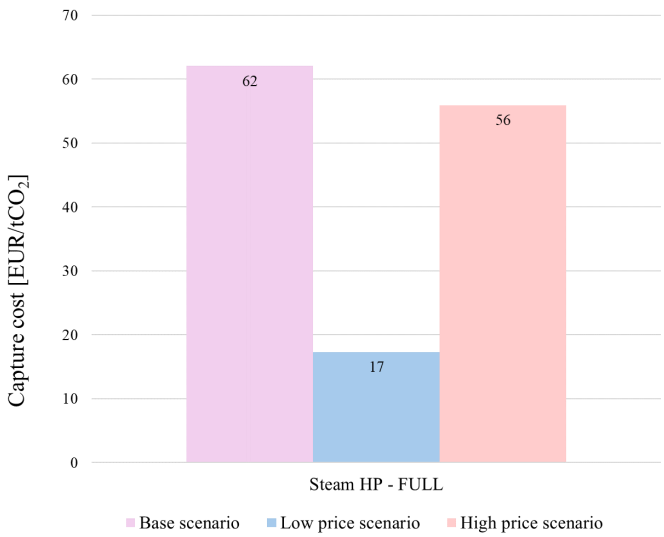

Figure 4.9: Capture cost for the Steam HP case (full heat pump load) evaluated for the different price scenarios. The base scenario, presented in purple, involves an electricity price of 700 SEK/MWh and DH price of 200 SEK/MWh. The other scenarios, low price and high price, refers to an equal price of 200 SEK/MWh as well as 1000 SEK/MWh and 500 SEK/MWh for electricity and DH respectively.

Comparing the base case, purple bar, with the low and high price scenarios in Figure 4.9, it is clear that the utility prices have significant impacts on the capture cost. With low prices on both electricity and DH, the electricity cost is reduced while the revenue from the increased DH delivery remains the same, resulting in a lower capture cost. In contrast, when the prices are increased, the cost of electricity outweighs the increase in DH revenues and the capture cost is of the same magnitude as in the base case.

4.4 Case: FBHE HP/LP

In this section, the results gathered from the analysis of the two FBHE cases are presented. The regeneration reactor is fluidized by a recirculating stream of CO_2 in both cases, but the FBHE HP case uses condensing HP steam as heat source while the FBHE LP case uses condensing LP steam.

4.4.1 Parameter study

The analysis of the regeneration reactor of both FBHE cases showed that the conversion of the sorbent reached 100 mole% for all reactor temperatures at, and above 130°C regardless of the fluidization gas flow. This pattern is shown in Figure 4.10, where the conversion of $KHCO_3$ is plotted as a function of the CO_2 flow.

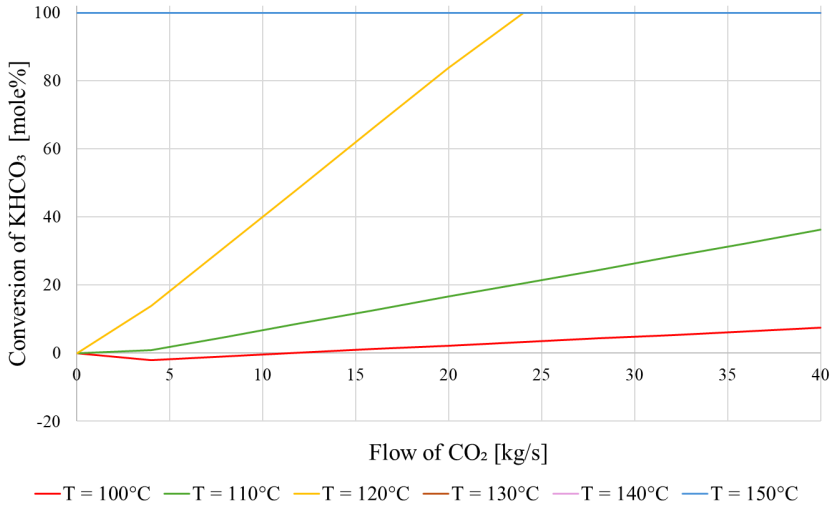

Figure 4.10: The conversion of $KHCO_3$ as a function of CO_2 flow at different reactor temperatures. Note that the graphs for 130°C and 140°C lay behind 150°C.

However, in the figure, it is also clear that some CO_2 flows result in negative conversion of $KHCO_3$ for the reactor temperatures 100°C and 110°C. According to the definition of the conversion of $KHCO_3$, see Section 3.3.4.2, a negative value indicates that $KHCO_3$ has been produced in the reactor. Investigating this further for the case of 4 kg/s CO_2 and a reactor temperature of 100°C in Table 4.11, it was clear that the compound $K_2CO_3{\cdot}(1.5H_2O)$ had reacted to form $KHCO_3$ and K_2CO_3 via reaction 4 and 3. Evidently, since the objective of the regeneration reactor is to regenerate K_2CO_3, reactor temperatures of 100 and 110°C were not suitable. In addition, to achieve a decent conversion of $KHCO_3$, large fluidization flows were required for these temperatures.

Table 4.11: Molar flows of the different compounds forming products and reactants in the regeneration reactor for the case of 4 kg/s of CO_2 flow and a reactor temperature of 100°C.

Compound	Inlet molar flow [kmol/h]	Outlet molar flow [kmol/h]
K_2CO_3	14.18	14.25
$KHCO_3$	585.08	596.66
$K_2CO_3{\cdot}(1.5H_2O)$	5.86	0

The regeneration reactor temperature for both FBHE cases were thereby set to 130 °C to reassure that 100% conversion to K_2CO_3 was reached. To confirm that the formed product was solely K_2CO_3, the inlet and outlet molar flows of the relevant compounds in the reactor are presented in Table 4.12. Evident in the table is that there is full regeneration of K_2CO_3 in the reactor. The reactor duty at 130°C is 14.12 MW.

The steam required to fulfill this heat demand in the FBHE reactors was investigated by letting HP and LP steam condense and cool to 140 °C in an external

Table 4.12: Molar flows of the different compounds forming products and reactants in the regeneration reactor for a reactor temperature of 130°C.

Compound	Inlet molar flow [kmol/h]	Outlet molar flow [kmol/h]
K_2CO_3	14.18	312.58
$KHCO_3$	585.08	0
$K_2CO_3 \cdot (1.5H_2O)$	5.86	0

cooler. The mass flow of steam required is shown at the intersection between the heat exchanger duty and the reactor duty in figures 4.11 and 4.12.

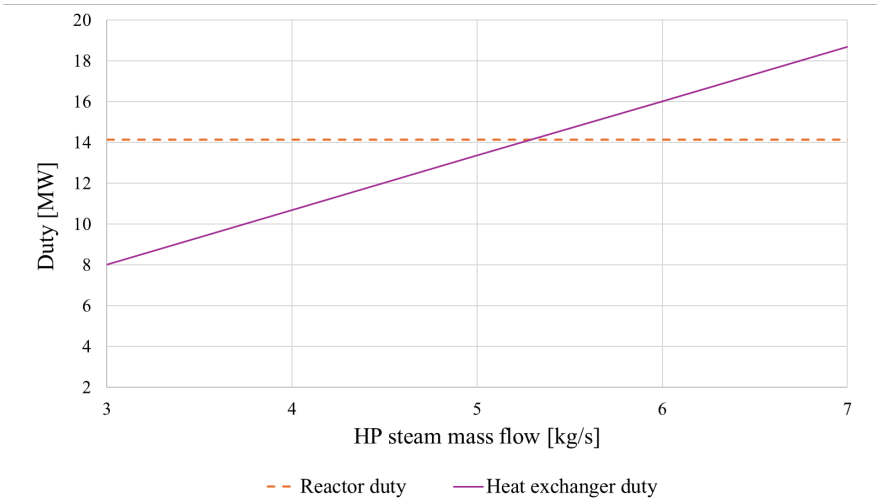

Figure 4.11: Heat exchanger duty as a function of HP steam flow satisfying the reactor duty (dotted line).

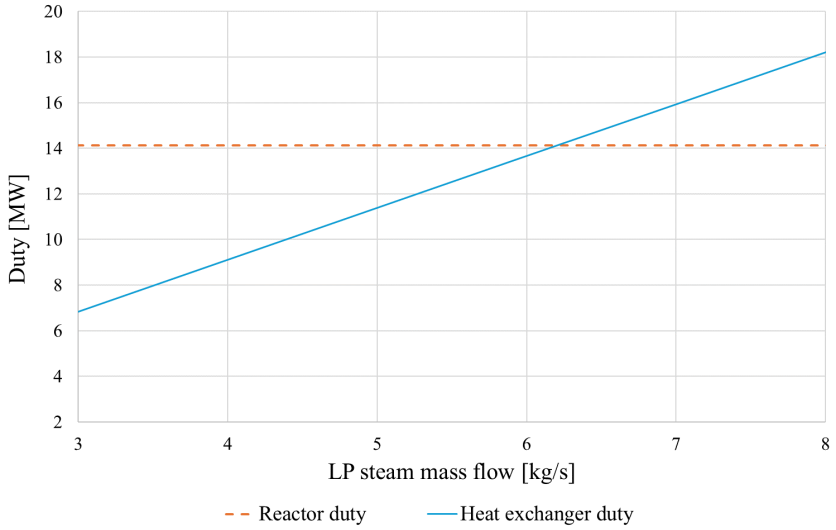

Figure 4.12: Heat exchanger duty as a function of LP steam flow satisfying the reactor duty (dotted line).

As can be seen in the figures, HP and LP steam mass flows of 5.19 kg/s and 6.20 kg/s, respectively, are required to satisfy the reactor duty. The key parameters for the two FBHE cases are shown in Table 4.13.

Table 4.13: Key parameters of the regeneration reactor in the FBHE case, using CO_2 as fluidization gas and HP as well as LP steam as heating medium.

FBHE case - Key parameters		
Steam condition	HP	LP
Reactor temperature	130 °C	130 °C
Reactor heat duty	14.12 MW	14.12 MW
Steam demand	5.19 kg/s	6.20 kg/s
CO_2 demand	3.95 kg/s	7.89 kg/s

4.4.1.1 Reactor dimensions

Following the methodology in Section 3.6.3, the dimensions for both the FBHE HP and FBHE LP reactors were obtained. In the FBHE HP case, the cross section area was 6 m^2 with a height of 2 m, and for the FBHE LP case the corresponding area and height were 12 m^2 and 5.1 m, respectively.

4.4.2 Integration of the DHPC process at the WtE plant

As discussed for the Steam HP case, applying the FBHE DHPC processes at the WtE plant implied affecting the outputs from the model as steam was extracted. For the FBHE HP case, the produced electricity and DH after application were 39.22 MW and 183.52 MW, respectively. The corresponding values for the FBHE LP case were 41.43 MW and 181.55 MW.

4.4.2.1 Pinch analysis

As mentioned in Section 4.3.2.1, the hot streams included in the pinch analysis were the same for both the FBHE HP and FBHE LP cases. The reason being that the condensate from the internal tubes of the FBHE, which differs between the cases, was excluded from the pinch analysis since it was returned to the feedwater chest.

In Table 4.14, the hot streams for the FBHE cases are presented. Following the same pattern as in Table 4.7, stream H3 was divided into three separate streams.

Table 4.14: List of the streams included in the pinch analysis for the FBHE cases.

Hot streams					
Name	*Location*	T_{start} *[°C]*	T_{end} *[°C]*	*Q [MW]*	*CP [MW/K]*
H1	Carbonation reactor load	70	55.52	11.50	0.79
H2	Sorbent cooler load	130	70	1.86	0.03
H3a	Water condenser (H_2O/CO_2)	130	100	0.09	0.002
H3b	Water condenser (H_2O/CO_2)	100.1	100	3.60	36.04
H3c	Water condenser (H_2O/CO_2)	100	10	0.66	0.01

Based on the data in Table 4.14, a hot composite curve was constructed which is found in Figure 4.13. In the graph, it is clear that the cumulative heat load is 17.70 MW.

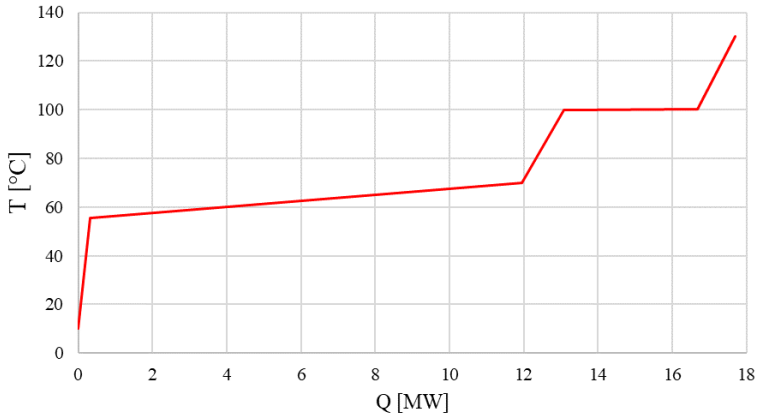

Figure 4.13: Hot composite curve for the streams included in the pinch analysis, which are related to the FBHE case.

Combining the hot composite curve with the cold composite curve in Figure 4.5 and shifting the cold curve, yielded Figure 4.14. Note that the graph is zoomed in to view details in the interaction between the curves, the entire hot composite is visible but not the cold one. In the figure, it can be seen that the minimum cooling demand ($Q_{C,min}$) is 0.24 MW and the maximum heat recovery (Q_{rec}) is 17.46 MW.

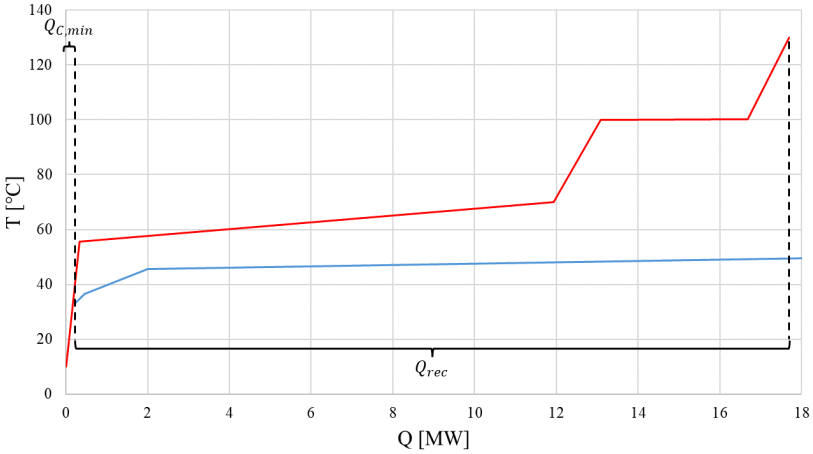

Figure 4.14: Combination of cold and hot composite curves for the FBHE cases shifted to satisfy the minimum temperature difference of 10 K.

4.4.2.2 Retrofit of the WtE plant

The same strategy as described for the Steam HP case was applied when retrofitting the two FBHE cases. As a result, the same retrofits but with other loads, were done at most parts of the system, except the retrofit considering the flue gas reheater. When investigating the possibility of replacing the steam as heating medium in this piece of equipment, it was realized that the decrease in steam demand would be counteracted by increasing the steam supply to the feedwater tank. This retrofit was therefore neglected.

The same approach used in the Steam HP case, with two alternative loads of the heat pumps, was used in the FBHE case. However, in this case, the heat pumps were operated at part load, instead of at minimum load, with the carbonation reactor load. This resulted in a decreased extraction of LP steam for the heat pump supply, while keeping the heat input to the DH system at a constant level. A description of all retrofits done in both FBHE cases are listed in Table 4.15.

Table 4.15: Description of all retrofits, their effects on the system as well as the streams matched in the two FBHE cases.

Retrofit description	System effects	Streams matched		Load of retrofit [MW]
		Hot	Cold	
Sorbent cooler duty to preheat air	Reduced steam demand in the air preheater	H2	C1	1.86
Condensing steam to preheat air	Reduced steam demand in the air preheater	H3b	C1	3.60
Carbonation reactor duty for DH	Increased DH delivery	H1	C5a	11.50
Total recovered heat (Heat pumps at full load)				16.96
Total recovered heat (Heat pumps at part load)				16.96

With all retrofits in Table 4.15 carried out, the hot streams with a duty larger than 1 MW in Table 4.14 had been matched with a suitable cold stream from Table 4.6. To summarize the effects of all retrofits in both FBHE cases, the produced electricity, delivered DH and percentage amount of recovered heat are shown in tables 4.16 and 4.17.

Table 4.16: Outputs from retrofitted WtE plant with FBHE HP DHPC process integrated.

FBHE HP		
Heat pump load [MW]	Full load 65.12	Part load 53.61
Produced electricity [MW]	39.71	40.27
Produced DH [MW]	199.89	194.48
Recovered heat [%]	97	97

Table 4.17: Outputs from retrofitted WtE plant with FBHE LP DHPC process integrated.

FBHE LP		
Heat pump load [MW]	Full load 65.12	Part load 53.61
Produced electricity [MW]	41.92	42.48
Produced DH [MW]	197.93	192.51
Recovered heat [%]	97	97

By comparing the results from both cases, it is evident that 97% of the maximum heat recovery was achieved in all situations. Evidently, 0.5 MW could not be integrated and was therefore seen as a cooling demand. The reason for that originates from the heat loads of stream H3a and H3c being less than 1 MW. Additionally, it was known from the beginning that the minimum cooling demand was 0.24 MW, leading to a total cooling demand of 0.74 MW.

4.4.3 System evaluation

The results from the system evaluation for both FBHE cases are presented in the following section.

4.4.3.1 Energy performance and capture rate

The energy performance indicators calculated for the FBHE HP case are presented in Table 4.18. To recall, the total energy efficiency of the WtE plant without carbon capture is 97.67%.

Table 4.18: Energy performance indicator values for the FBHE HP case.

FBHE HP			
Mode of operation	No heat integration	Heat pump full load	Heat pump part load
Total energy efficiency, η_{WtECC} [%]	91.90	99.12	97.04
Efficiency penalty, η_{loss} [%-units]	5.75	-1.47	0.61
Electricity energy penalty, EP_{El} [%]	9.95	8.51	6.89
DH energy penalty, EP_{DH} [%]	5.17	-3.29	-0.49

As seen in Table 4.18, the loss in efficiency was recovered when heat was integrated from the capture process. In fact, in the heat pump full load operational mode, the total energy efficiency reached even higher values than what was achieved for the original model, indicated as the negative value of the efficiency penalty. Mainly, this was due to DH being added to the system from the capture process, as seen in the negative value of the DH penalty. In the heat pump part load operational mode, the total energy efficiency almost managed to reach the same level as the original model, resulting in a low efficiency penalty. Evaluating the electricity and DH penalty for this situation and comparing to the heat pump full load operation, the electricity penalty is slightly lower while the DH penalty is higher, even if it is till negative. The energy performance indicators were also computed for the FBHE LP case and the results are presented in Table 4.19.

Table 4.19: Energy performance indicator values for the FBHE LP case.

FBHE LP			
Mode of operation	No heat integration	Heat pump full load	Heat pump part load
Total energy efficiency, η_{WtECC} [%]	92.00	99.22	97.14
Efficiency penalty, η_{loss} [%-units]	5.65	-1.57	0.51
Electricity energy penalty, EP_{El} [%]	3.52	2.09	0.47
DH energy penalty, EP_{DH} [%]	6.19	-2.27	0.53

Predictably, Table 4.19 displays similar results as the performance for the FBHE HP (Table 4.18). Numerically, the changes for the different operational modes in terms of total energy efficiency and the efficiency penalty are almost identical. However, the impact on the energy penalties differ significantly between the FBHE LP and HP cases but also among the operational modes within the LP case. In general, it can be observed that the electricity penalty is lower whereas the DH penalty is larger when utilizing LP steam instead of HP steam. Consequently, in the heat pump part load mode, both the original electricity and DH production can almost be recovered. Comparing this to the heat pump full load situation, which has higher total energy efficiency, the DH production is increased while the electricity is decreased compared to the original model.

The resulting captured amount of CO_2 was 3.58 kg/s for both FBHE cases, which is the exact same amount captured in the Steam HP case. Consequently the capture rate is 96% and the specific regeneration duty was 3.95 GJ/tCO_2 captured even for these cases. The equality of these values are due to the fact that the conversion of $KHCO_3$ to K_2CO_3 in the regeneration reactor, as well as the regeneration duty, was exactly the same in all cases.

4.4.3.2 Capture cost

For the FBHE HP/LP cases, the economic results are presented in the same way as for Steam HP, with the yellow dotted line representing the capture cost, in Figure 4.15.

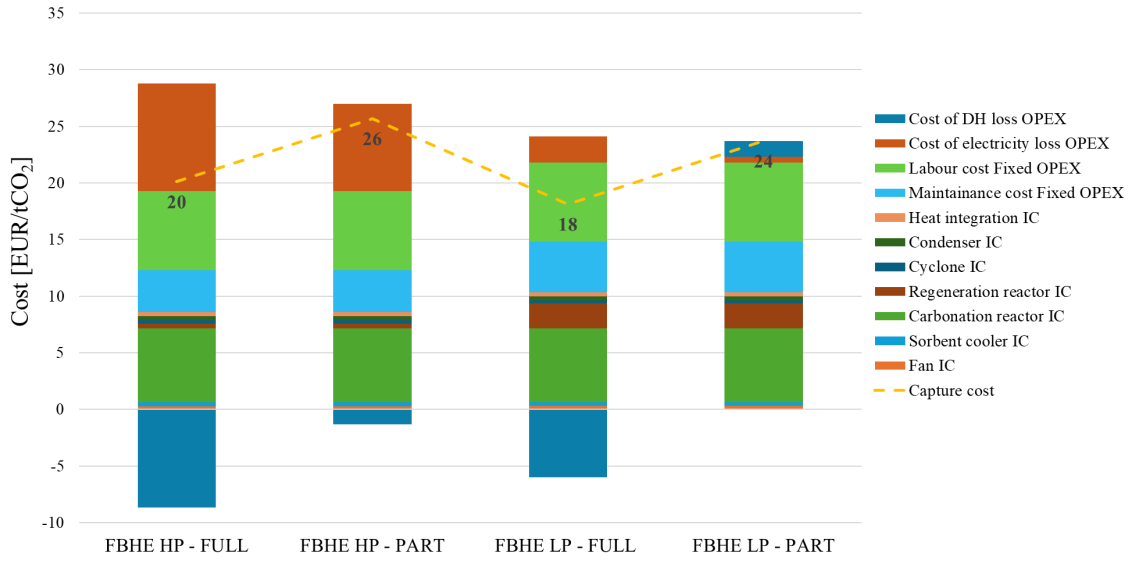

Figure 4.15: Cost contributions to the capture cost for the FBHE cases. Note that IC abbreviation refers to investment cost.

Comparing the investment costs of the FBHE HP and FBHE LP processes in Figure 4.15, it is clear that the regeneration reactor investment is higher in the LP case due to the larger size of the reactor. Other than that, the investments for all other equipment are close to equal between the two cases.

Furthermore, the lowest capture cost was obtained in the FBHE LP case, with the heat pumps working at full load. In general, the FBHE LP case resulted in lower capture cost than the FBHE HP case. This is a result from the increased revenues from DH (blue bars) which outweighs the cost of the loss in electricity generation (red bars). In contrast, the FBHE HP case has larger costs of electricity loss than what the increased revenues from DH can cover.

When instead comparing the two operational modes shown in Figure 4.15, it is clear that operating the heat pumps at full load leads to a lower carbon capture cost for

the same reason as explained for the Steam HP case. That being said, the different pricing scenarios were investigated for the full heat pump operational mode. The outcome of the price scenario analysis is shown in Figure 4.16.

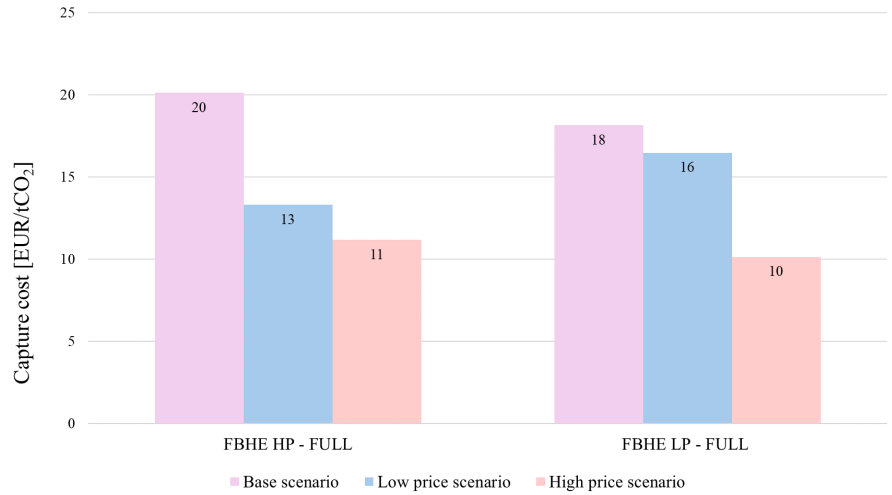

Figure 4.16: Capture cost for the FBHE cases (full heat pump load) evaluated for the different price scenarios.

Examining Figure 4.16 for the FBHE cases, it may be noted that the capture cost is decreased in the other scenarios compared to the base scenario. For the FBHE HP case, the outcome of the low price scenario relates to the reduction in electricity cost while maintaining the revenues from DH. Similar pattern can be seen in FBHE LP as well, but since the electricity demand is lower for this case compared to FBHE HP, the effect of the price reduction is lower. Focusing on the high price scenario, where both utility prices are increased, it is clear that the DH revenues have increased for both FBHE HP and LP, outweighing the increased electricity cost and resulting in a lowering of the capture cost.

4.5 Neglected cases

Even though six cases were constructed in Section 3.3.5, results have only been presented for three of them. As mentioned in the introduction of the results chapter, the Steam LP case and both preheated CO2 cases were not evaluated further than to the parameter study part of the analysis. The results from the parameter study, for these cases, are presented in Table 4.20.

Table 4.20: Summary of results for neglected DHPC cases.

	Steam case	**Preheated CO_2 case**	
	LP	HP	LP
Condenser duty [MW]	1151	3.68	3.68
Steam demand [kg/s]	469.72	5.19	6.20
CO_2 demand [kg/s]	-	114.25	>15 000

From Table 4.20, it can be concluded that the mass flows of fluidization gas differ between the neglected cases and are significantly larger compared to the cases studied in more detail, Steam HP and FBHE HP/LP. Actually, all three cases were considered unreasonable due to large steam flows or CO_2 flows. The maximum available steam flow, either LP or HP, at the plant is 72.13 kg/s (see Table 4.1). Evidently, the Steam LP case was unrealistic. As mentioned previously, the captured amount of CO_2 was 3.58 kg/s in all cases, indicating on the reasonable size of the circulating flow of CO_2. Therefore, the preheated CO_2 cases, using both HP and LP steam, appeared as unreasonable, as they exceed this number by far. As a result, the Steam HP case and the two preheated CO_2 cases were not considered for further investigation. For a more detailed description of the parameter studies of these cases, see Appendix E.

4.6 Summary and comparison of studied cases

Multiple designs of the DHPC process have been introduced in the different cases so far, each case with its own strengths and weaknesses. Some of the process variables were common between the cases but some were significantly different, resulting in clear distinctions when evaluating the systems further. The process variables for the Steam HP and the two FBHE cases are summarized in Appendix B. The objective with the following section will be to summarize a comparison of these cases.

An observation made in all three cases is that the operational mode, keeping the heat pumps at full capacity, gives a lower carbon capture cost than when the heat pumps are running at minimum/part load. This is a result of the DH revenues weighing over the added cost for lost electricity production in all full load operational modes. Thereby, the minimum/part load operational mode will not be discussed further in this section. In Table 4.21, a summary of the energy performance indicators, capture costs and reactors sizes for the three DHPC cases is presented. In accordance with the previous discussion, these values are for the full heat load operation.

Table 4.21: Summary of energy performance indicators, capture cost and reactor sizes for the Steam HP and the two FBHE cases, with heat pumps operating at full load.

	Steam HP	FBHE HP	FBHE LP
Electricity energy penalty, EP_{El} [%]	55.91	8.51	2.09
DH energy penalty, EP_{DH} [%]	-8.32	-3.29	-2.27
Capture Cost [EUR/tCO_2]	62	20	18
Regeneration reactor dimensions	2.6 m^2 x 6 m	6 m^2 x 2 m	12 m^2 x 5.1 m

Starting off with the Steam HP case, when integrated with the WtE plant, it has a large impact on the electricity and DH generation. This system also has a high capture cost compared to the FBHE cases. However, the reactor size is rather compact and similar to the reactor size of the FBHE HP case, see figure 4.17.

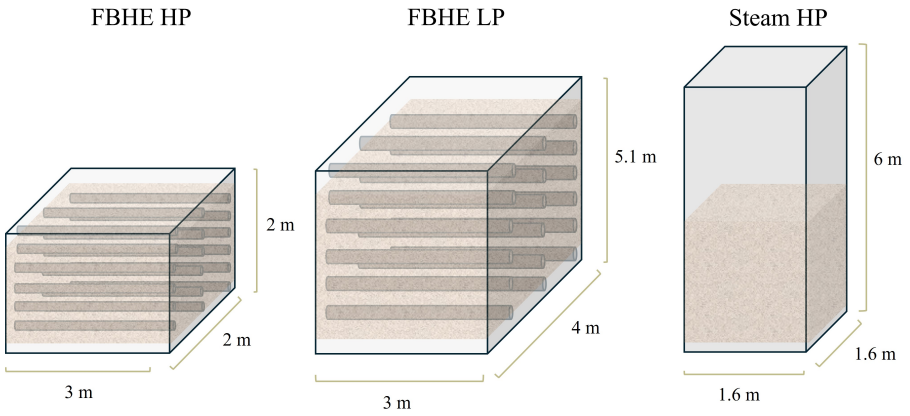

Figure 4.17: Comparison of reactor sizes for the regeneration reactors of the cases FBHE HP, FBHE LP and Steam HP.

Moving on to the FBHE HP case. As mentioned, this design is just as compact as the Steam HP reactor, but the electricity penalty is not even close to as large. Both FBHE cases had almost identical efficiency penalties, although the energy penalty in both electricity and DH were marginally higher for the FBHE HP. When it comes to the capture cost using the FBHE HP case, it lies between the capture costs of the two other cases, solely 2 EUR/tCO_2 more expensive than the capture cost for the FBHE LP case.

The FBHE LP case entailed the lowest loss in electricity production when integrated to the WtE plant, thereby resulting in the smallest electricity energy penalty and the lowest capture cost out of the three cases. However, these benefits comes with the cost of the reactor dimensions being more than twice the size of the reactors using HP steam as heating medium.

5
Discussion

Renova are planning to implement a CCS technology at their WtE plant in Sävenäs, in order to mitigate their CO_2 emissions. The design of a CCS technology, alternative to more commercial ones such as MEA, has therefore been investigated in this project. Namely, the DHPC process. With foundation in the research done on the process in Korea, the performance of the DHPC process in a Swedish context was of interest due to the possible integration of residual heat to the well established DH system. This chapter will discuss the results and elaborate on the achieved design of the DHPC process and its integration at Renova's WtE plant. The strengths and weaknesses of both models created to evaluate this will be discussed, as well as the performance of the system, in terms of energy penalties and capture rate. These discussions, together with the results presented in the previous chapter, will be the basis of the final conclusions of the project.

5.1 Elaboration on energy performance

Integrating the DHPC process to the WtE plant initially entailed a loss in energy efficiency when no heat integration actions were taken. However, this loss was able to be recovered through retrofits of the plant based on the pinch analysis. Therefore, heat integration is seen as a necessity for motivating application of the DHPC process at existing plants, such as Renova's WtE plant, as it allows maintaining most of the energy production. In fact, the results showed that in most cases the DH delivery could be increased when applying the DHPC process and integrating the excess heat. The increased DH delivery reveals the opportunity to gain revenue, which has a positive impact on the capture cost.

For the two FBHE cases, the heat integration of the DHPC process enabled an increase in total energy efficiency compared to the original plant. The efficiency penalty for the FBHE HP and the FBHE LP cases were 5.75%-units and 5.65%-units respectively when no heat integration actions were taken. The penalty in efficiency at a CHP plant has previously been reported as 15-16% when the more established MEA CCS technology has been applied [10]. Evident is that the DHPC process using FBHE reactors performs much better than MEA in terms of total energy efficiency. However, when integrating the DHPC process as suggested in previous research, namely the Steam HP case, the total energy efficiency loss was a lot higher, 35.10%. This demonstrates the importance of utilizing the extracted steam efficiently.

The specific regeneration duty, obtained for all studied cases, was 3.95 GJ/tCO_2 captured. Compared to the specific reboiler duty of the MEA process, 3.67 GJ/tCO_2 captured, the demand for heat to regenerate the sorbent is slightly higher for the DHPC process. However, the distinction between the two is not that large and, considering the previously mentioned difference in total energy efficiency, a slightly higher specific regeneration duty is not considered as an issue.

5.2 Limitations with the WtE plant model

Examining the performance of the WtE plant model by comparing it to the real process values from Renova, see Section 4.1, it is clear that the model produces values within a 2.5% margin of error. In absolute terms, this corresponds to an overestimation of electricity by 0.68 MW and an underestimation of DH by 4.16 MW. A potential reason behind the slight overestimation of the electricity lies in the limitations with Ebsilon as a simulation tool. In fact, when modelling the steam turbine, the inlet pressure of each turbine stage can be set by the modeler. However, by doing so, Ebsilon assumes saturated conditions of the steam at the extraction points. In reality, the LP steam extractions in the turbine are superheated. Consequently, the electricity produced in the generator, in the model, is overestimated since the steam is allowed to expand down to saturated conditions instead of superheated.

The underestimation of DH delivery is more complicated to trace as it is affected by several components in the WtE plant. However, there are some possible reasons for the deviation. First of all, the heat pump load is underestimated as well. As it is one of the main providers of heat to the DH system, if its load deviates, so will the DH delivery. Second of all, there are other providers of heat in the DH system, namely the heat exchangers which transfer heat from the hot water system and the direct condensation reactor, which in turn are affected by other components. A slight load deviation in these also result in a cascade effect. However, keeping in mind the relative error of 2.5% between the model and the real plant, the model is deemed to be sufficiently good for the application of this project.

An important feature of the WtE model is that it is instantaneous, while the real operation of the plant is transient. On one hand, this limits the relevance of the results to winter operation while the characteristics of the summer operation, plant running at part load, are not accounted for. This implies that operating the DHPC process during summer will generate large heat losses due to the production of excess heat which requires larger cooling capacity than during winter. In addition, the instantaneous property also overestimates the annual amount of captured CO_2 since it is calculated by multiplying the momentary captured mass flow with the operational hours. In that manner, the part load operation, which creates less CO_2 emissions, is not included. And this may lead to an underestimation of the capture cost. On the other hand, designing the DHPC process at the time of full load plant operation, winter mode, is of interest in order to dimension it properly to be able

to handle the largest amount of emissions. And since the aim of the project was to design the DHPC process, the model made sense in that manner.

Regarding the reliability of the model and the results of the energy performance, an uncertain parameter is the waste composition. Due to lack of investigation related to the waste content, the composition was assumed to be the same as the waste treated at Lillesjöverket in Uddevalla. Even though it can be representative for the composition of the waste at Renova, it is probably not exactly same, which can create deviations. Changes in waste composition will also affect the lower heating value which is estimated based on the composition by Ebsilon. This affects both the waste consumption and the fuel input flow in the model. Consequently, the uncertainty in estimating the properties of the waste is reflected in the energy performance indicators, in particular the total energy efficiency as it contains the fuel heat input in the denominator. However, since this uncertainty is universal for all simulations done during the project, the energy performance parameters are still valid for comparison.

In a larger context, there are more effects of changes in waste composition. For example, the fraction of carbon and volumes of the waste may change as a result of future reductions in waste generation. This affects the flue gas composition and flow, thereby the input to the DHPC process. Since the capture process is dimensioned, and the operating conditions are set based on a specific point in time, dynamic operation may be of importance in the future.

5.3 Impacts of the reactor temperatures

As mentioned in the theory section, the DHPC process is a novel technology and the research done on the subject is limited. There are no existing pilot plants in the same size range as the one proposed in this work, which makes it difficult to elaborate on the reasonableness of the design. Since the background material on the process is restricted, the design process involved a large number of free variables, some of which had no reference value found in literature. The final DHPC design is viewed as the best design of the process in terms of capture rate and energy penalties. However, there might be other aspects that could be analysed to achieve an even better design. For instance, the occurrence of byproducts and side reactions in the reactors.

The resulting temperature of the carbonation reactor, 70°C, was well in line with the temperature shown in previous research (50-100°C). However, the question about choosing a lower temperature in this reactor, to favor the exothermic carbonation reaction, could be raised. The results from the parameter study of the carbonation reactor, shown in Table 4.2, state that more CO_2 was captured at lower temperatures. However, since it was desirable to choose a higher temperature that could effectively be integrated to the DH cycle, 70 °C was selected even though the amount of captured CO_2 was lower. It would therefore be of interest to investigate the profitability of integrating the carbonation reactor duty to the DH cycle, versus capturing more CO_2 and thereby avoid paying for a few more ETS permits.

The regeneration reactor temperature range suggested in theory is 150-200°C, while the suggested temperature in this work is 130°C. The aim was to set the regeneration reactor temperature as low as possible to decrease the reactor duty, while still obtaining a high degree of sorbent regeneration. Using the model created in this study made it possible to regenerate 100% of sorbent already at 130°C. This was probably due to the fact that the model is ideal, not considering possible heat losses and fluidized bed dynamics that are present in reality. For instance, due to the choice of using Gibbs reactors, no properties from a real fluidized bed, such as mixing and interactions between solid particles and gas, were considered in the simulation. Since the experiments and pilot plants studied in previous research have not been ideal to the same extent, the temperature for regeneration has probably been set higher to ensure full regeneration of the sorbent. If the model conditions were to change to less ideal and more realistic ones, there is a possibility that the same parameter study would result in a higher regeneration temperature within the range suggested in literature.

In the light of the discussions above, the most crucial parameters of the proposed DHPC design are the reactor temperatures of 70°C and 130°C, for the carbonation and regeneration reactors, respectively. For instance, it has been made clear that the amount of captured CO_2 is strictly dependent on the temperature, due to the specifics of the reactions occurring in each reactor. As expected, the capture rate found in this project, 96%, is significantly higher than the corresponding value obtained in the pilot plants of 80%. A potential reason for that is the ideal property of the Aspen simulation. However, this does not invalidate its relevance. On the contrary, the DHPC simulation could work as a guideline when constructing future pilot plants.

5.4 Presence of byproducts and side reactions

As mentioned in Section 3.3.2, the hydrated version of K_2CO_3 was included in the DHPC simulation, wich made it possible for side reactions, including this parameter, to occur in the reactors. During the course of the Steam HP case parameter study, a shift regarding which reaction taking place in the regeneration reactor was noted. At 120°C, all sorbent was regenerated through reaction 3 and at 130 °C, reaction 2 occurred instead. One would expect there to be a gradient in the shift where both reactions could take place partly in the reactor. This could not be seen during the analysis and a potential cause could be a possible limitation in the Aspen model. To simulate the gradual shift between the reactions it could be of importance to exchange the Gibbs reactors to less ideal ones, and by this action taking other parameters, for instance kinetics, into account than only minimizing the Gibbs free energy.

No other side reactions were taken into consideration during the simulations. For example, the component $KAl(CO_3)(OH)_2$ and other possible side reactions, occuring between the impurities in the flue gas and the sorbent, were not considered.

Solely including $K_2CO_3 \cdot (1.5H_2O)$ implied accounting for one competing reaction, when there probably are more of them in reality. This may have affected the results of the simulation negatively in terms of its credibility, since it implies that the performance of processes such as the CO_2 uptake and the regeneration of sorbent could be overestimated. However, it is questionable if the inclusion of more byproducts would improve the model proposed in this work due to the same reason previously purposed, the choice of the Gibbs reactors. To add more possible side reactions may not give a more realistic behaviour of the DHPC process, since the only variable taken into consideration is the minimization of the Gibbs free energy. Probably, the rapid shift in reactions between temperature steps, as seen for the hydrated version of K_2CO_3, could arise again.

5.5 Simplicity of size dimensioning method

To dimension the reactors used in the DHPC process, a simplistic approach was used. The calculations give an indication of the reactor sizes but many assumptions are made in the process. For instance, the same residence time as in the pilot scale reactors proposed in theory were assumed to obtain the height of the reactors. Since the same reactions occur at pilot scale as in full scale, this assumption is seen as a reasonable approach for the reactor size calculations.

Moreover, the heat coefficients used for calculation of total heat exchange area in the FBHE cases were roughly approximated. Especially, the one representing the condensation of steam inside the tubes, which can be seen in Appendix C. In previous applications of FBHE reactors, the situation has been the opposite, heat has been exchanged from the bed particles to superheat steam inside the tubes. The reversed process, condensation inside tubes, is not as studied and would have to be validated. For instance, evaluating whether the condensation of the LP steam, with the small temperature gradient between the steam and reactor bed, requires more or less heat exchange area than what has been proposed in the project.

5.6 Capture cost limitations and future energy price scenarios

There are some limitations associated with the method used for computing the capture cost. First of all, the calculations of the cost of electricity and DH losses are questionable. By multiplying the annual production of electricity and DH with their corresponding assumed prices and the factor discussed in Section 3.7 (equation 3.6), the seasonal price variations are not accounted for. Ideally, the hourly production should be multiplied by the factor and the momentary price, especially for the electricity, and then summarizing this over the year. By doing so, the price drop during summer would be accounted for and the results could show how the balance between the utility costs vary over the course of the year. However, this computation would

require a lot of detailed data which were unavailable, for instance the momentary DH price. Second of all, the investment costs for the equipment are rough estimations that need to be refined. Additionally, the CAPEX is not complete. For instance, the investment costs for piping, pumps and throttles are not considered. However, even though these limitations exist, the capture cost is mainly used for comparison, as stated in Section 3.7, and still gives an indication on the potential magnitude.

In terms of the two future price scenarios, the capture costs decreased for all three cases in both price predictions. For the Steam HP case, the capture cost was decreased the most in the low price scenario while for the FBHE cases high price scenario lead to the largest cost reduction. Applying the low price scenario on all cases lead to the capture cost being almost equal for Steam HP and FBHE LP at 17 and 16 EUR/tCO_2 respectively and FBHE HP at the lowest capture cost of 13 EUR/tCO_2. However, with the high price scenario, the dissimilarities are more evident as the capture cost for Steam HP case is more than 5 times the cost for the two FBHE cases. This being said, for both price scenarios presented, the capture cost will be lower for the two FBHE cases than for the Steam HP case but the decrease in capture cost will not be as drastic. This suggests that the operational costs of the two FBHE cases are more robust compared to the corresponding costs of the Steam HP case. If relating the analysis of the future pricing scenarios for the FBHE cases to Renova, this also indicates that the capture cost will remain relatively stable or, even decrease, if the economic situation would change in the future, assuming that the investment costs will be constant.

5.7 Implications for summer operation

As previously discussed, the results from this project are mainly applicable to winter operation. First of all, as the CO_2 emissions follow the load of the WtE plant, summer operation would imply decreasing the load of the DHPC process. However, excess heat, mainly from the carbonation reactor, would still be produced to some extent and if no other actions are taken, this would be an additional cooling demand to the plant. Another plausible option would be to use the heat in another process on site, for instance in future recovery processes that may be applied at the plant. Another possibility to enable an energy effective summer operation of the DHPC process could be to increase the carbonation reactor temperature, implying that the reactor duty decreases which reduces the excess heat. However, the higher reactor temperature results in a decrease in the capture rate as a cause of the exothermic reaction.

5.8 Future work

Even though research has been done on the DHPC capture process, the technology is still immature. Considering the potential that has been revealed through this project, large scale experiments and more pilot plants are needed for the process to develop into a market leading carbon capture technology. In particular, since the

DHPC process involves fluidized bed reactors, experiments studying the dynamics of these reactors, for instance the interactions between the solid sorbent particles and the flue gas, are crucial to enable commercial up-scaling.

This project also proposed a new design of the regeneration reactor, namely the FBHE. The results show that utilizing this configuration in the DHPC system is beneficial for the application at the WtE plant, because it minimizes the energy penalties and capture cost, all with a compact reactor design. However, since the research on this component is limited, thorough investigations are needed to confirm and map its function and opportunities in industrial processes. At a later stage, estimating the investment cost more accurately by contacting potential vendors is also important to be able to include it in future carbon capture analyses and designs.

6
Conclusion

The aim of the project was to investigate the possibilities of implementing the DHPC process at Renova's WtE plant. In accordance with their emission mitigation strategy, which aims at applying CCS by 2030, an alternative capture method than the conventional MEA is potentially now found. In fact, the results of this study indicate that a suitable design of the DHPC capture process could provide low impacts on the normal operation of the WtE plant. The low impact description entails low efficiency penalty, compact design and low capture cost accompanied with a high capture rate.

In more detail, the analysis made in the project consisted of several major parts selected to investigate the research questions. Firstly, the Ebsilon model of the WtE plant was constructed which laid the foundation of the project and enabled simulating the DHPC process in Aspen Plus with a design proposed in research. The temperature for the carbonation reactor is 70°C which corresponds to a reactor duty of 11.50 MW (Q1). However, it was found that the regeneration reactor had limitations regarding its significant steam demand, which resulted in developing a new type of reactor: the FBHE. In the light of the results, the FBHE reactor provides a solution with compact design and low energy penalty compared to original regeneration reactor used in the Steam case. In particular, using LP steam in the tubes of the FBHE reactor is the most optimal option as it maintains the energy production at Renova to a higher extent than HP steam. The suitable temperature for this reactor is 130°C which yields a reactor duty of 14.12 MW (Q1). Physically, the sizes of the carbonation and regeneration reactors are 2.6 m^2 x 6 m and 12 m^2 x 5.1 m, respectively.

Extracting the steam required to fulfill the steam demand of the FBHE LP case at the WtE plant implies that the total energy efficiency decreases by 5.65%, in absolute terms. To make up for the loss, heat integration measures were investigated. It turns out that, integrating the carbonation reactor load into the DH system is accomplishable, which is one of the main motivations behind the project. Other heat loads in the DHPC process can be recovered as well, for instance the condenser load. In fact, 97% of the maximum recovered heat potential, obtained in the pinch analysis, is achieved. By doing so, the total energy efficiency of Renova's WtE plant, with carbon capture implemented, increases by 1.57%. The reason being that the DH delivery increases by 2.27% while the power production reduces by 2.09% (Q2). In reality, this means that it is possible for Renova to almost maintain its energy production, even when carbon capture has been applied.

Evaluating the capture cost (Q3), it is found that balance between the cost of electricity loss and the gain of revenue from increased DH delivery is vital. A low capture cost is obtained when the DH revenue exceeds the cost of electricity loss, which is the case for FBHE LP. With a capture rate of 96%, the resulting capture cost is 18 EUR/tCO_2, the lowest among all studied DHPC system cases. Investigating future price scenarios, including situations where electricity and DH prices are high and low, concludes that the operational cost of the DHPC process are likely to decrease in the future and will be more robust for the two FBHE cases compared to the Steam HP case.

To summarize, it is highly recommended for Renova to investigate the DHPC process further, especially the FBHE LP configuration. However, to enable a future implementation of this system, more research is needed in the field of FBHE. Potentially, a short-term operated pilot plant could be a first step forward. In addition, to validate the potential of the heat integration and the physical footprint of the reactors, a detailed analysis of the proposed retrofits and available space at the WtE plant is required to evaluate their practical feasibility. It is also important to elaborate more on the summer operation of the DHPC process to find a suitable way of dealing with it, in terms of operating conditions and cooling demand.

Bibliography

[1] United Nations -Climate Change, "The Paris Agreement," n.d. Accessed: 2024-01-17.

[2] Encyclopedia Britannica, "global warming," 2023. Accessed: 2024-01-23.

[3] European Environment Agency, "Annual European Union greenhouse gas inventory 1990–2021 and inventory report 2023." https://www.eea.europa.eu//publications/annual-european-union-greenhouse-gas-2, 2023. Accessed: 2024-01-29.

[4] M. Bui, C. S. Adjiman, A. Bardow, E. J. Anthony, A. Boston, S. Brown, P. S. Fennell, S. Fuss, A. Galindo, L. A. Hackett, J. P. Hallett, H. J. Herzog, G. Jackson, J. Kemper, S. Krevor, G. C. Maitland, M. Matuszewski, I. S. Metcalfe, C. Petit, G. Puxty, J. Reimer, D. M. Reiner, E. S. Rubin, S. A. Scott, N. Shah, B. Smit, J. P. M. Trusler, P. Webley, J. Wilcox, and N. Mac Dowell, "Carbon capture and storage (CCS): the way forward," *Energy Environ. Sci.*, vol. 11, pp. 1062–1176, 2018.

[5] International Energy Agency , "Carbon Capture, Utilisation and Storage," n.d. Accessed: 2024-01-17.

[6] M. Biermann, F. Normann, F. Johnsson, R. Hoballah, and K. Onarheim, "Capture of co2 from steam reformer flue gases using monoethanolamine: Pilot plant validation and process design for partial capture," *Industrial & Engineering Chemistry Research*, vol. 61, no. 38, pp. 14305–14323, 2022.

[7] J. Beiron, F. Normann, and F. Johnsson, "A techno-economic assessment of co2 capture in biomass and waste-fired combined heat and power plants – a swedish case study," *International Journal of Greenhouse Gas Control*, vol. 118, p. 103684, 2022.

[8] Z. Zhang, D.-N. Vo, J. Kum, S.-H. Hong, and C.-H. Lee, "Enhancing energy efficiency of chemical absorption-based co2 capture process with advanced waste-heat recovery modules at a high capture rate," *Chemical Engineering Journal*, vol. 472, p. 144918, 2023.

[9] S.-Y. Oh, M. Binns, H. Cho, and J.-K. Kim, "Energy minimization of mea-based co2 capture process," *Applied Energy*, vol. 169, pp. 353–362, 2016.

[10] T. R. Kumar, J. Beiron, M. Biermann, S. Harvey, and H. Thunman, "Plant and system-level performance of combined heat and power plants equipped with

different carbon capture technologies," *Applied Energy*, vol. 338, p. 120927, 2023.

[11] Y. Guo, J. Sun, R. Wang, W. Li, C. Zhao, C. Li, and J. Zhang, "Recent advances in potassium-based adsorbents for CO2 capture and separation: a review," *Carbon Capture Science and Technology*, vol. 1, p. 100011, 2021.

[12] Y. C. Park, S.-H. Jo, J.-Y. Kim, Y. Won, H. Nam, C.-K. Yi, T.-H. Eom, and J.-B. Lee, "Carbon dioxide capture from a real coal-fired flue gas using K-based solid sorbents in a 0.5 MWe-scale test-bed facility," *International Journal of Greenhouse Gas Control*, vol. 103, p. 103192, 2020.

[13] J. Jung, Y. S. Jeong, Y. Lim, C. S. Lee, and C. Han, "Advanced co2 capture process using mea scrubbing: Configuration of a split flow and phase separation heat exchanger," *Energy Procedia*, vol. 37, pp. 1778–1784, 2013. GHGT-11 Proceedings of the 11th International Conference on Greenhouse Gas Control Technologies, 18-22 November 2012, Kyoto, Japan.

[14] R. Notz, H. P. Mangalapally, and H. Hasse, "Post combustion co2 capture by reactive absorption: Pilot plant description and results of systematic studies with mea," *International Journal of Greenhouse Gas Control*, vol. 6, pp. 84–112, 2012.

[15] Renova AB, "Här blir avfall till el och värme. Avfallskraftvärmeverk i Sävenäs, Göteborg.," 2023.

[16] Renova AB, "Rena fakta 2023, om avfallsvärmevärket," 2023.

[17] A. Hellström. personal communication.

[18] S. Wang, Z. Liu, A. T. Smith, Y. Zeng, L. Sun, and W. Wang, "Dry hydrated potassium carbonate for effective CO2 capture," *Dalton Trans.*, vol. 49, pp. 3965–3969, 2020.

[19] M. Wang, A. Lawal, P. Stephenson, J. Sidders, and C. Ramshaw, "Post-combustion co2 capture with chemical absorption: A state-of-the-art review," *Chemical Engineering Research and Design*, vol. 89, no. 9, pp. 1609–1624, 2011. Special Issue on Carbon Capture Storage.

[20] Y. C. Park, S.-H. Jo, C. K. Ryu, and C.-K. Yi, "Demonstration of pilot scale carbon dioxide capture system using dry regenerable sorbents to the real coal-fired power plant in korea," *Energy Procedia*, vol. 4, pp. 1508–1512, 2011. 10th International Conference on Greenhouse Gas Control Technologies.

[21] Y. C. Park, S.-H. Jo, D.-H. Kyung, J.-Y. Kim, C.-K. Yi, C. K. Ryu, and M. S. Shin, "Test operation results of the 10 mwe-scale dry-sorbent co2 capture process integrated with a real coal-fired power plant in korea," *Energy Procedia*, vol. 63, pp. 2261–2265, 2014. 12th International Conference on Greenhouse Gas Control Technologies, GHGT-12.

[22] P. Gunjal and V. Ranade, "Chapter 7 - catalytic reaction engineering," in

Industrial Catalytic Processes for Fine and Specialty Chemicals (S. S. Joshi and V. V. Ranade, eds.), pp. 263–314, Amsterdam: Elsevier, 2016.

[23] P. Biniaz, N. A. Shirazi, T. Roostaie, and M. R. Rahimpour, "12 - wastewater treatment: employing biomass," in *Advances in Bioenergy and Microfluidic Applications* (M. R. Rahimpour, R. Kamali, M. Amin Makarem, and M. K. D. Manshadi, eds.), pp. 303–327, Elsevier, 2021.

[24] V. Dhyani and T. Bhaskar, "Chapter 9 - pyrolysis of biomass," in *Biofuels: Alternative Feedstocks and Conversion Processes for the Production of Liquid and Gaseous Biofuels (Second Edition)* (A. Pandey, C. Larroche, C.-G. Dussap, E. Gnansounou, S. K. Khanal, and S. Ricke, eds.), Biomass, Biofuels, Biochemicals, pp. 217–244, Academic Press, second edition ed., 2019.

[25] H. Hofbauer and M. Materazzi, "7 - waste gasification processes for sng production," in *Substitute Natural Gas from Waste* (M. Materazzi and P. U. Foscolo, eds.), pp. 105–160, Academic Press, 2019.

[26] C.-K. Yi, S.-H. Jo, Y. Seo, J.-B. Lee, and C.-K. Ryu, "Continuous operation of the potassium-based dry sorbent co2 capture process with two fluidized-bed reactors," *International Journal of Greenhouse Gas Control*, vol. 1, no. 1, pp. 31–36, 2007. 8th International Conference on Greenhouse Gas Control Technologies.

[27] Y. C. Park, S. H. Jo, S.-Y. Lee, J.-H. Moon, C. K. Ryu, J.-B. Lee, and C.-K. Yi, "Performance analysis of k-based kep-co2p1 solid sorbents in a bench-scale continuous dry-sorbent co2 capture process," *Korean Journal of Chemical Engineering*, vol. 33, pp. 73–79, 2015.

[28] J. Ma, J. Zhong, X. Bao, X. Chen, Y. Wu, T. Cai, D. Liu, and C. Liang, "Continuous co2 capture performance of k2co3/al2o3 sorbents in a novel two-stage integrated bubbling-transport fluidized reactor," *Chemical Engineering Journal*, vol. 404, p. 126465, 2021.

[29] K.-W. Park, Y. S. Park, Y. C. Park, S.-H. Jo, and C.-K. Yi, "Study of co2 carbonation-regeneration characteristics of potassium-based dry sorbents according to water vapor contents of inlet gas and regeneration temperature in the cycle experiments of bubbling fluidized-bed reactor," *Korean Chem. Eng. Res*, vol. 47, pp. 349–354, 2009.

[30] K.-C. Kim, K.-Y. Kim, Y. C. Park, S.-H. Jo, H.-J. Ryu, and C.-K. Yi, "Study of hydrodynamics and reaction characteristics of k-based solid sorbents for co2 capture in a continuous system composed of two bubbling fluidized-bed reactors," *Korean Chem. Eng. Res*, vol. 48, pp. 499–505, 2010.

[31] K. KC, P. Y.C., and J. S. et al, "The effect of co2 or steam partial pressure in the regeneration of solid sorbents on the co2 capture efficiency in the two-interconnected bubbling fluidized-beds system," *Korean J. Chem. Eng*, vol. 28, p. 126465, 2011.

[32] V. Stenberg, F. Lind, and M. Rydén, "Measurement of bed-to-tube surface heat

transfer coefficient to a vertically immersed u-tube in bubbling loop seal of a cfb boiler," *Powder Technology*, vol. 381, pp. 652–664, 2021.

[33] V. Stenberg, M. Rydén, and F. Lind, "Evaluation of bed-to-tube heat transfer in a fluidized bed heat exchanger in a 75 mwth cfb boiler for municipal solid waste fuels," *Fuel*, vol. 339, p. 127375, 2023.

[34] A. Gomez, A. Jayakumar, and N. Mahinpey, "Experimental verification of the reaction mechanism of solid k2co3 during postcombustion co2 capture," *Industrial Engineering Chemistry Research*, vol. 55, 09 2016.

[35] A. Jayakumar, A. Gomez, and N. Mahinpey, "Post-combustion co2 capture using solid k2co3: Discovering the carbonation reaction mechanism," *Applied Energy*, vol. 179, pp. 531–543, 2016.

[36] A. Jayakumar, A. Gomez, and N. Mahinpey, "Study of the kinetic behavior of solid k2co3 under post-combustion co2 capture conditions," *Industrial Engineering Chemistry Research*, vol. 56, 01 2017.

[37] N. Shigemoto, T. Yanagihara, S. Sugiyama, and H. Hayashi, "Material balance and energy consumption for co2 recovery from moist flue gas employing k2co3-on-activated carbon and its evaluation for practical adaptation," *Energy & Fuels*, vol. 20, no. 2, pp. 721–726, 2006.

[38] C. Zhao, X. Chen, C. Zhao, and Y. Liu, "Carbonation and hydration characteristics of dry potassium-based sorbents for co2 capture," *Energy & Fuels*, vol. 23, no. 3, pp. 1766–1769, 2009.

[39] STEAG Energy Services GmbH System Technologies, "EBSILON®Professional - The Planning Tool for the Power Plant Process," n.d.

[40] Aspen Tech, "Aspen Plus - Leading Process Simulation Software," 2024.

[41] Aspen Tech, "Aspen Plus V14 Help - RKS-BM," 2024.

[42] D. Mallick, B. Buragohain, P. Mahanta, and V. S. Moholkar, *Gasification of Mixed Biomass: Analysis Using Equilibrium, Semi-equilibrium, and Kinetic Models*, pp. 223–241. Singapore: Springer Singapore, 2018.

[43] R. P. Lively, R. R. Chance, and W. J. Koros, "Enabling low-cost co2 capture via heat integration," *Industrial & Engineering Chemistry Research*, vol. 49, no. 16, pp. 7550–7562, 2010.

[44] Åsa Eliasson, E. Fahrman, M. Biermann, F. Normann, and S. Harvey, "Efficient heat integration of industrial co2 capture and district heating supply," *International Journal of Greenhouse Gas Control*, vol. 118, p. 103689, 2022.

[45] S. Hall, "24 - energy conservation," in *Branan's Rules of Thumb for Chemical Engineers (Fifth Edition)* (S. Hall, ed.), pp. 375–385, Oxford: Butterworth-Heinemann, fifth edition ed., 2012.

[46] Chalmers University of Technology, "KVM013 INDUSTRIAL ENERGY SYSTEMS Course Compendium – Autumn 2022."

https://chalmers.instructure.com/courses/21146/files/2347251?module$_i tem_i d = 310192, 2022. *Accessed* : 2024 − 04 − 04.

[47] P. Catrini, D. Curto, V. Franzitta, and F. Cardona, "Improving energy efficiency of commercial buildings by combined heat cooling and power plants," *Sustainable Cities and Society*, vol. 60, p. 102157, 2020.

[48] K. Gustafsson, R. Sadegh-Vaziri, S. Grönkvist, F. Levihn, and C. Sundberg, "Beccs with combined heat and power: Assessing the energy penalty," *International Journal of Greenhouse Gas Control*, vol. 108, p. 103248, 2021.

[49] A. Lyngfelt, B. Leckner, and T. Mattisson, "A fluidized-bed combustion process with inherent co2 separation; application of chemical-looping combustion," *Chemical Engineering Science*, vol. 56, no. 10, pp. 3101–3113, 2001.

[50] H. Ali, N. H. Eldrup, F. Normann, R. Skagestad, and L. E. Øi, "Cost estimation of co2 absorption plants for co2 mitigation – method and assumptions," *International Journal of Greenhouse Gas Control*, vol. 88, pp. 10–23, 2019.

[51] M. Biermann, C. Langner, S. Roussanaly, F. Normann, and S. Harvey, "The role of energy supply in abatement cost curves for co2 capture from process industry – a case study of a swedish refinery," *Applied Energy*, vol. 319, p. 119273, 2022.

[52] S. Gardarsdottir, E. De Lena, M. Romano, S. Roussanaly, M. Voldsund, J.-F. Pérez-Calvo, D. Berstad, C. Fu, R. Anantharaman, D. Sutter, M. Gazzani, M. Mazzotti, and G. Cinti, "Comparison of technologies for co2 capture from cement production—part 2: Cost analysis," *Energies*, vol. 12, p. 542, 02 2019.

[53] Chalmers University of Technology, "MEN120 HEAT AND POWER SYSTEMS ENGINEERING Course Compendium – Autumn 2022." https://chalmers.instructure.com/courses/20160/files/folder/Case Accessed: 2024-04-22.

[54] B. Ren, L. Zhang, H. Xu, J. Cao, and Z. Tao, "Experimental study on condensation of steam/air mixture in a horizontal tube," *Experimental Thermal and Fluid Science*, vol. 58, pp. 145–155, 2014.

[55] Chalmers University of Technology, "KVM071 DESIGN OF INDUSTRIAL ENERGY EQUIPTMENT," 2021. Accessed: 2024-04-24.

A

Appendix 1

In this Appendix more detailed information about the Ebsilon model of the WtE plant will be presented. At first a few figures showing the layout of the original model will be shown. Secondly a detailed list of all components used in the model as well as important input data for the simulation is displayed.

A.1 Original Ebsilon model

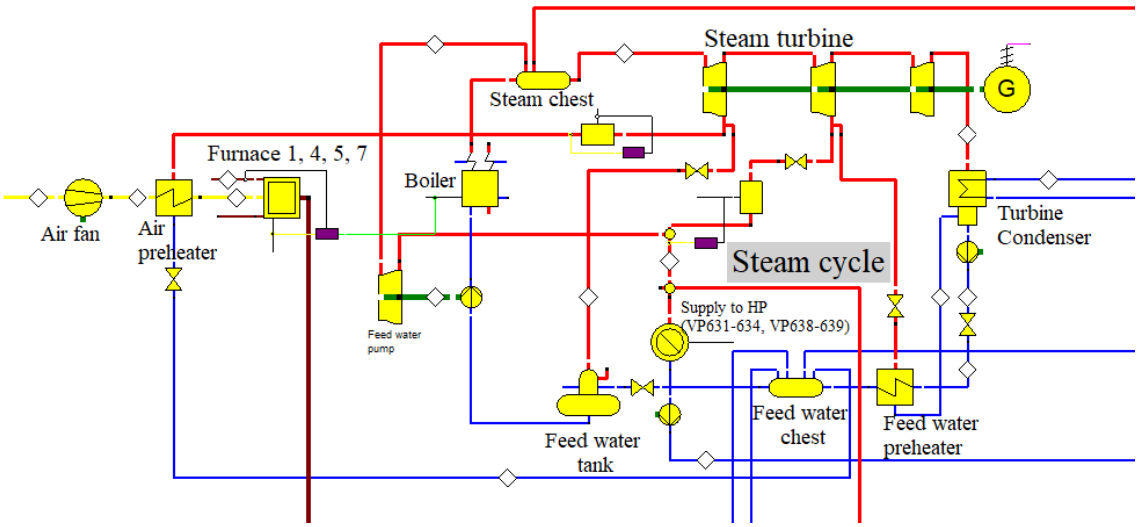

Figure A.1: Steam cycle of the original Ebsilon model.

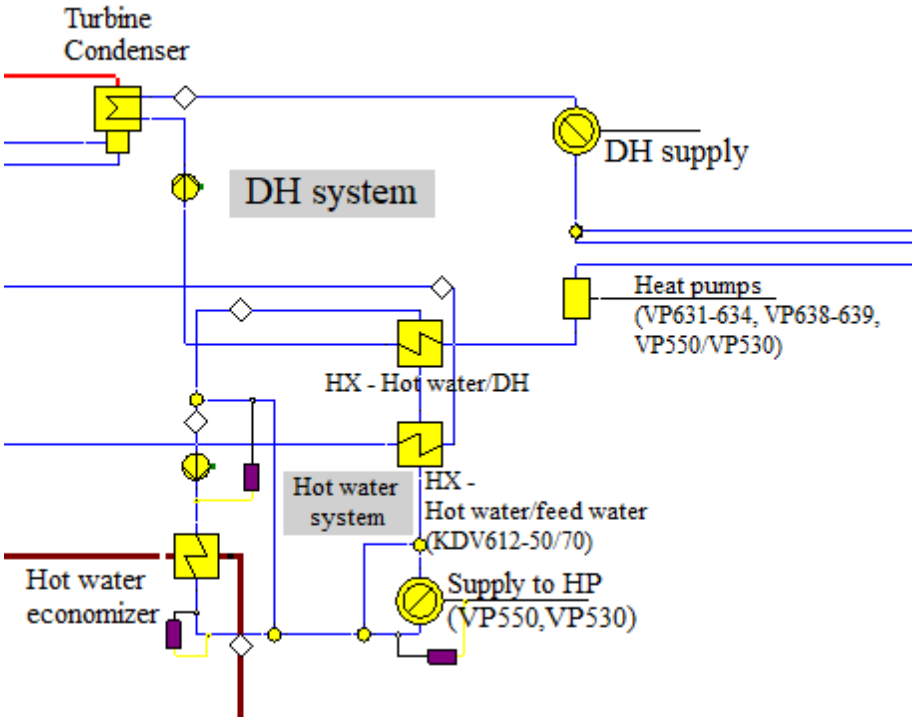

Figure A.2: DH system and hot water cycle of the original Ebsilon model.

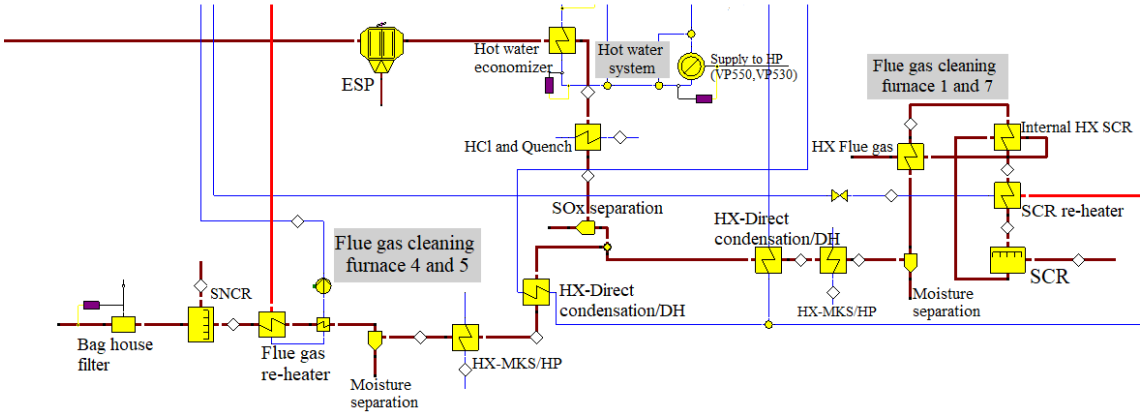

Figure A.3: Fluegas cleaning system of the original Ebsilon model.

A.2 Components list - WtE model in Ebsilon

Table A.1: Component list for the WtE plant in Ebsilon.

Description	Component name and number in Ebsilon
Combustion Chamber	Combustion Chamber - 21
Air fan	Compressor - 24
Air preheater	Feedwater preheater - 10
Boiler	Steam generator - 5
Steam chest	Tank - 28
Feedwater pump	Turbine - 6
Steam turbine	Turbine - 6
Turbine condenser	Condenser - 7
Generator	Generator - 11
Feedwater tank	Deaerator - 9
LP Feedwater preheater	Feedwater preheater - 10
Feedwater chest	Tank - 28
Supply to HP	Heat consumer - 35
Hot water economizer	Heat exchanger - 61
Heat exchanger Hot water/Condensate	Heat exchanger - 26
Heat exchanger Hot water/DH	Heat exchanger - 26
DH supply	Heat consumer - 35
Heat pump delivery	Heat injection - 16
Electrostatic percipitator	Electrostatic percipitator - 85
HCl and Quench step	Air preheater - 25
SO_2 separation	Selective splitter - 52
Heat exchanger Direct condensation/DH	Air preheater - 25
Heat exchanger Direct condensation/HP	Air preheater - 25
Moisture separation	Selective splitter - 52
Flue gas re-heater	Feedwater preheater - 10
SNCR/SCR	NOx removal - 86
Bag house filter	Heat injection - 16
Heat exchanger Flue gas	Air preheater - 25
Heat exchanger SCR internal	Air preheater - 25
SCR re-heater	Feedwater preheater - 10

A.3 Input data in the WtE model

Table A.2: Input specifications for the waste as fuel in the WtE model in Ebsilon.

Waste conditions and composition		
Lower heating value, LHV[1]	11990	kJ/kg
Composition[2]		
Water in fuel	36.0	mole%
Carbon	29.8	mole%
Oxygen	15.4	mole%
Ash	13.2	mole%
Hydrogen	4.2	mole%
Nitrogen	0.6	mole%
Chlorine	0.6	mole%
Sulphur	0.2	mole%

[1]Calculated by Ebsilon based on the composition of the fuel.
[2]Data taken from [53].

Table A.3: Design specifications for WtE model in Ebsilon. Data collected from Renova's WtE plant, on the 6th of November 2022.

Combustion		
Combustion efficiency	90	%
Air outlet temperature from air preheater	120.8	°C
Flue gas exhaust temperature	227.7	°C
Steam cycle		
Generator efficiency	95	%
HP steam temperature	399.5	°C
HP steam pressure	40.2	bar
LP steam pressure	3.6	bar
LP extraction steam flow to heat pumps	16.1	kg/s
LP extraction steam temperature to heat pumps	150	°C
LP steam temperature to air preheater	150	°C
Turbine feed steam flow	69.4	kg/s
Steam flow to feed-water turbine	2.46	kg/s
Turbine outlet pressure	0.8	bar
Feedwater chest pressure	6.5	bar
Condensate temperature after Supply to HP (VP631-634, VP638-639)	96.7	°C
Condensate temperature after HX - Hot water/condensate KDV612-50/70	130.0	°C
DH cycle		
DH pressure	9.3	bar
Delivery temperature (out from the plant)	90.2	°C
Return temperature (to the plant)	40.2	°C
Temperature after HX - Hot water/DH	63.8	°C
Hot-water cycle		
HW cycle pressure	16.9	bar
Inlet temperature to Hot water economizer	120.0	°C
Outlet temperature to Hot water economizer	150.4	°C
Flue gas cleaning system (Line 1 and 7)		
Temperature after hot-water economizer	147.6	°C
Temperature after HCl and Quench	63.4	°C
Temperature after HX-direct condensation/DH	43.3	°C
Temperature after HX-MKS/HP	28.8	°C
Temperature between HX Flue gas and Internal HX SCR	110.5	°C
Temperature between Internal HX SCR and SCR re-heater	223.9	°C
Temperature between Internal SCR re-heater and SCR	236.0	°C
Flue gas cleaning system (Line 4 and 5)		
Temperature after hot-water economizer	147,6	°C
Temperature after HCl and Quench	63.4	°C
Temperature after HX-Direct condensation/DH	43.3	°C
Temperature after HX-MKS/HP	33.2	°C
Temperature after Flue gas re-heater	67.3	°C
Temperature after Bag house filter	83.3	°C

B

Appendix 2

In this appendix the general settings of the Aspen Plus model of the DHPC process are shown initially. Thereafter the rest of the results from the parameter study of the carbonation reactor temperature are introduced. Finally, a summary of the process variables used in the Aspen simulations for each case is presented.

B.1 General settings - DHPC model in Aspen Plus

Component	**Type**
CO	Conventional
CO_2	Conventional
H_2O	Conventional
O_2	Conventional
N_2	Conventional
SO_2	Conventional
HCl	Conventional
NOx	Nonconventional
NH_3	Conventional
Ash	Nonconventional
TOC	Nonconventional
K_2CO_3	Solid
$KHCO_3$	Solid
Al_2O_3	Solid
$K_2CO_3 \cdot (1.5H_2O)$	Solid
Property method	RKS-BM

B.2 Results from parameter study - Carbonation reactor

In the following section some of the results from the parameters study of the carbonation reactor will be shown. As mentioned, the percentage captured CO_2 in the reactor as a function of sorbent flow for different reactor temperatures and moisture levels are plotted in the following graphs.

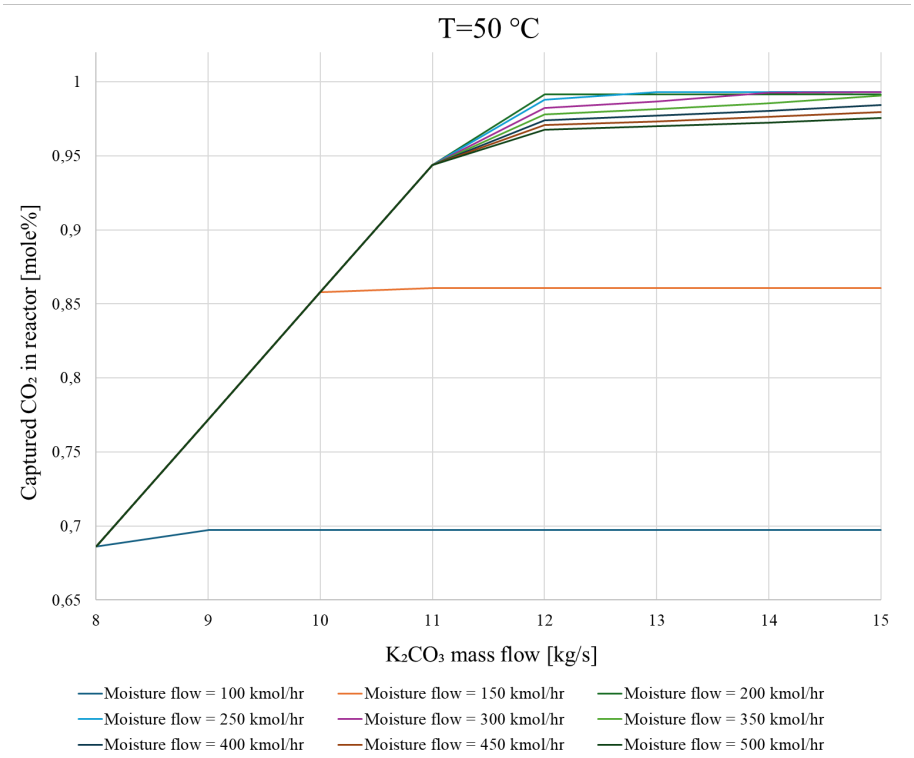

Figure B.1: Captured CO_2 in the carbonation reactor against sorbent flow for different moisture flows at a reactor temperature of 50°C.

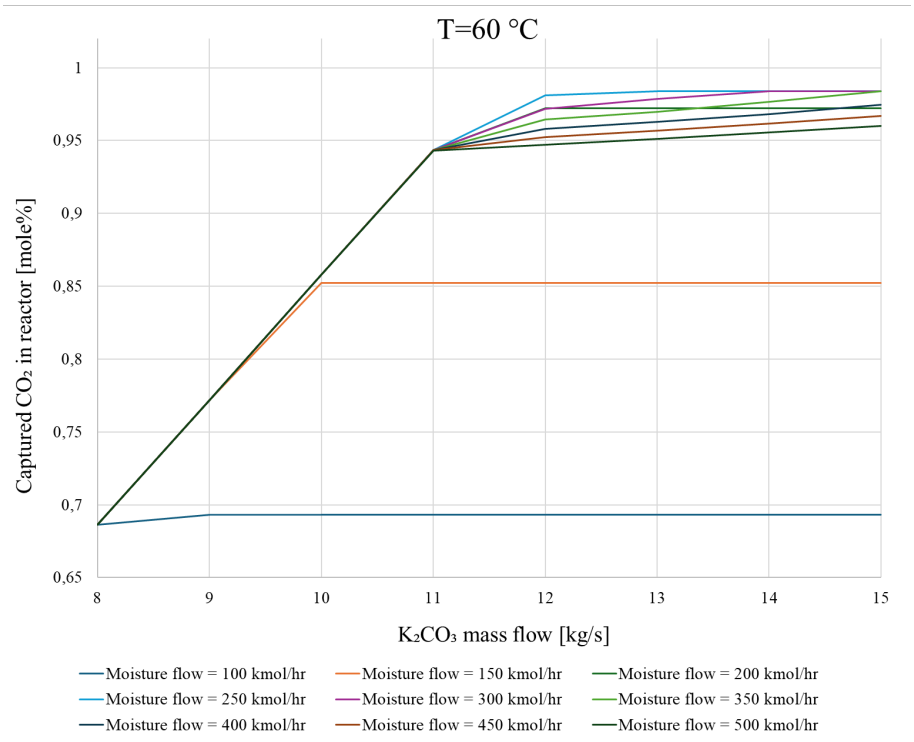

Figure B.2: Captured CO_2 in the carbonation reactor against sorbent flow for different moisture flows at a reactor temperature of 60°C.

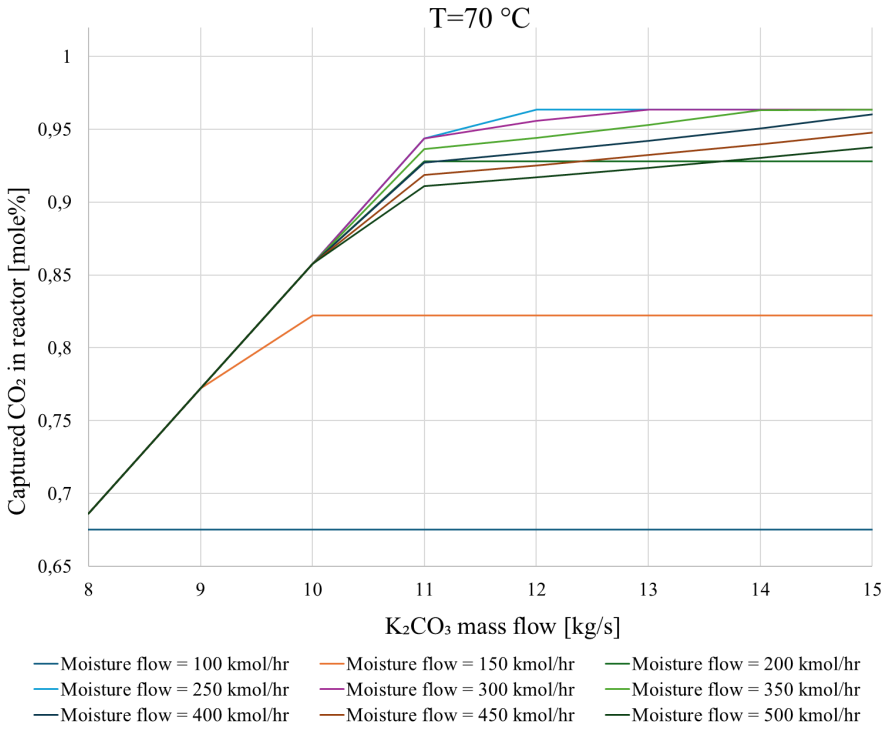

Figure B.3: Captured CO_2 in the carbonation reactor against sorbent flow for different moisture flows at a reactor temperature of 70°C.

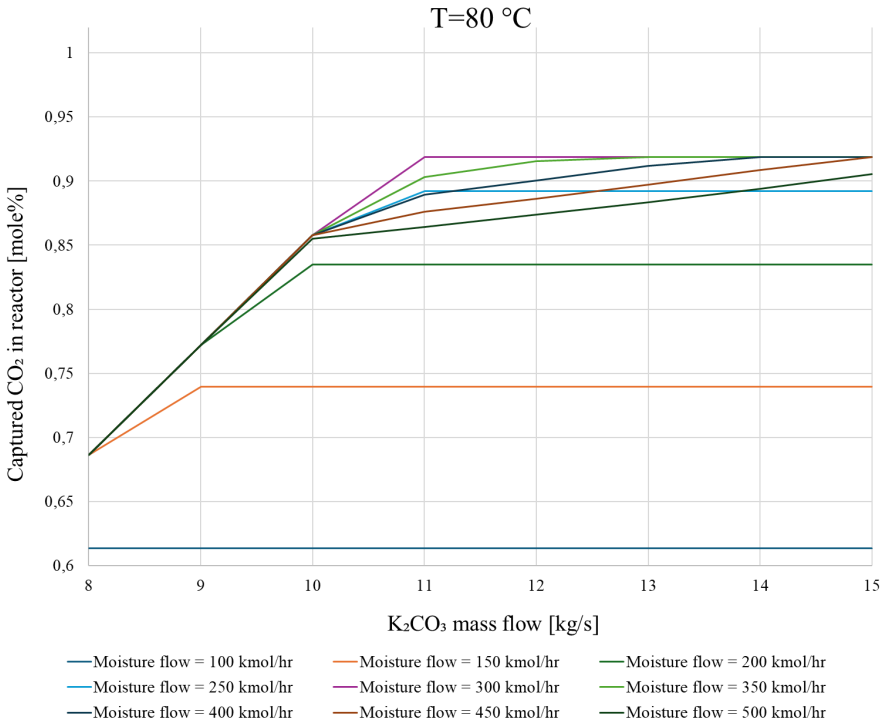

Figure B.4: Captured CO_2 in the carbonation reactor against sorbent flow for different moisture flows at a reactor temperature of 80°C.

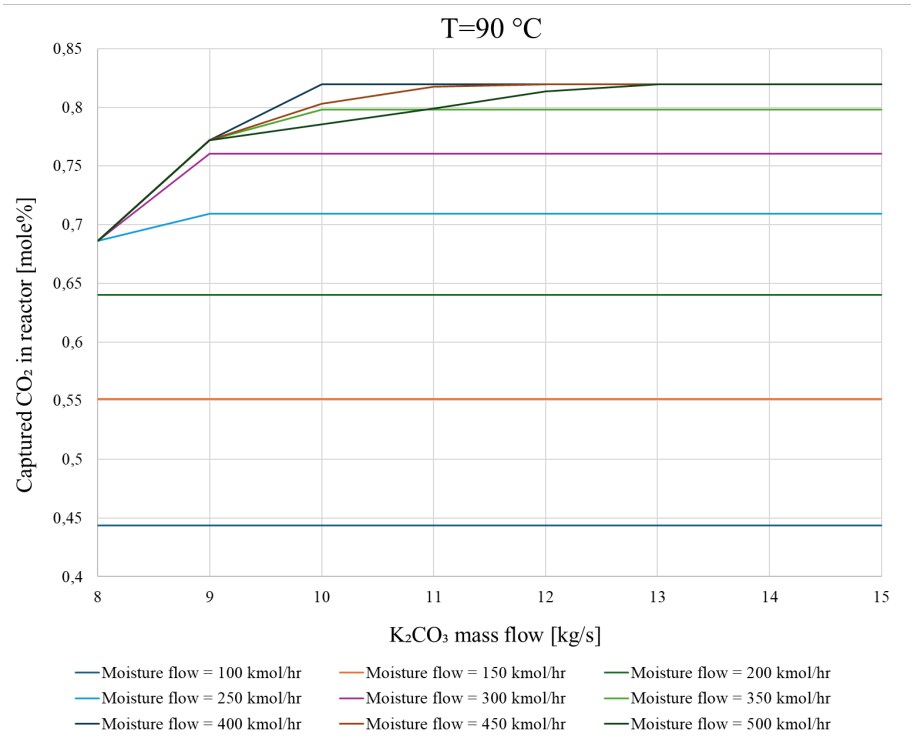

Figure B.5: Captured CO_2 in the carbonation reactor against sorbent flow for different moisture flows at a reactor temperature of 90°C.

B.3 Summary of process variables

For all of the studied DHPC system cases the carbonation reactor had the same design. As a consequence of the parameter study, also the regeneration reactor temperature and duty as well as other process variables were identical among the cases. Consequently, there are a few joint parameters for the Steam HP, FBHE HP and FBHE LP cases which are summarized in Table B.1.

Table B.1: Summary of common process variables for the DHPC cases.

Carbonation reactor temperature [°C]	70
Carbonation reactor heat duty [MW]	-11.50
Regeneration reactor temperature [°C]	130
Regeneration reactor heat duty [MW]	14.12
Sorbent cooler duty [MW]	1.86
Degree of sorbent regeneration [%]	100
Capture rate [%]	96.4
Captured flow of CO_2 [kg/s]	3.58

However, there are clear distinctions in terms of other process variables between the system cases and these are summarized in Table B.2. For instance, since the choice of fluidization gas differs, so does the condenser duty. In addition, the demand of steam is significantly higher in the Steam HP than in the FBHE cases. Also, there is a CO_2 demand in the FBHE cases, but not in the Steam HP.

Table B.2: Summary of diverging results for the DHPC cases.

	Steam case	**FBHE case**	
	HP	HP	LP
Condenser duty [MW]	76.40	3.68	3.68
Steam demand [kg/s]	29.76	5.19	6.20
CO_2 demand [kg/s]	-	2.37	4.73

C
Appendix 3

The procedure for estimating the dimensions of the FBHE reactors, the calculated heat coefficients for this case and a summary of all the reactor sizes are included in this appendix.

C.1 Dimensions of FBHE reactors

In contrast to the calculations described for the Steam HP regeneration reactor, in the FBHE cases, the flow of CO_2 fluidizing the reactor bed was not known in advance. Therefore, these size calculations were done in a different way. The procedure used for dimensioning the FBHE reactors is based on a method used to dimension a fluidized bed reactor used for chemical looping combustion applications [49]. However, some adjustments and simplifications were made to more accurately suite the method to the FBHE reactors.

Before initiating the calculations, some parameters for the heat exchanger tubes inside the reactor were estimated based on knowledge gained through discussions with the supervisors. These parameters as well as other estimated values are listed in Table C.1.

Table C.1: Specifications of the internal tubes of the FBHE reactor.

Tube specifications		
Outer diameter, d_o	0.04	m
Inner diameter, d_i	0.0336	m
Wall thickness, w	0.0032	m
Pitch	0.06	m
Length	3	m
Outer heat transfer coefficient, ho	500	W/m^2K
Other assumed values		
Steam quality, x	0.5	
Superficial velocity	0.5	m/s
Bed voidage, e	0.4	

The overall heat transfer coefficient, U, for steam condensing inside horizontal tubes was then estimated. The expression for U is shown in equation C.1, where h_o and h_i are the thermal resistance on the outside and inside of the tubes and d_o and d_i are the outer and inner diameter of the tubes.

$$\frac{1}{U} = \frac{1}{h_o} + \frac{d_o}{d_i} + \frac{1}{h_i} \tag{C.1}$$

h_o in equation C.1 had already been estimated in Table C.1 while h_i was estimated trough the Nusselt correlation shown in equation C.2. Equation C.2 is valid for stratified flows were x is the steam quality, ρ is the density (kg/m^3), g is the gravitational constant, h_{fg} is the entalphy of vaporisation (J/kg), k_l is the thermal conductivity (W/m^2°C), μ is the dynamic viscosity (Pas), d is the tube diameter (m) and δT is the temperature difference between the saturation temperature and the tube wall [54]. The flow inside the tubes is assumed to be stratified, to account for the gravitational effects as it condenses.

$$Nu_{strat} = 0.728 \left[1 + \frac{1-x}{x}\left(\frac{\rho_v}{\rho_l}\right)^{2/3}\right]^{-0.75} \left[\frac{\rho_l(\rho_l - \rho_v)g h_{fg} d_3}{k_l \mu_l \Delta T}\right]^{0.25} \tag{C.2}$$

When Nu had been found, h_i was computed through the definition of the Nusselt number. With U established, the total heat transfer area of the tubes could be calculated through the general equation for heat transfer across a surface, presented in equation C.3. Where Q is the total transferred heat (W), U is the overall heat transfer coefficient (W/m^2°C), A is the total heat transfer area and ΔT_{lm} is the logarithmic mean temperature.

$$Q = UA\Delta T_{lm} \tag{C.3}$$

Since the dimensions of each individual tube had already been established and shown in Table C.1, the number of tubes could then be obtained. The depth of the reactor was assumed and consequently the tubes could be evenly distributed over the cross section area with the pitch distance in mind. The number of tube layers in the vertical direction was calculated by dividing the total number of tubes by the number of tubes in each horizontal layer. The reactor height could thereafter be calculated as the pitch times the number of tubes in the vertical direction.

When the cross sectional area of the reactor was set, the dimensions could be used to calculate the volume flow of CO_2 required to fluidize the reactor bed. At first a superficial velocity was assumed at 0.3 m/s and the volume flow of CO_2 could be calculated using the area. With use of the density the mass flow of CO_2 for fluidization was then obtained. In addition to the dimensions of the reactor the pressure drop was calculated through equation C.4 where ρ_s is the density of the solid bed particles (kg/m^3), e is the bed voidage and H is the height of the reactor bed (m).

$$\Delta P = (\rho_s - \rho_l)g(1-e)H \tag{C.4}$$

C.2 Summary of results from reactor dimension calculations

The resulting heat coefficients used to establish the FBHE reactor sizes are presented in Table C.2.

Table C.2: Heat coefficients for the two FBHE cases.

	FBHE HP	FBHE LP
h_o [W/m^{2}K]	500	500
h_i [W/m^{2}K]	3220	6460
U [W/m^{2}K]	422	458

In Table C.3, the sizes of the carbonation reactor, FBHE reactors and Steam HP regeneration reactor are presented.

Table C.3: Dimensions of carbonation reactor and the regeneration reactors in the Steam HP and FBHE cases.

	Carbonation reactor	FBHE HP	FBHE LP	Steam HP
Fluidizing velocity [m/s]	3	0.5	0.5	0.5
Height [m]	25.6	2.0	5.1	6
Cross section [m]	7.2	6	12	2.6
Pressure drop [bar]	0.14	0.14	0.33	0.32
Bed height [m]	0.72	0.72	1.7	1.64
Solid flux [kg/m^{2}s]	4.8	-	-	-
Heat exchange area [m^2]	-	424	2140	-

D
Appendix 4

This appendix aims at describing the size and cost estimation of the remaining process equipment. In addition, a summary of the investment costs and the assumptions used in the economic analysis, are presented.

D.1 Other DHPC equipment

Besides the reactors in the DHPC process, the size of other components in the process were estimated in order to evaluate the investment cost of the DHPC process as a whole.

For all heat exchanging equipment, the procedure for dimensioning was based on estimating the overall heat transfer coefficient, U, and then calculating the total heat transfer area through equation C.3. The estimations of U were based on theory presented in [55], and strictly dependent on the two media that heat was transferred between. In addition to the equipment required in the stand alone DHPC process, the heat exchangers and condensors required for heat integration were also dimensioned to enable the economic analysis. The assumed values of U for the equipment exchangeing heat between different media are presented in Table D.1.

Table D.1: Assumed overall heat transfer coefficients, U, for all equipment exchanging heat in the DHPC process.

Process fluids	U [W/m^{2}C]
Air/solids	100
Water/water	1000
Condensing steam/water	1300
Condensing steam/air	250
Water/air	200

When evaluating the size and cost of the equipment needed for the retrofit of the plant, decisions regarding the type of heat exchanger and whether there were old equipment that could be reused, had to be made. The condenser used as a final step in the DHPC process, assumed to be of shell and tube type, is considered suitable to reuse when retrofitting the air preheating process. The flue gas reheater was also considered possible to reuse in the retrofitted plant in the Steam HP case since the function of heater was the same as before the retrofit, the only difference being the

source of the hot stream. Thus no additional investments in heat new exchanger equipment was considered to enable these retrofits at the plant.

For integrating the carbonation reactor load with the DH water, the added investment costs are calculated based on cost functions for plate and frame heat exchangers. These costs are the only retrofit costs considered for the two FBHE cases.

D.2 Summary of equipment investment costs

All the equipment included in the CAPEX for the DHPC cases, for both capture process and heat integration, together with their corresponding investment cost are presented in Table D.2.

Table D.2: Euipment investment costs for the DHPC cases.

Equipment [kEUR][1]	**Steam case** HP	**FBHE case** HP	LP
Flue gas fan	268	268	268
Steam fan	47.9	-	-
CO_2 fan	-	39.3	68.7
Carbonation reactor	7262	7262	7262
Regeneration reactor	621	484 (FBHE)	2422 (FBHE)
Sorbent cooler (Air cooled HX)	375	375	375
Condenser (Shell and Tube HX)	1922	405	405
Cyclone	324	324	324
Carbonation reactor load (Plate HX)	402	400	400
Total	11223	9508	11480

A summary of the assumptions for the economic calculations can be seen in Table D.3.

[1] All investments were evaluated using year 2022 as reference.

Table D.3: Assumptions made for the economic calculations.

Economic assumptions		
Plant life time	25	years
Interest rate	7.5	%
Maintenance cost	4	% of EIC[2]
Annualized factor	10.8	
Operational hours	8000	h/yr
Labour costs		
Operator salary	90	EUR 2022
Engineer salary	176	EUR 2022

[2]EIC stands for equipment investment cost.

E

Appendix 5

The parameter studies of the neglected cases: Steam LP and Preheated CO_2 HP/LP, are presented in this appendix.

E.1 Case: Steam LP

E.1.1 Parameter study

Following the same procedure as for the HP steam case, the conversion of K_2CO_3 was plotted against the flow of LP steam, which can be seen in Figure E.1. Evident is that the behaviour of the different reactor temperatures follow the exact same pattern as in Figure 4.3.

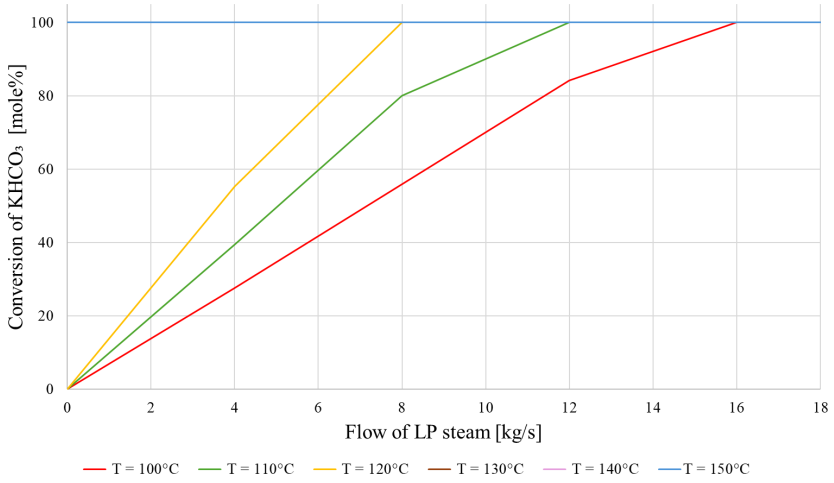

Figure E.1: Conversion of $KHCO_3$ as a function of the flow of LP steam at different reactor temperatures. Note that the graphs for 130 and 140°C lays behind the 150 °C graph.

When evaluating the demand of LP steam to cover the heat duty of the regeneration reactor the same groupings can be seen as for the HP steam case, but the results differ significantly. In Figure E.2, the reactor heat duty is plotted as a function of LP steam flow.

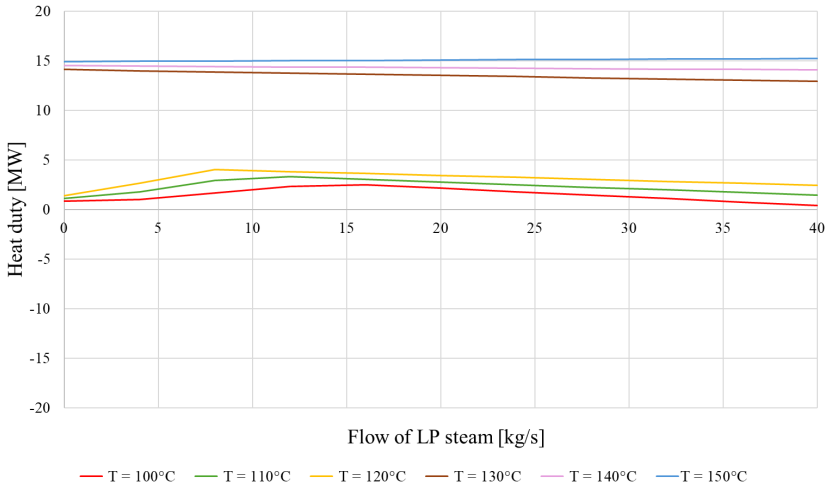

Figure E.2: Regeneration reactor heat duty as a function of the flow of LP steam flow at different reactor temperatures.

For the same reasons as discussed for the HP steam case, the lower reactor temperatures that converted $KHCO_3$ to the hydrated form of K_2CO_3 will not be considered further. Evident is that the required flow of LP steam, independent of reactor temperature, is about ten times the amount required in HP steam. In particular, maintaining a reactor temperature of 130°C requires 469.72 kg/s of LP steam to cover the heat duty of 14.12 MW. The key parameters for the regeneration reactor in the Steam LP case are presented in Table E.1.

Table E.1: Key parameters of the regeneration reactor in the Steam LP case, using LP steam as both fluidizing agent and heating medium.

Steam LP case - Key parameters	
Steam condition	LP
Reactor temperature	130 °C
Reactor heat duty	14.12 MW
Steam demand	469.72 kg/s

E.2 Case: Preheated CO_2 HP/LP

E.2.1 Parameter study

For the preheated CO_2 case, the first part of the parameter analysis, evaluating the conversion of $KHCO_3$ by varying the CO_2 flow at different reactor temperatures, was exactly the same as for the FBHE HP/LP case. In Figure 4.10, the conversion for different flows of CO_2 fluidizing the reactor bed is shown. Using the same reasoning as previously and considering that the CO_2 is circulated from the reactor outlet stream, the relevance of its size compared to the amount of captured CO_2 can be discussed. The reactor temperature is thereby chosen to be 130 °C even in this case.

However, in this case there were a few more parameters to analyze than with the other cases. In addition to the purpose of driving the reaction, the CO_2 flow also functions as heating medium. Therefore, for this case the external heat exchanger preheating the recirculating CO_2 also had to be analyzed. As mentioned previously, steam is used to preheat the CO_2. And from the above analysis, the reactor duty at 130°C was found. Consequently, it was possible to find the mass flow of HP and LP steam required to satisfy this heating demand. The resulting mass flows from these calculations were 5.19 kg/s and 6.20 kg/s for HP and LP steam respectively, assuming that the steam is allowed to condense and cool to a temperature of 140°C.

When the mass flow of steam was set in the external heat exchanger, the size of the CO_2 stream required to deliver the heat to the reactor was found. Figure E.3 shows the minimum temperature difference obtained in the CO_2 preheater for different mass flows of CO_2 at 130°C. The minimum temperature difference in the heat exchanger was set to 10 °C. Therefore, the minimum mass flow of the CO_2 stream fulfilling this requirement, is obtained at the point where the graph crosses the 10 °C line. However, for the chosen reactor temperature of 130°C, the heat exchange was only viable when using HP steam as it would require >15 000 kg/s of CO_2 for the case with LP steam. The reason behind that was the low driving force, temperature difference, due to the set outlet condensate temperature of 140°C and the LP steam temperature of 150°C, requiring a significant mass flow to deliver the heat. Consequently, the Preheated CO_2 case using LP steam was not further evaluated. Therefore, Figure E.3 is solely for the heat exchange between CO_2 and HP steam.

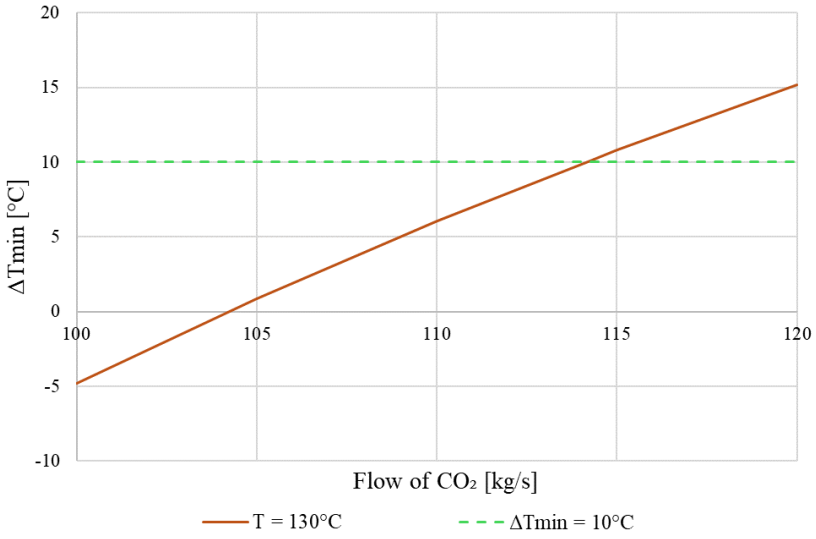

Figure E.3: The minimum temperature difference in the external heat exchanger of the Preheated CO_2 case as a function of CO_2 flow at 130°C.

As is evident in Figure E.3, this mass flow of CO_2 was 114.25 kg/s resulting in a outlet temperature of 254.2°C for the CO_2 stream as can be seen in Figure E.4.

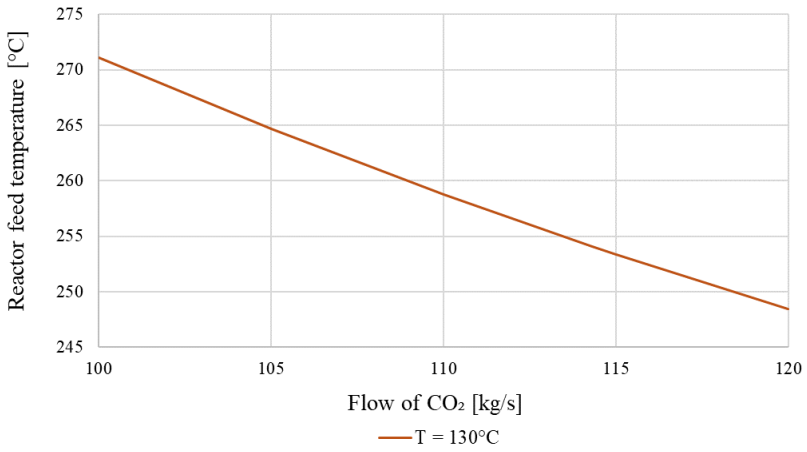

Figure E.4: The outlet temperature of the fluidizaton gas from the external heat exchanger of the Preheated CO_2 case as a function of CO_2 flow at 130°C.

The key performance parameters for the regeneration reactor using preheated CO_2 as the fluidizing agent and HP as well as LP steam as heating medium are shown in Table E.2.

Table E.2: Key parameters of the regeneration reactor in the Preheated CO_2 case, using CO_2 as fluidization gas and HP as well as LP steam as heating medium.

Preheated CO_2 case - Key parameters		
Steam condition	HP	LP
Reactor temperature	130 °C	130 °C
Reactor heat duty	14.12 MW	14.12 MW
Steam demand	5.19 kg/s	6.20 kg/s
CO_2 demand	114.25 kg/s	>15000 kg/s

DEPARTMENT OF SOME SUBJECT OR TECHNOLOGY
CHALMERS UNIVERSITY OF TECHNOLOGY
Gothenburg, Sweden
www.chalmers.se

CHALMERS
UNIVERSITY OF TECHNOLOGY